PN-AAU-997

49922

3860465

AN EXPERIMENTAL INVESTIGATION OF THE EFFECT OF WATER REMOVAL AND REPLACEMENT ON THE THERMAL STRATIFICATION IN A HORIZONTAL WATER STORAGE TANK

TECHNICAL REPORT 4

by

Li-Yun Wu

Richard B. Bannerot

Mechanical Engineering Department

University of Houston-University Park

Houston, Texas 77004

November 1984

Any opinions, findings, conclusions or recommendations expressed in this publication are those of the author(s) and do not necessarily reflect the views of the U.S. Agency for International Development (USAID).

AN EXPERIMENTAL INVESTIGATION OF THE WATER REMOVAL AND REPLACEMENT ON THE THERMAL STRATIFICATION IN A HORIZONTAL WATER STORAGE TANK

TECHNICAL REPORT 4

Prepared by: Li-Yun Wu
Research Associate

Approved by: Richard B. Bannerot
Principal Investigator

Prepared as part of the project, "Medium Temperature, High Efficiency Tracking and Non-tracking Solar Energy Collectors for Rural and Industrial Applications" for the Agency for International Development under the Agreement for Projects under USAID Grant Agreement Dated August 26, 1978 between the President of India and USAID for Technologies for the Rural Poor.

USAID Project Grant No. 386-0465

November 1984

ACKNOWLEDGEMENTS

This work was supported by United States Agency for International Development (USAID).

Li-Yun Wu

Richard B. Bannerot

ABSTRACT

The temperature distribution in a horizontal water tank simulating the thermal storage for a solar thermosyphon water heating system was investigated experimentally in two different tank plumbing configurations, for eight different flow rates and different temperature levels, and for both continuous and interrupted flows. Stratification was characterized with a stratification coefficient,

$$St = \sum_i m_i (T_i - T_{avg})^2 / M_{total}$$

and an extraction efficiency,

$$COEF = (T_{output} - T_{makeup})/(T_{avg} - T_{makeup}).$$

Using the stratification coefficient, St, the data were correlated with inlet flow Reynolds number and pseudo Grashof number based on the tank diameter to yield formulas to predict the occurence and degree of thermal stratification for the storage tank.

Based on the stratification coefficient, St, three stratification regimes were identified:

For $St > 5$, the tank is stratified.

For $1 < St < 5$, the tank is in a transitional condition.

For $St < 1$, the tank is fully mixed.

TABLE OF CONTENTS

		Page
Acknowledgement		iv
Abstract		v
Table of Contents		vi
List of Symbols		viii
List of Figures		x
List of Tables		xiii
Chapter 1	Introduction	1
Chapter 2	Experimental Apparatus	8
2.1	Tank	8
2.2	Solar Simulation	8
2.3	Load Simulation	11
Chapter 3	Instrumentation	12
3.1	Data Logger	12
3.2	Temperature Measurement	13
3.3	Thermocouple Probe	14
3.4	Flow Rate	16
Chapter 4	Experimental Procedure	23
4.1	Introduction	23
4.2	Procedure	26
Chapter 5	Preliminary Results and Analysis	30
5.1	Temperature Profiles	30
5.2	Storage Efficiency	36
Chapter 6	Results for Continuous Load Flow	43
6.1	Inlet and Outlet on the Same Side, Continuous Load	43
6.2	Inlet and Outlet on the Opposite sides, Continuous Load	54
6.3	Discussion	65
6.4	Correlation of Data for Continuous Flow	74
Chapter 7	Results for Periodic Flow	80
Chapter 8	Conclusions	108
References		111

Page

Appendix A	An Estimate of Thermal Losses from the "Thermal Flow Meter"	112
Appendix B	Tabulated Data	116
Appendix C	Additional Results for Temperature Distributions in the Tank at Specific Times	144

LIST OF SYMBOLS

COEF	Differential (instantaneous) energy extraction efficiency (Eqn. (1.2))
c_p	Specific heat of water at constant pressure
d	Pipe diameter
D	Tank diameter
g	Acceleration due to gravity
Gr	Grashof number (Eqn. (6.1))
L	Vertical distance between inlet and outlet of tank
$\dot{m}$	Mass flow rate of water, load
m_i	Water mass in section i
M_{total}	Mass of water in entire tank
Pe	Peclet number (eqn. (5.7))
Q_{loss}	Energy lost from tank
Re	Reynolds number (Eqn. (5.7))
Ri	Richardson number (Eqn. (5.6))
St	Stratification coefficient (Eqn. 1.1))
t	Time
T_{avg}	Average temperature of the water in the tank
T_e	Exit water temperature, load
T_i	Temperature of water in section i
T_{in}	Temperature of inlet water
T_{makeup}	Make-up water temperature
T_o	Initial temperature
T_{output}	Output water temperature
u_{io}	Average inlet velocity
U_{tank}	Energy remaining in the tank after a time t (Eqn. (5.2))

β	Volumetric expansivity of water
ν	Kinematic viscosity of water
η	Extraction efficiency defined by Lavan (Eqn. (5.2))
η_1	Energy extraction efficiency defined by Young (Eqn. (5.1))

LIST OF FIGURES

Figure	Title	Page
2.1	Schematic of the Simulated Solar Thermosyphon System	9
2.2	The Tank Dimensions	10
3.1a	The Streamline Contour for the Thermocouple Probe	15
3.1b	The Profile of the Thermocouple Probe	15
3.2	The Thermocouple Positions in the Tank	17
3.3	Schematic Diagram of the Thermal Flowmeter	19
3.4	The Calibration Curve for the Thermal Flowmeter	21
4.1	The Thirty Portions of the Tank	26
5.1	Temperature Profile for Section A and Six Positions	31
5.2	Temperature Profile for Section C and Six Positions	32
5.3	Temperature Profile for Section F and Six Positions	33
5.4	Temperature Profiles for Five Axial Sections and Six Positions	34
5.5	Correlations of Extraction Efficiency Data	40
5.6	Degree of Stratification as Function of Richardson and Peclet Numbers	42
6.1	Stratification Coefficient History for Same-Side Configuration, Continuous Output	44
6.2	Extraction Efficiency History for Same-Side Configuration, Continuous Output	45
6.3	Vertical Temperature History at Middle Probe for Continuous Output	48
6.4	Vertical Temperature History at Middle Probe for Continuous Output	49

Figure	Title	Page

6.5 Vertical Temperature History at Middle Probe for Continuous Output....50

6.6 Stratification Coefficient History for Opposite-Side Configuration, Continuous Output....55

6.7 Extraction Efficiency History for Opposite-Side Configuration, Continuous Flow....56

6.8 Vertical Temperature History at Middle Probe for Continuous Output....58

6.9 Vertical Temperature History at Middle Probe for Continuous Output....59

6.10 Vertical Temperature History at Middle Probe for Continuous Output....60

6.11 A Comparison Between the Data for the Two Different Configurations....62

6.12 A Comparison Bewteen the Data for the Two Different Configurations....63

6.13 A Comparison Between the Data for the Two Different Configurations....64

6.14 The Temperature Distribution in the Tank....66

6.15 The Temperation Distribution in the Tank....67

6.16 The Temperature Distribuiton in the Tank....68

6.17 The Temperature Distribution in the Tank....69

6.18 The Temperature Distribution in the Tank....70

6.19 The Temperature Distribution in the Tank....71

6.20 Correlation of Stratification Coefficient, St, Data for the Opposite-Side Configuration, Continuous Flow..76

6.21 Correlation of Stratification Coeffieient, St, Data for the Same-Side Configuration, Continuous Flow....77

7.1 Stratification Coefficient History for Periodic Output....81

7.2 Stratification Coefficient History for Periodic Output....82

Figure	Title	Page

7.3 Extraction Efficiency History for Periodic Output.....83

7.4 Extraction Efficiency History for Periodic Output.....84

7.5 Correlation of Stratification Coefficient, St, Data for Same-Side Configuration, Continuous and Periodic Output.....86

7.6 Correlation of Stratification Coefficient, St, Data for Opposite-Side Configuration, Continuous and Periodic Output.....87

7.7 A Comparison Between the Data for the Two Different Configurations.....88

7.8 A Comparison Between the Data for the Two Different Configurations.....89

7.9 A Comparison Between the Data for the Two Different Configurations.....90

7.10 The Temperature Distribution in the Tank.....92

7.11 The Temperature Distribution in the Tank.....93

7.12 The Temperature Distribution in the Tank.....94

7.13 The Temperature Distribution in the Tank.....95

7.14 The Temperature Distribution in the Tank.....96

7.15 The Temperature Distribution in the Tank.....97

7.16 The Temperature Distribution in the Tank.....98

7.17 The Temperature Distribution in the Tank.....99

7.18 The Temperature Distribution in the Tank.....101

7.19 The Temperature Distribution in the Tank.....102

7.20 The Temperature Distribution in the Tank.....103

7.21 The Temperature Distribution in the Tank.....104

7.22 The Temperature Distribution in the Tank.....105

7.23 The Temperature Distribution in the Tank.....106

LIST OF TABLES

Table	Title	Page
4.1	Experimental Program	29

CHAPTER 1

INTRODUCTION

Heating water with the sun is one of the oldest applications of solar energy. There are basically three methods to accomplish the heating: 1) a batch process, 2) a force circulation process and 3) a thermosyphon process.

In the batch method a fixed amount of water is exposed to the sun until the desired temperature is achieved. This is by far the simplest and cheapest method to heat water. However, the process is slow and usually limited to temperatures considerably below those attainable with the other processes.

For domestic hot water production the forced circulation system utilizing a flat plate collector is usually used in climates in which freezing is common. The pump is controlled both by the demands of the system and the availability of sunlight. To protect against freeze damage in the collector, drain down or drain back techniques are utilized as well as anti-freeze chemicals which then require that a heat exchanger be incorporated into the system. The pump, the controls, the other additional equipment and the electrical power to operate them, all contribute to the additional cost of the forced circulation system over that required for a basic thermosyphon system.

The thermosyphon system takes advantage of the natural circulation that develops as a result of the decrease in the density of water as it is heated. A storage tank is located above the collector. As the water in the collector is heated, it rises through the collector and exits at the top. It continues to rise through the piping network and is introduced into the top of the storage tank. Cooler water is displaced from the tank and directed to the bottom of the collector. A natural circulation develops. The flow rate is proportional to the amount of solar irradiation. The actual flow rate varies from system to system and depends, of course, on the flow restrictions and the hydrostatic head in the system. In most systems, however, the temperature difference across the collector (and between the top and the bottom of the storage tank) stabilizes at about 6 to 10°C.

The efficiency of the collector (the fraction of the available solar energy that is actually transferred to the water) depends strongly on the design of the collector. For a given collector, the primary dependence is on the operating temperature or the inlet temperature since the temperature increase in the collector is fairly constant. Therefore, it is desirable to keep the collector inlet water temperature as low as possible. Under no load conditions (that is, when hot water is not being drawn from the storage tank) the water circulates in a closed system, and the inlet water temperature can be minimized only by maintaining maximum thermal stratifi-

cation in the storage tank. The degree of stratification is, of course, limited by the temperature rise across the collector. This stratification occurs naturally in the closed loop system. The problems develop when hot water is drawn from the top of the storage tank, and cold make-up water replaces it at the bottom of the tank. The induced flow in the tank due to this process disrupts the natural stratification. Diffusers and baffles have been used to dissipate this adverse effect.

Several studies have appeared in the literature which have investigated the thermal stratification in storage tanks in solar water heating systems [1,2,3,4].* However, until recently all have considered only "vertical" tanks, that is, cylindrical tanks where the length is several times greater than the diameter and oriented with the long axis vertical. This orientation helps to maintain the stratification by increasing the distance between the top and the bottom of the tank. Unfortunately, practical installation considerations, like wind loading and the concentrated structural load, have resulted in a trend toward "horizontal" tanks where the tanks are laid on their sides, greatly reducing the vertical depth of the tank. While aesthetically more pleasing and structurally more sound, the thermal stratification is more difficult to maintain.

Young and Baughn [5] and Firl, Schmitt and Young [6] have recently investigated the thermal behavior of a horizon-

---

*Numbers in []'s refer to references listed at the end.

tal storage tank. They claimed that the axial temperature gradients were negligible compared to vertical temperature gradients. Consequently, they utilized a one-dimensional model to simulate the tank's performance. For these horizontal tanks it can be a good approximation. However, significant vertical mixing between the top and bottom of the tank was observed in their study for loads greater than 19 liters (about 5 gal or 10% of the total tank volume) at withdrawal rates of above 11 liters/min (about 3 gpm). In some cases a significant axial temperature gradient developed during the withdrawal. Young et al. utilized a convection-conduction model with some degree of mixing at the boundaries to compare with their experimental results. The top tank temperatures were predicted fairly well, whereas the bottom tank temperatures deviated from the numerical predictions. The discrepancies between theory and experiment indicated that some interior mixing occurred. This mixing was probably responsible for reducing the otherwise large temperature stratification that was predicted by their model.

The objective of the current study is to investigate experimentally the thermal stratification in a water storage tank similar to those currently in use in thermosyphon solar water heating systems. In the experiment the water is heated in a thermosyphon loop with an electric heater simulating the solar input. The load (hot water withdrawal) is imposed by draining hot water from the top of the tank and replacing it

with tap water at the bottom.

The laboratory system is instrumented with seventy thermocouples. A typical "run" takes a day. The system is first stabilized to keep the tank at a constant uniform temperature (19.7 ± 0.4°C). Then the heater is activated, inducing a buoyancy driven flow through the tank. A stable stratification is established. On different runs various load profiles and load flow rates are imposed on the system. The resulting thermal effects are monitored with the thermocouples. The temperature distributions as a function of "percent output volume of the tank" are used to determine the flow pattern and how the stratification is effected by the various system operating parameters.

"Stratification" has not previously been satisfactorily characterized by a single parameter. Such quantities as maximum temperature difference do not reflect the temperature distribution. Without a satisfactory characterization it is not possible to fully investigate the effect that the system parameters have on the stratification. Because of the large number of temperatures measured in the current project it was possible to evaluate a stratification coefficient St:

$$St = \sum_i [m_i (T_i - T_{avg})^2] / M_{total} \qquad (1.1)$$

Where i runs over all the "elements" of the water that taken together represent all the water in the tank.

The stratification coefficient is the mass weighted sum

of the squares of the deviations of temperature T_i' (the local temperature measured for each mass, m_i) from the mean temperature, T_{avg}. It indicates the square of average deviation of temperature from the mean -- the higher St, the better the stratification. As St approaches zero, the tank approaches a uniform temperature. Hence the magnitude of St will be used to indicate the degree of thermal stratification in the tank. This parameter allowed the "status of the stratification" to be evaluated at any given time.

A differential (instantaneous) energy extraction efficiency, COEF, was also defined:

$$COEF = (T_{output} - T_{makeup})/(T_{avg} - T_{makeup}) \qquad (1.2)$$

and used to study the effect on stratification. It is a dimensionless output temperature indicating the output performance. It represents an indirect and less precise measure of stratification. However, it is more easily obtained and is commonly used. Since the make-up water temperature is essentially constant, this parameter is really a measure of the load supply temperature or the temperature at the top of the tank.

The effects on the stratification and on the storage function as characterized by the two parameters defined above were studied as a function of two different tank plumbing configurations, eight different load flow rates and different temperature levels. The results were then presented as a function of an inlet Reynolds number based on inlet pipe diameter and a pseudo Grashof number based on tank diameter.

As a result of this work, it is hoped that a better understanding of the process involved will be developed and that eventually this understanding will lead to more effective system design and operating procedures.

CHAPTER 2
EXPERIMENTAL APPARATUS

All the experimental measurements reported were taken from a simulated solar thermosyphon system constructed in the laboratory. A schematic of the system is presented in Fig. 2.1.

2.1 Tank

The storage tank was cylindrical, 103 cm in length and 57 cm in diameter. The tank, containing 264 liters water, was insulated with 9 cm of fiberglass batt.

The tank inlets and outlets were constructed of 3/4-inch, schedule 40 galvanized pipe, and their positions are shown in Fig. 2.2. Two different tank plumbing configurations were established by connecting individually to either outlet A or B. (Fig. 2.1)

Six nipples were welded in place along the top of the tank to allow access for measuring the temperature distribution and water level, and insulated with 1.9 cm of foam plastic.

2.2 Solar Simulation

An electrically heated riser was used to simulate a steady solar input in place of a collector. The steady 1.02 kW input power supplied to the electric heater was controlled by a variable autotransformer, and monitored by a digital multimeter (accuracy ± 1.0% of reading) and an iron-vane ammeter (accuracy ±2.0% of full scale).

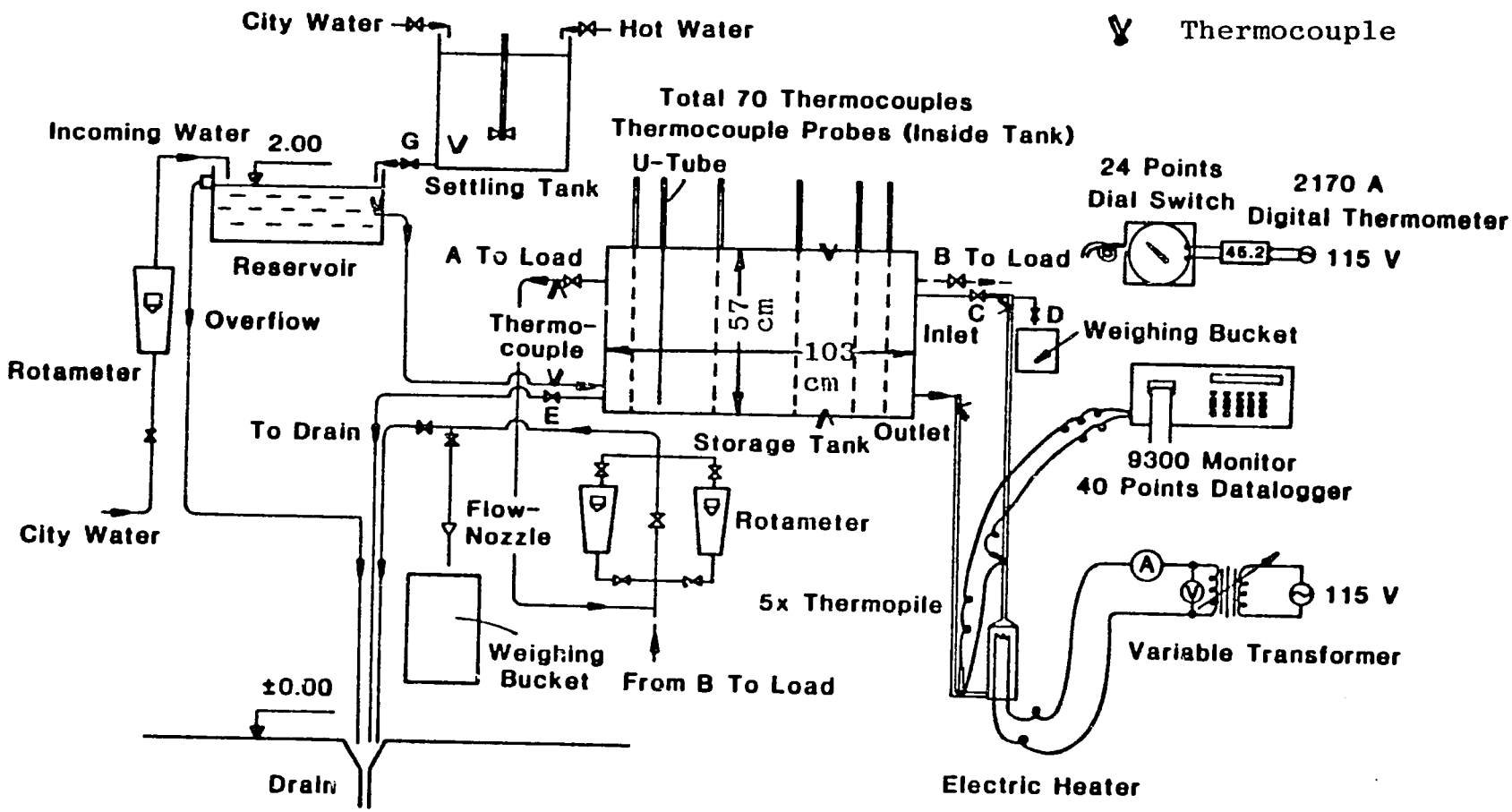

Fig. 2.1: Schematic Diagram of The Simulated Solar Thermosyphon System

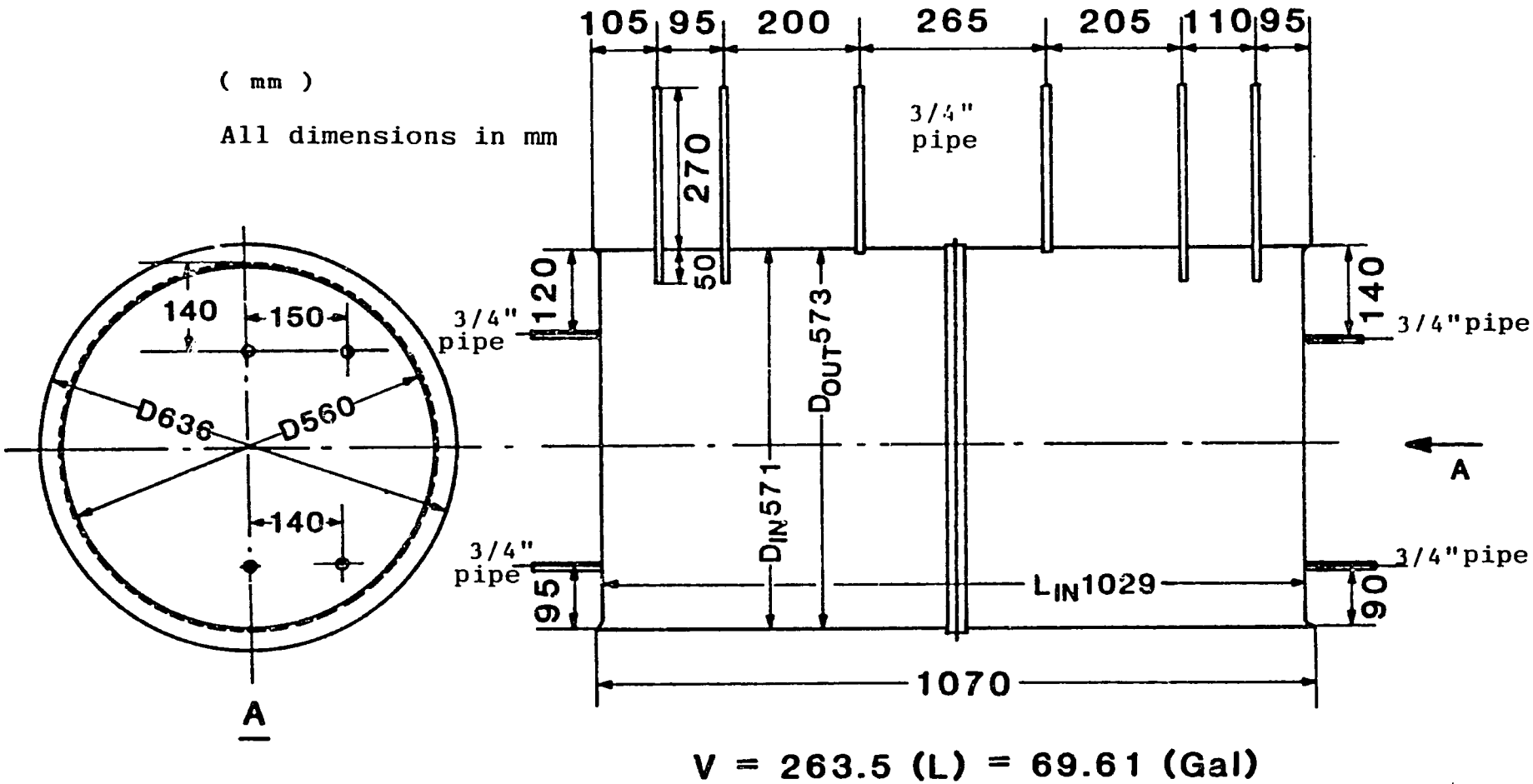

Fig. 2.2: The Tank Dimensions

The connection between the tank and the riser was made with one-inch schedule 40 galvanized pipe and was insulated with 1.7 cm of foam plastic

2.3 Load Simulation

Hot water was withdrawn from the tank through take-off port A or B. The water passed through a gate valve, a rotameter (or a flow nozzle), and an offset to a weighing bucket which was used to remove prescribed loads (to simulate a user removing hot water). All the above connecting pipe were 3/4-inch schedule 40 galvanized pipe and was not insulated.

A reservoir with an overflow outlet provided a constant system pressurization to insure the load flow rate stability. A settling tank provided a constant, prescribed temperature for the make-up water.

CHAPTER 3
INSTRUMENTATION

The primary measurements were made to determine the temperature distribution within the water storage tank. However, temperatures were also recorded in other parts of the system. Flow rates and heating rates were also determined in various parts of the system. The instrumentation used to make and record these measurements is discussed below.

3.1 Data Logger

Simultaneous acquisition of large quantities of data can be accomplished accurately and reliably by using an automated data logging system. A forty channel, multipurpose data logger (Monitor Labs-9300) was used in this experiment. The Monitor Labs-9300 is an interactive, programmable data logger that is capable of rapidly scanning forty signals sequentially. Results can be recorded on printed paper and/or stored on a cassette tape.

With the ten channel input connector and copper-constantan thermocouples, the accuracy is 0.28°C at standard speed and in the range from room temperature to 400°C. The accuracy includes NBS conformity error of 0.05°C, digitizer error, relay offsets and reference junction error. The accuracy does not include sensor or sensor-induced errors.

Each ten input channels has a common compensator.

Therefore, four compensators were used to obtain forty channels, but each compensator's reference voltage was not exactly the same. Each compensator must be calibrated separately. Using the corrective coefficient of -0.045, -0.064, -0.009 and 0.009, the deviation was less than ±0.1°C. Including this deviation, the accuracy for the ML-9300 becomes:

$$\sqrt{0.28^2 + 0.1^2} = 0.297 = \pm 0.3°C.$$

3.2 Temperature Measurement

Type T (copper-constantan) thermocouples made from special-limits-of-error wire (Omega cat no. TT-T-30) were used for all of the temperature measurements. The special-limits-of-error wire ensured the accuracy of the thermocouples to ±0.42°C in the range of -70 to 90°C. All thermocouples were fabricated with a thermocouple welder in the laboratory.

Both the thermocouples and ML-9300 together were calibrated with a mercury thermometer (division: 0.1°C, accuracy: 0.3°C, and range: 0 to 50°C). The results showed that in the range 0° to 50°C, the difference of the readings between the ML-9300 and the mercury thermometer were all within ±0.3°C, without exception. The accuracy of the temperature measurements was estimated as:

$$\sqrt{0.3^2 + 0.3^2} = \sqrt{0.18} = 0.43°C.$$

Since more than forty temperature measurements were

required, a 2170A-T digital thermometer and thermocouple switch were used for the additional readings. In the range 0 to 400°C, the maximum error (including reference junction and conformity errors, excluding thermocouple errors) was 0.4°C at calibration and 0.5°C after 20 min. to 24 hrs. With both the type T thermocouple and the 2170A-T thermometer, the accuracy of temperature measurement was estimated as:

$$\sqrt{0.5^2 + 0.3^2} = \pm 0.59°C$$

3.3 Thermocouple Probe

The temperature distribution in the tank was measured with specially constructed thermocouple probes. Each probe contained four to six thermocouples. The probe had to be rigid enough to maintain its position accurately but small enough to minimize the interference with the temperature and flow field in the tank. The resultant design has a streamline contour as illustrated in Fig. 3.1a. Its major and minor dimensions are 6.5mm and 3.2mm. Four to six 0.56 mm x 0.96 mm insulated copper-constantan thermocouples were passed through the probe tube and were wrapped around the probe at the prescribed height. Each thermocouple extends out about 3 mm from the probe. The probe is illustrated in Fig. 3.1b. Each thermocouple was calibrated prior to mounting in the probe tube.

A total of twelve probes were utilized. Five axial stations and up to four transverse stations were fitted with

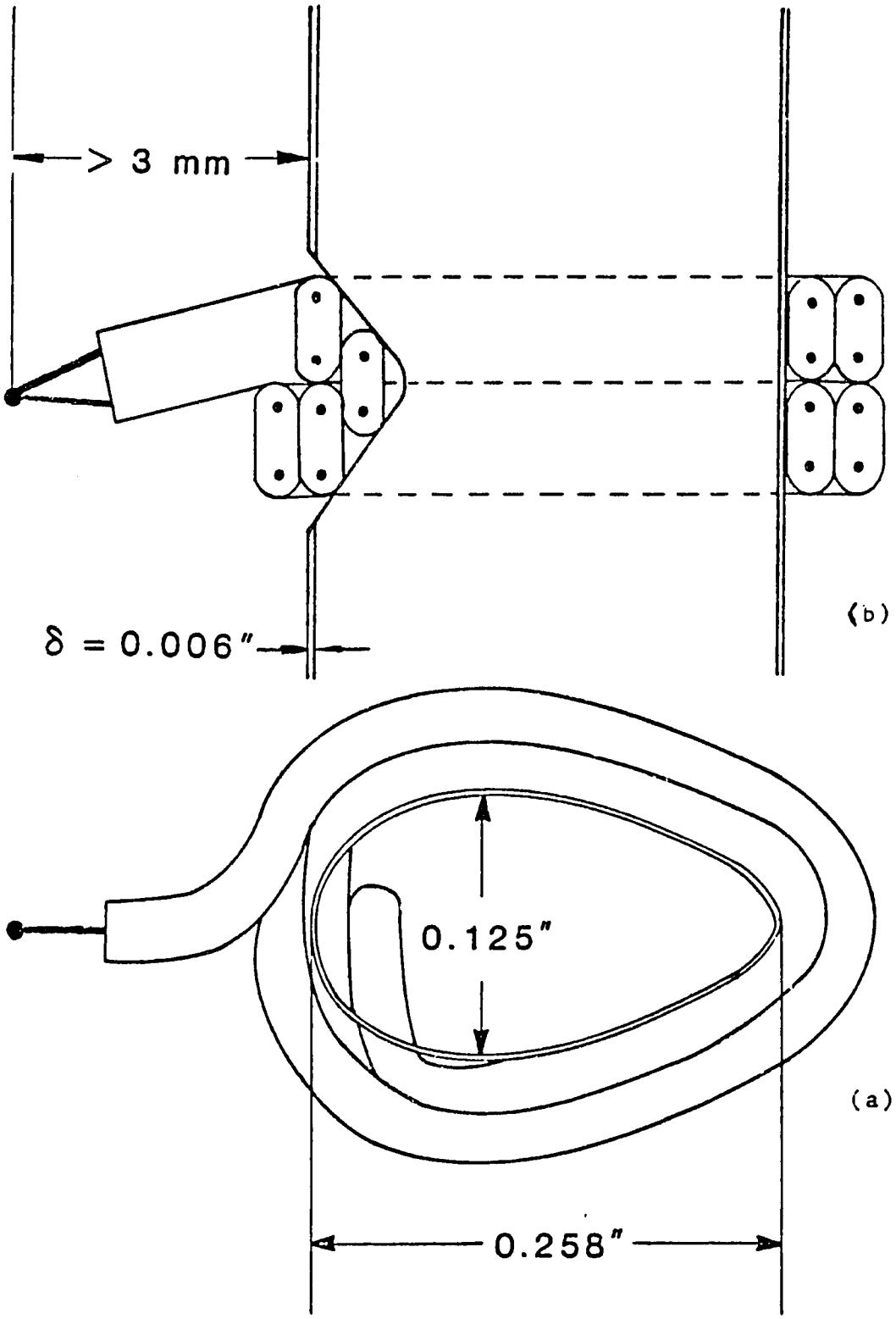

Fig. 3.1: (a) The Streamline Contour for The Thermocouple Probe

(b) The Profile of The Thermocouple Probe

probes as illustrated in Fig. 3.2. At each of the axial stations a six-thermocouple probe extended through the center line of the tank (thirty thermocouples). In addition, axial station A had a six- and a four-thermocouple probe (ten thermocouples) located outward 105mm and 210mm from the central probe and parallel to it. Axial station C had three additional probes (fourteen thermocouples). Axial station D had one additional probe (four thermocouples). Axial station F had two additional probes (ten thermocouples). These sixty-eight thermocouples are all shown in Fig 3.2.

3.4 Flow Rate

3.4.1 Load System (Simulated Use)

Two calibrated rotameters (range: 0 to 53 ml/s, and 0 to 98.4 ml/s) were arranged in parallel and used to monitor the five flow rates: 29.3, 38.2, 53.0, 98.4, 151.4 ml/s used in the study. The accuracies were ± 1.5% full scale.

Calibrated flow nozzles were used to monitor the other three flow rates: 221, 353, 442 ml/s. The hot water removed from the storage tank was directed to buckets, and the flow rate was checked by weighing. The results of the independent determinations were within ±2% of each other. The accuracy of the reported removal rates were estimated as about ±3%.

3.4.2 Collector Circulation Rate

"Collector" mass flow rate measurements were complicated by the relatively low velocities of the natural circulation system. A flowmeter placed in the flow with even a small

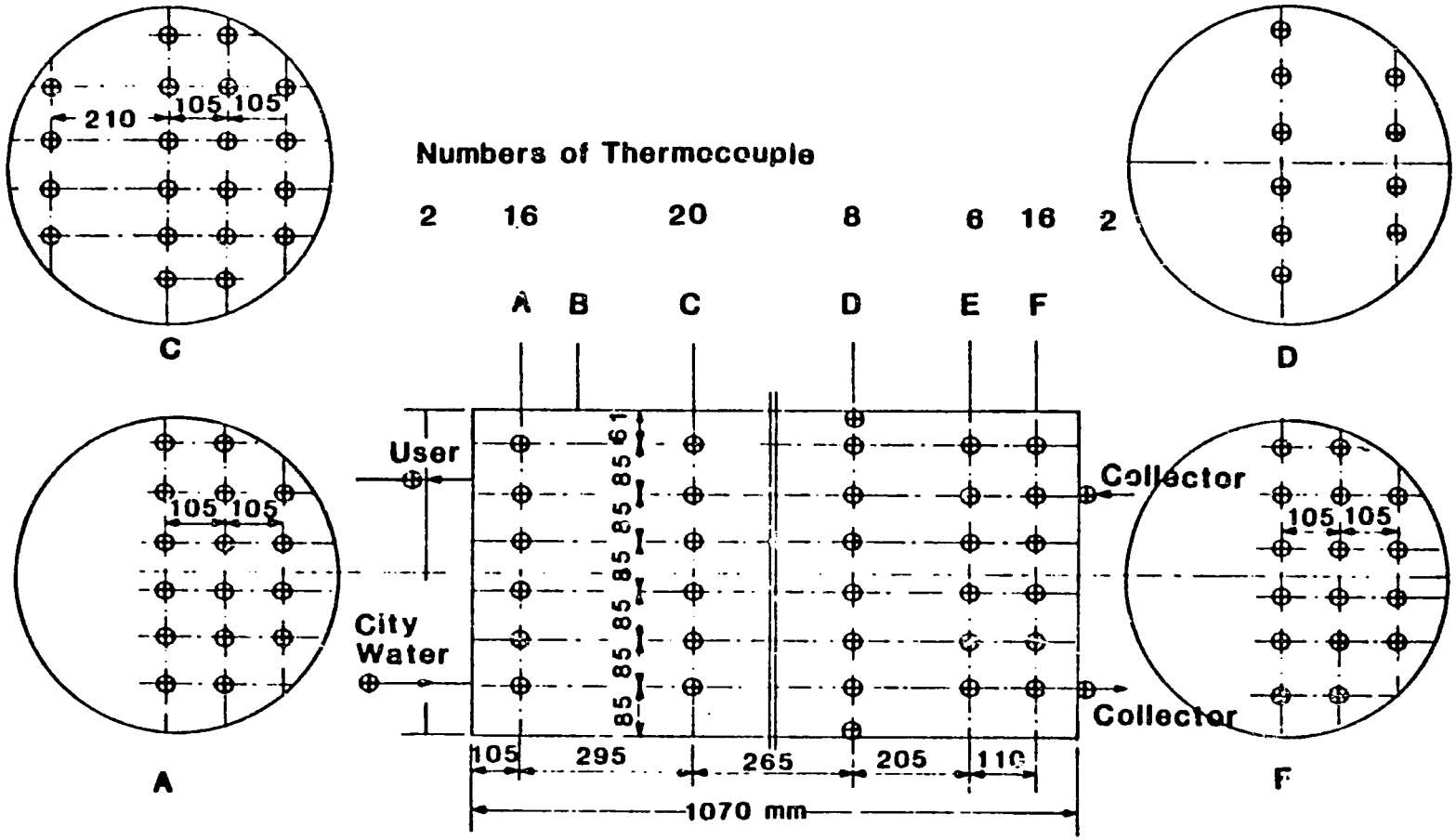

Fig. 3.2: The Thermocouple Positions in the Tank

flow restriction could drastically reduce the flow and change the hydrodynamic behavior of the system.

A laser doppler anemometer has been used by Morrison and Ranatunga [7] to measure collector mass flow rates. Accuracies of two percent were reported in that work. Although a laser anemometer does not introduce any restrictions in the flow field, it is expensive and extremely complex.

Young and Bergquam [1] used an energy balance on the storage tank to calculate the collector mass flow rate. This method is of course limited to steady state conditions since it is really an averaging technique. It also depends on the use of a large number of temperature measurements.

In the current study, a "thermal flowmeter" was developed and utilized to measure the "collector" loop circulation rate. The "thermal flowmeter" was based on a careful energy balance in which the temperature rise in the fluid is measured for a known energy input (electric heater). With the fluid heat capacity known, its flow rate can be determined. The input electrical power was controlled to be a constant (about 1020 W) by a variable autotransformer and a digital multimeter (accuracy ± 1.0%). The "thermal flowmeter" is illustrated in Fig. 3.3.

In Appendix A the thermal losses (the energy that the heat dissipates that does not end up in the fluid) for the meter are estimated to be less than 2W or 0.2%.

The calibration of the "thermal flowmeter" was performed by blocking the return pipe to the tank and bleeding

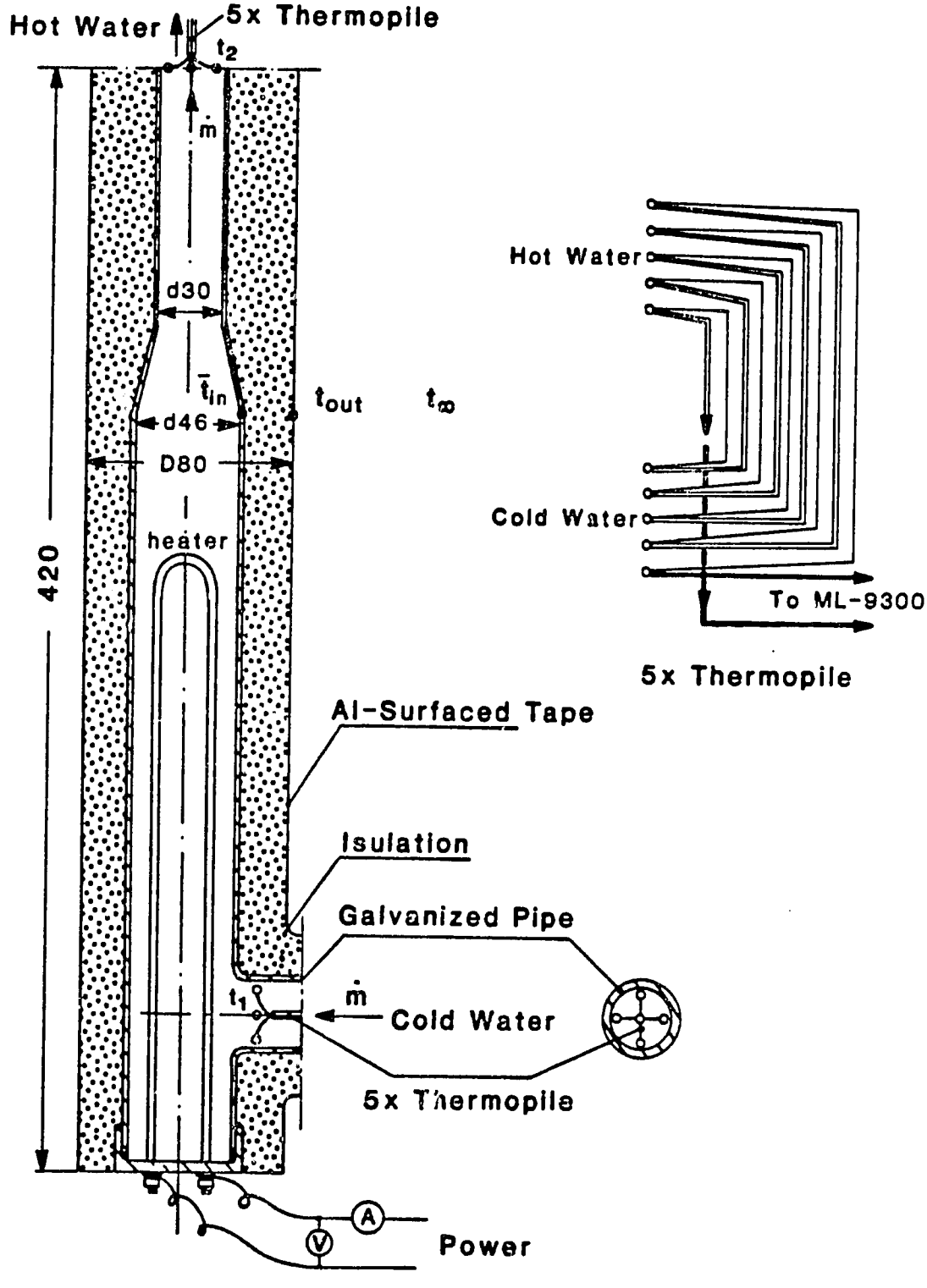

Fig. 3.3: Schematic Diagram of The Thermal Flowmeter

flow from the top of the heater (by opening valve D and closing valve C in Fig. 2.1). The flow rate, $\dot{m}$, was measured directly by collecting the flow from the heater and then weighing it with a balance (accuracy ±2g). The temperature difference between outlet and inlet, $(T_{out} - T_{in})$, was measured with a 5x thermopile and recorded with the data logger ML-9300. Figure 3.4 is the plot of measured flow rate against the thermal emf and is the required calibration curve. In operation the simple thermal emf measurement determines the mass flow rate.

Some fluctuations of the temperature difference between outlet and inlet were observed. The average values of the temperature differences during the interval of testing were used.

Based on the accuracy of the thermocouple, the data logger ML-9300 and the weighing method, the accuracy of the "thermal flowmeter" was estimated as follows:

For the thermocouple and ML-9300:

$$\sqrt{5 \times 0.417^2 + 0.3^2} = \pm 0.9795°C$$

The reading of ML-9300 was about 5x12 = 60°C.

Then 0.98/60 = 1.63%

For weighing:

The error of the time measurement was less than ±1.0 second, and the reading of the stop watch was 120 seconds. The accuracy of the time measurement was better than 1.0/120 = ±0.83%.

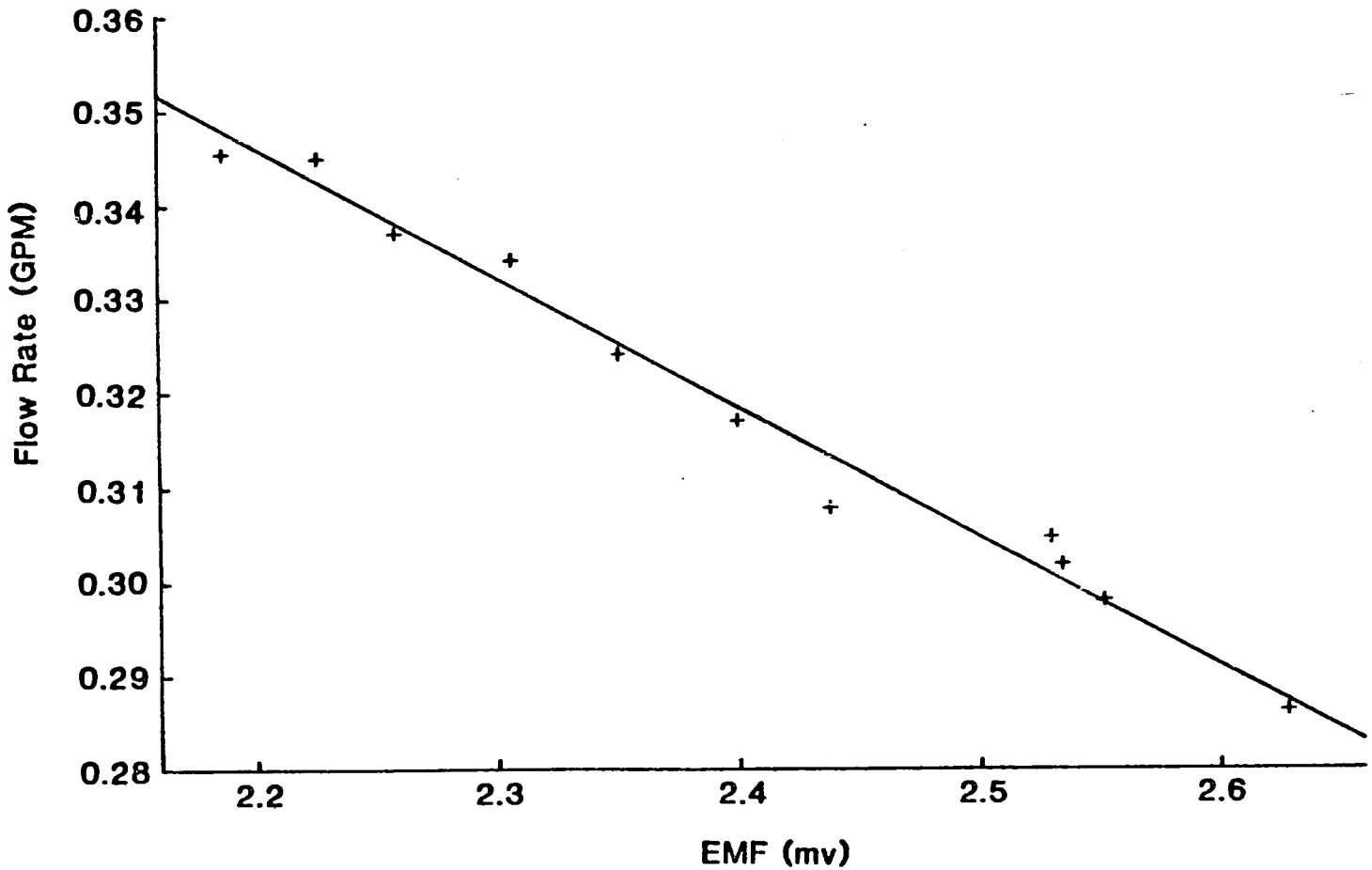

Fig. 3.4: The Calibration Curve for the Thermal Flowmeter

The error in weighing was less than 2 grams. The accuracy in weighing for the 2000 gram balance was better than

$$2/2000 = \pm 0.1\%.$$

The accuracy of weighing was estimated as:

$$\sqrt{0.83^2 + 0.1^2} = \pm 0.84\%.$$

The accuracy of the thermopile, ML-9300, and weighing was estimated as:

$$\sqrt{0.84^2 + 1.63^2} = \pm 1.84\%$$

With consideration of the fluctuation of input power, the temperature difference, and average error, the accuracy of the "thermal flowmeter" was estimated as ±3%.

CHAPTER 4

EXPERIMENTAL PROCEDURE

4.1 Introduction

Thermosyphon solar domestic hot water systems typically have collector flow rates that vary between 14 and 32 ml/s (0.22 and 0.51 gpm) [6]. These flow rates vary throughout the day with insolation and with the hot water use pattern. The experimental results reported here, however, were obtained using a constant electrical energy input of 1.02KW, and a steady flow rate of about 18.9 ml/s (0.3 gpm). The temperature increase across the electrical heater was about 12°C. The hot water inlet Reynolds number was about 1540 (based on inlet pipe diameter).

Solar domestic hot water systems are sometimes operated with severe hot water use patterns; for example, 38-76 liters (10-20 gals) are removed in consecutive intervals. Examples include showers taken back to back, or dishwashers and washing machines operated simultaneously. For a typical solar domestic hot water system, 76 liters could constitute about 30% of the storage tank volume. Typical hot water use patterns are usually a combination of light and heavy loads. Since water use patterns vary widely, two kinds of extreme withdrawn patterns were used in this study: continuous load and half-hour periodic loads. Both patterns were utilized with six different output flow rates: 53.0, 98.4, 151.4, 221, 353 and 442 ml/s (0.84, 1.56, 2.44, 3.5, 5.4, and 7.0 gpm). The con-

tinuous load was utilized with two additional output rates: 29.3, 38.2 ml/s (0.464, 0.605 gpm). For the periodic loads the same quantity of water (about 20% volume of the tank) was removed in each half-hour period. Since the volume withdrawn for each cycle was kept nearly constant, as the flow rate increased, the duration of the flow within the half-hour period was reduced. For example, if 60 liters were withdrawn each half-hour, it would correspond to a 100 ml/s flow for ten minutes followed by twenty minutes of no flow, or a 500 ml/s flow for two minutes followed by twenty-eight minutes of no flow.

The volume of the tank was subdivided (mathematically) into 30 portions as illustrated in Fig. 4.1, so that each thermocouple was alloted an appropriate portion of the volume. As described later, an energy balance was made on the tank to determine an average tank temperature in which it was assumed that the temperature indicated by the thermocouple for the associated volume was uniform throughout that volume. For a given time interval the change in the energy content in the tank was proportional to the change in the average temperature of the water in the tank.

$$\Delta T_{avg} = T_{avg} - T_{makeup} = \sum_{i=1}^{30} (T_i - T_{makeup}) \times V_i/V$$

$$= \sum_{j=1}^{5} \sum_{k=1}^{6} (T_{jk} - T_{makeup}) \times S_k/S \times L_j/L \qquad (4.1)$$

FORMULA: $a = \sqrt{2h\gamma - h^2}$

$$\Delta S = \frac{4\pi \arctan(h/a)}{360}\gamma^2 - a\sqrt{\gamma^2 - a^2}$$

Using These Formulas, Find ΔS_1 And ΔS_6 First, And Then Others.

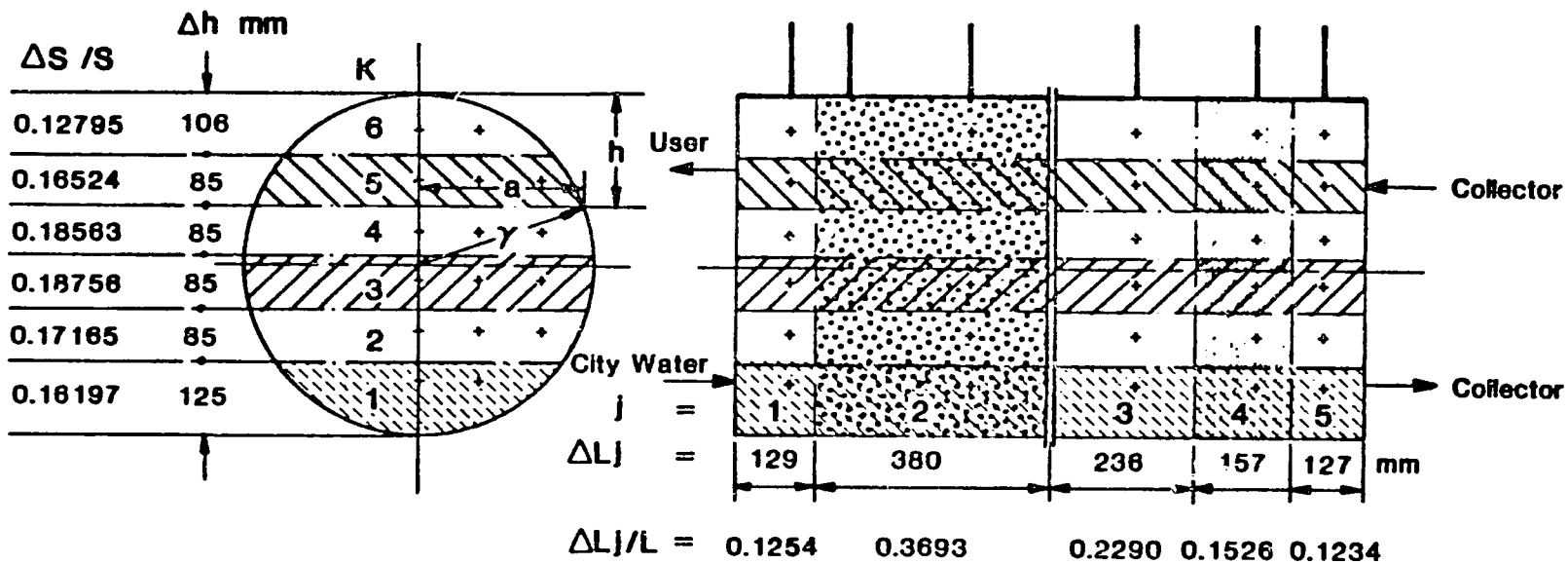

Fig. 4.1: The Thirty Portions of The Tank

where:

T_{avg} = average temperature in the storage tank, °C.

L = the length of the storage tank, m.

L_j = the length of the portion of the tank associated with axial element j,m.

S = the cross section area of the storage tank, m^2.

S_k = the cross sectional area of the portion of the tank associated with section k, m^2.

V = the volume of the storage tank, m^3.

V_i = the volume of the portion of the tank associated with element i,m^3.

4.2 Procedure

The experimental procedure was as follows:

1. The outlet valve E (see Fig. 2.1) was opened so that the tank was flushed with a large flow (about 0.5 liters per second) of cold water (city water) for about one-half hour. The jet momentum of the city water pressure was utilized for mixing the water in the tank

2. As each temperature reading of the water in the tank came into the range of 19.7±0.4°C (the average water temperature T_{avg} should be in the range 19.7±0.3°C), valve E was closed. The electrical heater in the simulated solar collector loop was turned on. This simulated the no load heating of the tank water and

and established the stratification. The electric power input was controlled by controlling voltage at 102±0.4V with a variable autotransformer and a digital multimeter TRIPLETT 3500 during the entire procedure.

3. The temperature of the water in the settling tank and the reservoir were maintained at the initial T_{avg} ±0.4°C during the entire procedure.
4. All instruments were checked and adjusted.
5. All data were recorded as the heating continued for three hours at which time the stratification was established.
6. The load flow rate was adjusted quickly to the prescribed load flow rate was maintained during the remainder of the procedure by the valves. All data were recorded.
7. For the periodic load flow rate, the flow rate was adjusted as described previously. All data were recorded at the end of each flow period and just before the start of each flow.
8. The storage continued to supply the load until either the total output volume exceeded twice the volume of the storage tank for the continuous load or exceeded 80% of the volume of the storage tank for the half-hour periodic loads (four periods or more).

A summary of the parameters in the experimental program is given in the Table 4.1. This procedure was the same in all experiments.

Configuration	Output Pattern and Load Magnitude	Output Flow Rate (ml/s)
Inlet and Output Ports on the Same Side	Continuous Output Until Total Load Volume Exceeded Twice the Volume of the Tank	29.3, 38.2, 53.0, 98.4 151, 221, 353, 442
	Half-hour Periodic Output, About 20% of the Tank Volume for Each Output and 4 or 5 Output Cycles	53.0, 98.4, 151,221, 353, 442
Inlet and Output Ports on the Same Side	Continuous Output Until Total Load Volume Exceeded Twice the Volume on the Tank	29.3, 38.2, 53.0, 98.4 151, 221, 353, 442
	Half-hour Periodic Output, About 29% of the Tank Volume for Each Output and 4 or 5 Output Cycles	53.0, 98.4, 151, 221, 353, 442

Table 4.1: Experimental Program

CHAPTER 5

PRELIMINARY RESULTS AND ANALYSIS

5.1 Temperature Profiles

Temperature is plotted as a function of time for the configuration with the inlet and outlet on the same side, for three transverse locations at three sections (Section A in Fig. 5.1, Section C in Fig. 5.2 and Section F in Fig 5.3), and for five axial locations (Fig. 5.4). The section locations are illustrated in Fig. 3.2.

These figures show that the temperature gradients in the axial and the transverse directions are small (The temperature difference usually is less than 0.5°C.) compared with the gradient in the vertical direction (The temperature differences are usually greater than 6°C.) except at position 6 of Sections A and F, and at position 5 of Section F. At position 6 of Sections A and F, a lower temperature was detected in the center of the tank. The cooler temperature regions were formed as the result of a pipe nipple attached to the tank wall that acted like a heat sink and caused a 0.5 to 1.5°C drop in temperature relative to the surrounding regions.

At position 5 of Section F, the temperature of the central region was first higher and then lower by 0.5 to 2.5°C than the temperature of surrounding regions. These temperature differences were due to the water returned from the

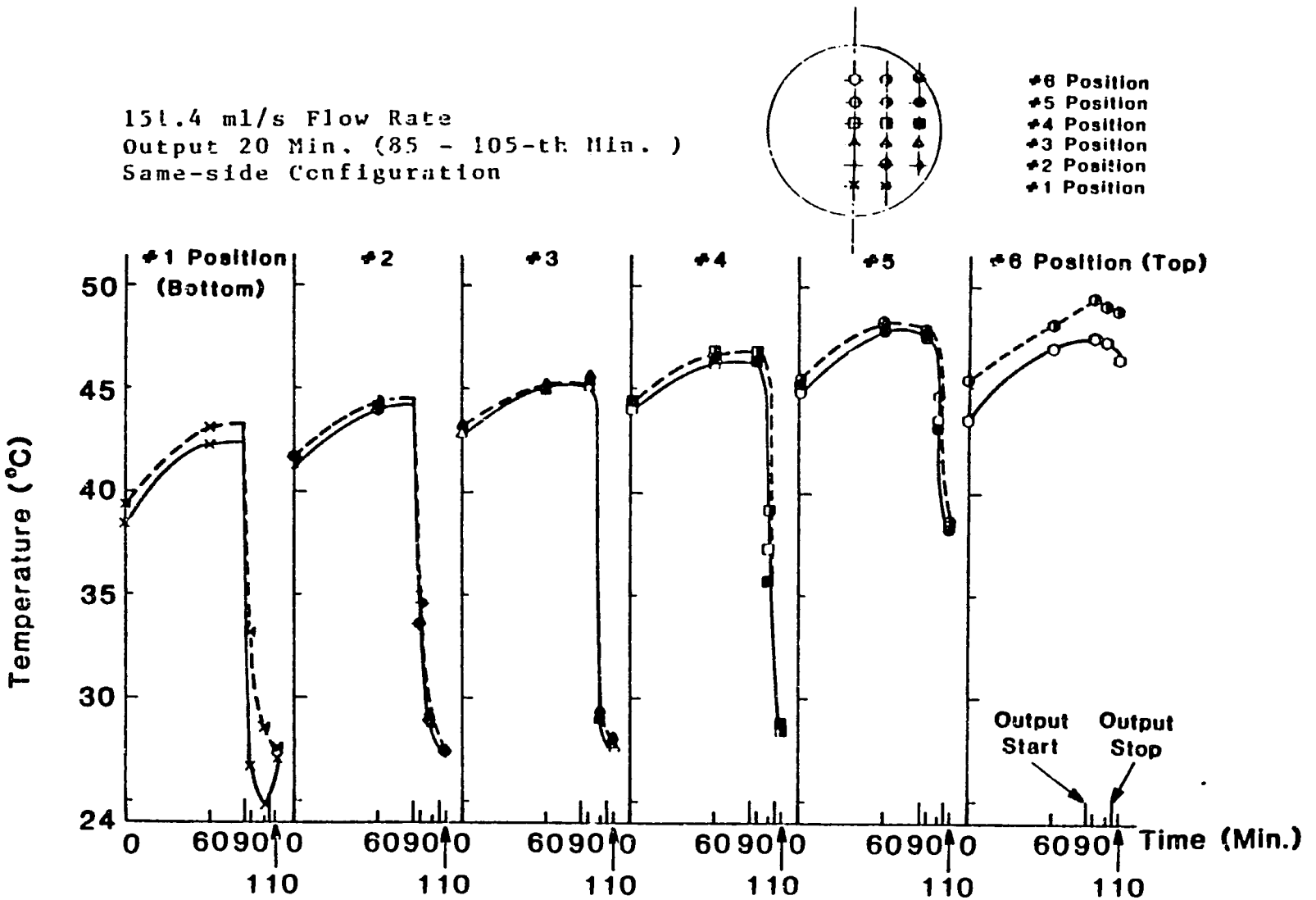

Fig. 5.1: Temperature Profile for Section A and Six Positions

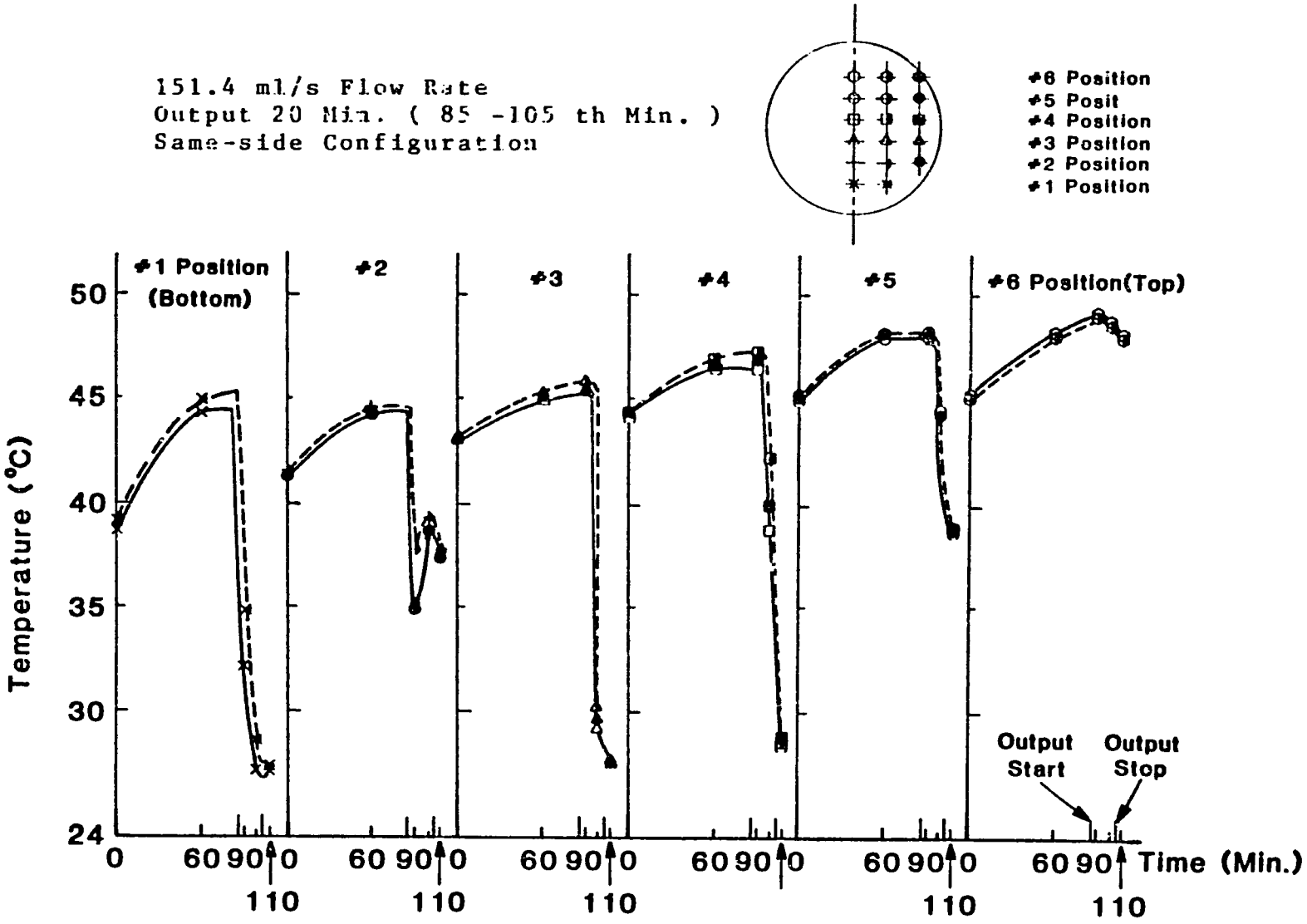

Fig. 5.2: Temperature Profile for C Section and Six Positions

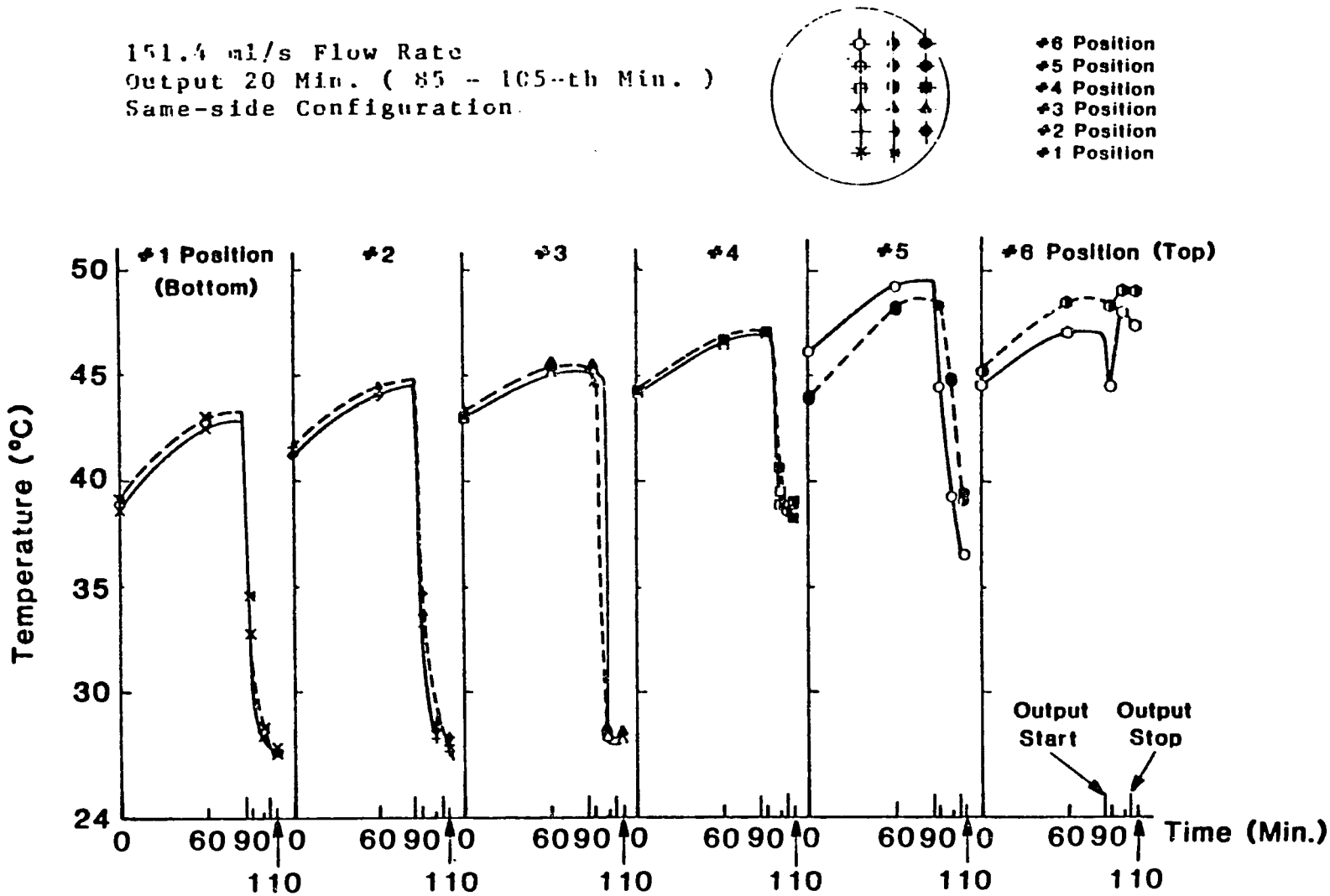

Fig. 5.3: Temperature Profile for F Section and Six Positions

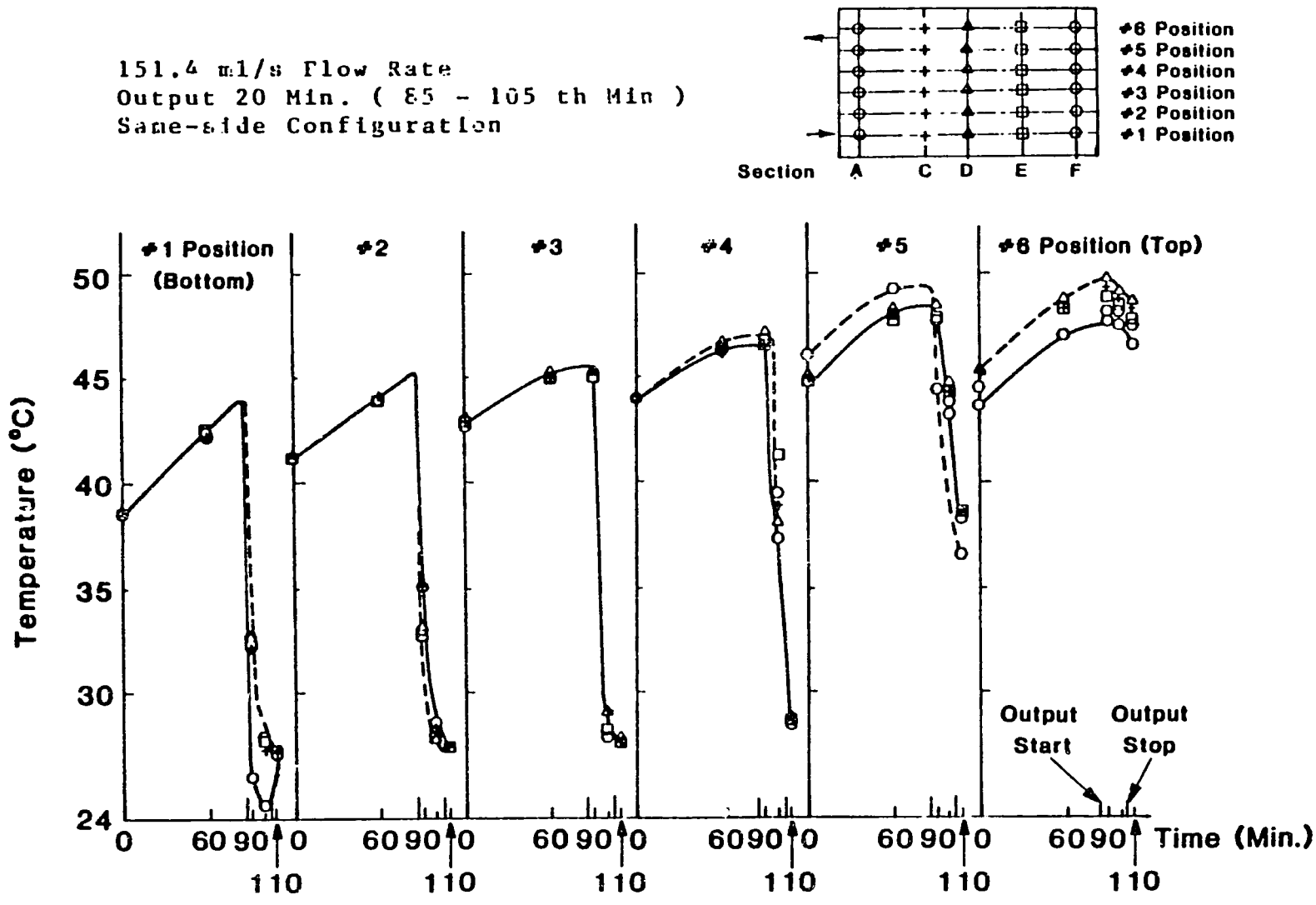

Fig. 5.4: Temperature Profile for Five Axial Sections and Six Positions

simulated collector. Initially, the collector return water was above the local water temperature by about 0.5 to 1.0 °C. Later, as the bottom of the tank was cooled by the make-up water, the collector with its fixed thermal input was not able to heat the water to as high a temperature. Therefore, the collector return actually began to cool the water in the top of the tank. The central temperature was lower than the surroundings by 1.0 to 2.5°C.

In the fully mixed condition, the minimum value of stratification coefficient, defined in Eqn (1.1), should be zero. In this experiment, the minimum measured value of St was 0.048 at a load flow rate of 7.0 gpm. If it is assumed that at every point the temperature in the tank was the same as the average value at that time, the estimated standard deviation of the measurement method and the instrument, s, (the positive square root of St):

$$s = \sqrt{St} = \sqrt{0.048} = 0.22°C$$

This quantity represents a measure of the preciseness of a sample of data.

As the load was being withdrawn, axial and transverse temperature variation increased showing the effects of the injection of cold water at the bottom and the withdrawal of the hot water at the top of the tank. The thermocouples opposite the make-up water inlet indicated that the temperature dropped about 2 to 5°C below the surroundings.

Due to practical considerations the number of thermocouples in the tank were limited to seventy. Even this

large number of thermocouples was not enough to allow a complete description of the temperature field. Symmetry about the vertical axial plane was assumed (and verified with a few measurements), and thermocouples were concentrated to one side of this plane.

5.2 Storage Efficiency

The ultimate objective of this and similar work reported in the literature is to develop a more efficient method for storing thermal energy derived from the solar thermosyphon system. Due to their widespread use and simplicity, cylindrical tanks, both vertical and horizontal have been examined extensively.

Results from different investigators are difficult to compare since each has his own idea as to what constitutes storage "efficiency". Despite these various efficiency definitions, it is really the "quality" of the stratification that ultimately determines the storage withdrawal efficiency.

Among the factors that could influence the thermal stratification in the storage tank are:

- the location of the inlet and outlet ports,
- the mass flow rate,
- the detailed geometry of inlet and outlet ports (diffusers),
- the size of the storage tank,
- the overall length to diameter ratio for the tank,
- the inlet and outlet temperatures and

the pattern of the energy draw.

This study has concentrated on the effects of mass flow rate and the energy draw pattern for two locations of the inlet and outlet ports.

The output temperature was first measured with a thermocouple inserted in the output pipe close to the tank. It was noted, however, that as output flow rate approached zero, the thermocouple indicated a temperature below that measured in the tank. This was due to the fact that the heat loss from the pipe was larger than from the tank. The temperature measured by the thermocouple in the proble inserted in the tank then was used for T_{out} instead of the temperature measured by the thermocouple inserted in the output pipe.

The stratification coefficient, St, and an instantaneous energy extraction efficiency, COEF, were defined in Eqns. (1.1) and (1.2). Results in this work have been reported in terms of these two parameters. However, other "efficiency" parameters have been suggested in the literature and they are reviewed below:

G.G. Firl, B.J. Schmitt, and M.F. Young defined an overall energy extraction efficiency, η_1, as: [6]

$$\eta_1 = m_1 c_p (T_1 - T_{makeup})/U_{tank} \tag{5.1}$$

where U_{tank} is the energy remaining in the tank after a time t, and is found from:

$$U_{tank} = \int_0^t (V^2/R)dt - m_1 c_p (T_1 - T_{makeup}) - Q_{loss} \tag{5.2}$$

where

V = voltage across heater

R = resistance of heater

T_1 = bulk temperature of hot water removed

m_1 = mass of water removed up to time t

This overall energy extraction efficiency is a measure of the energy removed from the tank as hot water relative to the total energy remaining in the tank. For a particular hot water use pattern this efficiency indicates the required energy input to the tank, and hence the collector area needed to satisfy the projected energy demand. However, the overall energy extraction efficiency cannot be utilized as a criterion for the stratification. It is meaningful only to compare its values for the same output flow rate and the same process because the numerator is evaluated instantaneously while the denominator is evaluated over an interval of time. This integrated effect will be different for different processes and geometries. Therefore, both the numerator and the denominator will be changing in a manner which will make it difficult to interpret results.

Zalman Lavan and James Thompson [2] reported work for a vertical tank and defined an extraction efficiency as

$$\eta = \dot{Q}t/V. \tag{5.3}$$

Here t is the time at which the current make-up inlet and load exit temperature difference has decreased ten percent from its initial value: i.e.:

$$(T_e - T_{in} / (T_o - T_i) = 0.9 \qquad (5.4)$$

where

$\dot{Q}$ = volume flow rate

V = tank volume

T_e = exit water temperature (load)

T_{in} = inlet water temperature (make-up)

T_o = initial temperature

Their basic testing sequence was to fill the tank with hot water at about 40.5°C and then to pump cold water into the bottom of the tank while draining hot water from the exit port at the top. By monitoring the inlet-exit temperature difference, the hot water extraction efficiency was evaluated.

They hypothesized that the tank length to diameter ratio, L/D, the inlet Reynolds number, Re_d, the Grashof number (based on the tank diameter), Gr_D and the difference between the inlet and output temperature would correlate the data for η. A least-square fit of all the data taken in ninety-six cases yielded the correlation shown in Fig. 5.5. The curve can be expressed mathematically as:

$$\eta = 1 - \exp [-0.067 \, Re_d^{-0.55} \, Gr_D^{0.35} \, (L/D)^{0.58}] \qquad (5.5)$$

This extraction efficiency does reveal some information about the tank's performance but does not address the stratification question directly.

B.J. Sliwinski, A.R. Mech, and T.S. Shih [3] char-

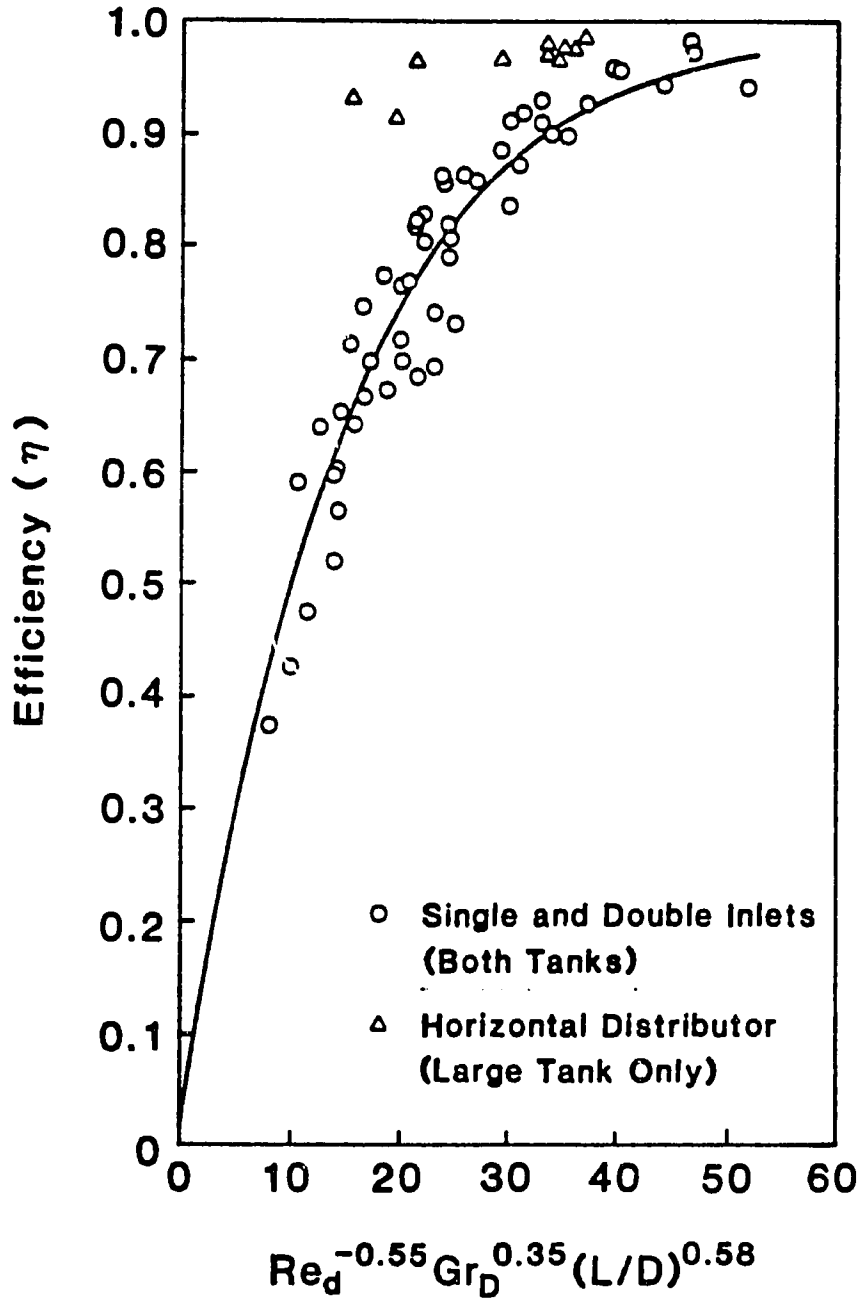

Fig. 5.5: Correlation of Extraction Efficiency Data

acterized the degree of stratification of the thermal storage tank by the magnitude of the temperature gradient in the "boundary region" or thermocline in the tank. From their graphs of temperature vs. depth, it can be observed that there is a region of nearly constant temperature gradient which moves down the tank as the tank is charged. This is the boundary region. This gradient was determined for a 300 liter tank. The tank initially contained uniform temperature water. It was charged by adding constant, higher temperature water at a constant flow rate to the top of the tank, while withdrawing water at the bottom.

The initial tank temperature, the difference between input and initial tank temperature, and flow rate were varied in the ranges 21 to 65°C, 5.6 to 27.8°C, and 0.76 to 4.5 liter/min, respectively. The magniture of the gradient was observed to be a function of both the modified Richardson number, Ri, and the inverse Peclet number, Pe:

$$Ri = g\,\beta\,\Delta T\,L/u_{io} \tag{5.6}$$

where

L = vertical distance between inlet and outlet

ΔT = average temperature difference between T_{in} and T_o

u_{io} = average inlet velocity

g = acceleration of gravity

β = volumetric expansivity

$$Pe = Re\ Pr \tag{5.7}$$

where

$Re = u_t D/\nu$

D = tank diameter, m

u_t = velocity of fluid in tank (ratio of volumetric flow rate to tank cross-sectional area), m/s

The relationship between the temperature gradient, the Richardson number and the inverse Peclet number is shown in Fig. 5.6. The correlation suggests a measure of stratification but cannot be used directly for a comparison between storage tanks used in solar systems.

In the work discussed above several parameters were introducted which attempted to characterize the degree of stratification. But these parameters are useful only for the particular system described. Neither the extraction efficiency nor the temperature gradient in the thermocline region was determined in the present experiment. The extraction efficiency is a measure of the average performance and does not contain any detailed information about the quality of the stratification. The thermocline temperature gradient method assumes a one-dimensional model, and the gradient itself is difficult to determine accurately. The stratification coefficient, St, previously defined in Egn. (1.1) more accurately accounts for the detailed two-dimensional effects of stratification.

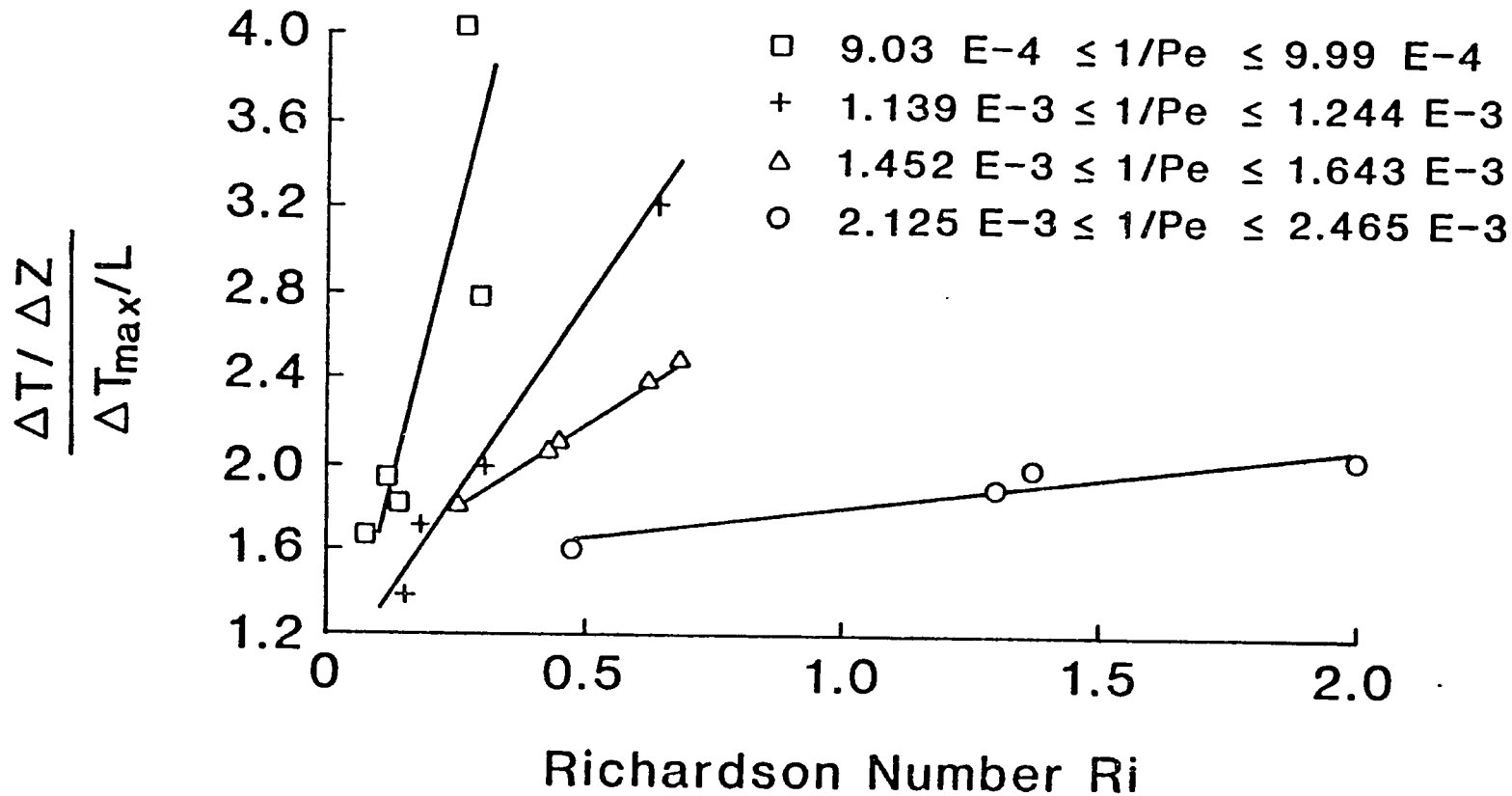

Fig. 5.6: Degree of Stratification as Function of Richardson and Peclet Numbers

CHAPTER 6

RESULTS FOR CONTINUOUS LOAD FLOW

The results for eight load flow rates and for four different combinations of load pattern and geometry are presented in this chapter. The independent variable used is the "output volume," the volume of water removed expressed as a percent of the storage tank volume. This parameter is actually a time parameter scaled by the extraction flow rate.

The results presented will be for the following four cases:

1. Inlet and outlet nozzles on the same side of the tank with a continuous withdrawal for the loads.
2. Inlet and outlet nozzles on the opposite sides of the tank with a continuous withdrawal for the loads.
3. Inlet and outlet nozzles on the same side of the tank with a periodic withdrawal for the loads.
4. Inlet and outlet nozzles on the opposite sides of the tank with a periodic withdrawal for the loads.

As discussed in the Experimental Procedure Chapter the duration of each periodic withdrawal is determined for each flow rate such that about 20% of the tank volume is withdrawn in each one-half hour interval.

6.1 Inlet and Outlet on The Same Side, Continuous Load.

Plots of St and COEF versus dimensionless output volume for each output flow rate, are shown in Figs. 6.1 and 6.2. Based on the results depicted in Fig. 6.1 as well as others

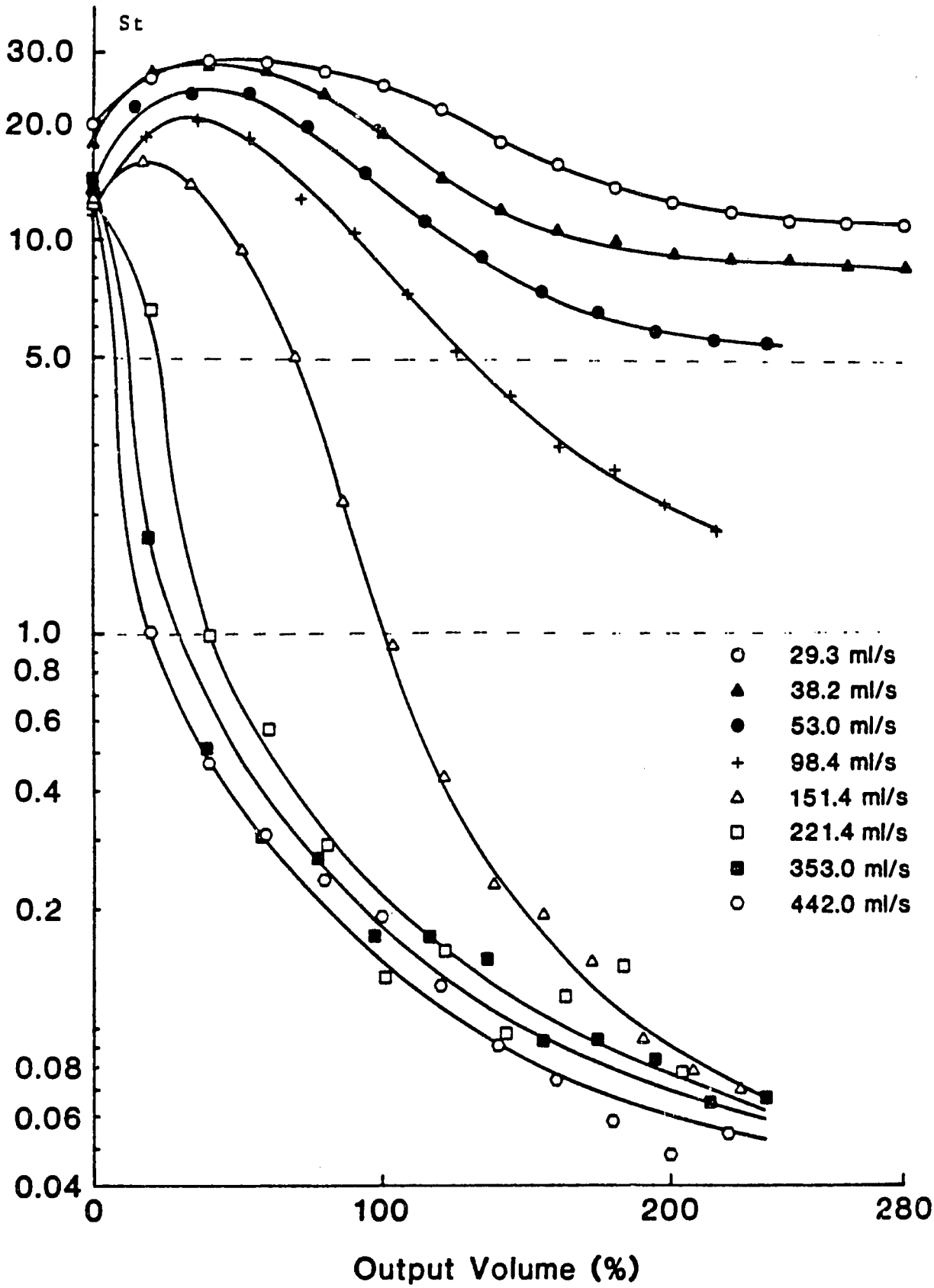

Fig.6.1: Stratification Coefficient History for Same-side Configuration Continuous Output

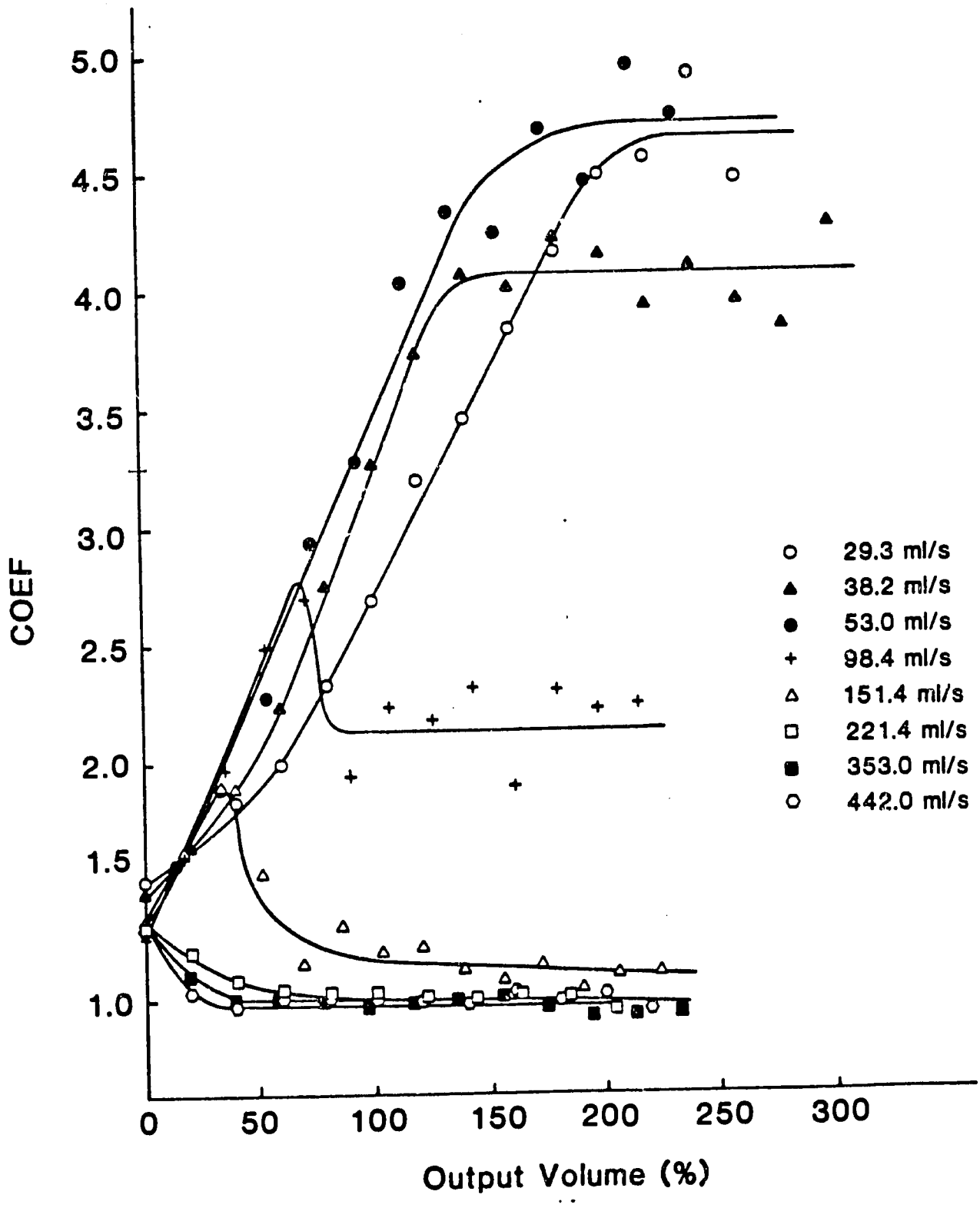

Fig. 6.2: Extraction Efficiency History for Same-side Continuous Output

to follow, three stratification regimes can be identified:

For St > 5, the tank is thermally stratified and appears stable as the experiment continues. This condition occurs for $\dot{m}$ < 60 ml/s ($\dot{m}$ < approximately 1 gpm).

For St < 1, the tank is in a fully mixed condition as the experiment continues. This condition occurs for $\dot{m}$ > 200 ml/s ($\dot{m}$ > 3 gpm)

For 1 < St < 5, the tank is in a transition condition.

According to the above criterion, the curves in Fig 6.1 can be divided into three groups:

In the first group the tank experiences perfect thermal stratification. Even though the output volume increases to over 250% of the total tank volume, the tank is still thermally stratified (St > 5). These cases correspond to make-up water flow rates of 29.3, 38.2, and 53.0 ml/s, corresponding to Re < 3400, based on the make-up water inlet diameter and velocity.

The second group is in the fully mixed condition. The value of St drops quickly from its initial value and for the output volume less than about 40% of the tank volume, the tank is already fully mixed (St < 1). These cases correspond to make-up water flow rates of 221, 353, and 442 ml/s, corresponding to Re > 14,200 based on the make-up water inlet diameter and velocity.

The third group represents a transitional condition

between the first and the second. The value of St initially increases, then decreases as the output increases (output volume over 40%). For one of the flow rates tested a completely mixed condition develops as output volume approaches about 100%. The other flow appears headed to this condition but has not yet reached it at 250% output volume. These cases correspond to the make-up water flow rates of 98.4 and 151.4 ml/s; or 6,000 < Re < 9,600 based on the make-up water inlet diameter and velocity.

Similar results can be identified in Fig. 6.2 where COEF is plotted. However, the trends are not so clearly established.

The output and vertical tank temperature histories for each of the three situations described above are shown in Fig. 6.3 ($\dot{m}$ = 38.2 ml/s) Fig. 6.4 ($\dot{m}$ = 353 ml/s), and Fig 6.5 ($\dot{m}$ = 151 ml/s). The vertical tank temperatures were measured with the center probe (D section).

6.1.1 Full Thermal Stratification

The full thermal stratification case is shown in Fig. 6.3, where the temperature history is for a 38.2 ml/s output flow rate. As flow was initiated, the temperature at the bottom of the tank decreased rapidly to within 0.3°C of the inlet water temperature. Because the input hot water (from the simulated collector) entered the tank through the inlet located at the top of the tank and the output hot water left the tank from the outlet located at the top region, the top

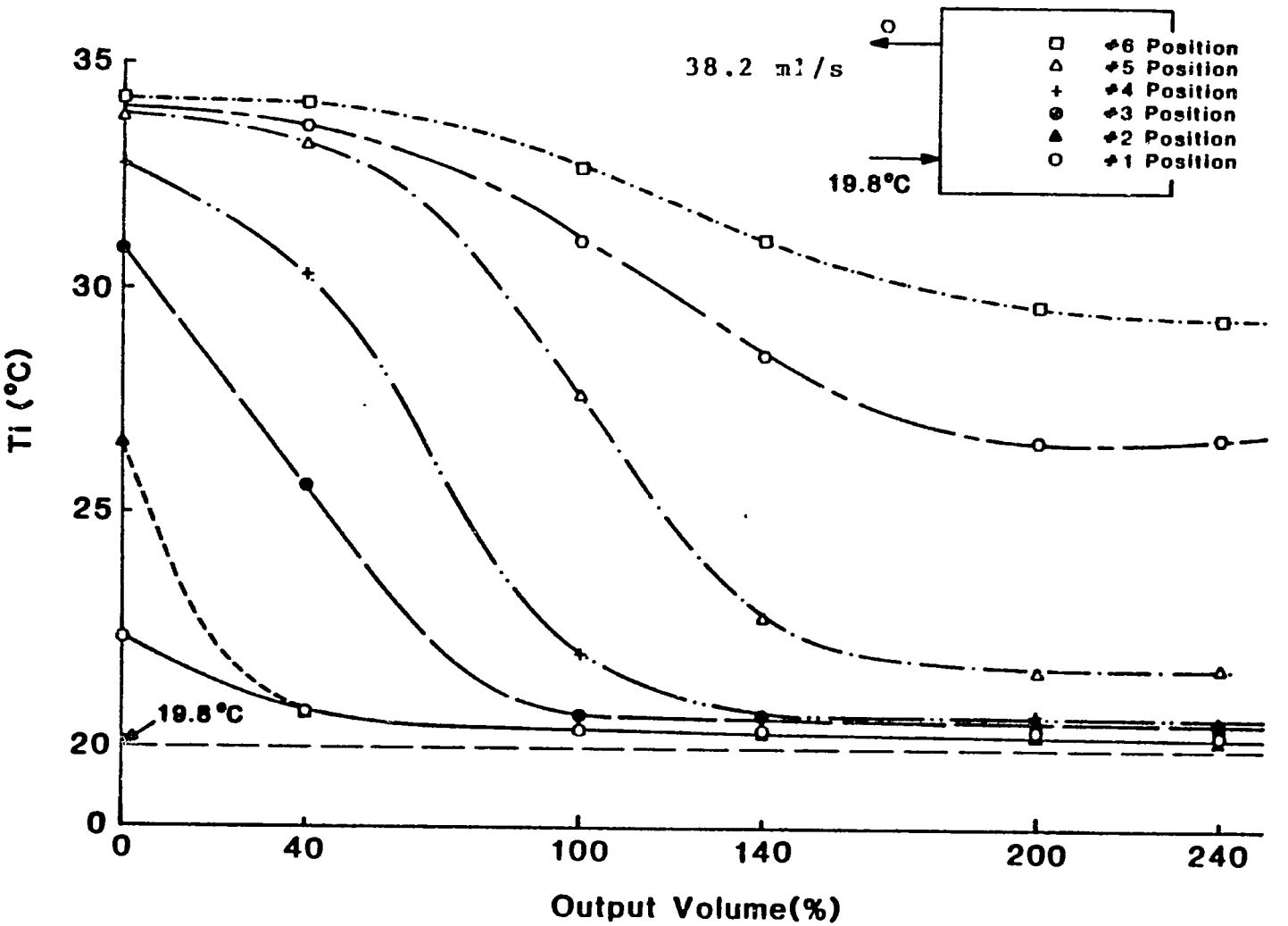

Fig. 6.3: Vertical Temperature History at Middle Probe for Continuous Output

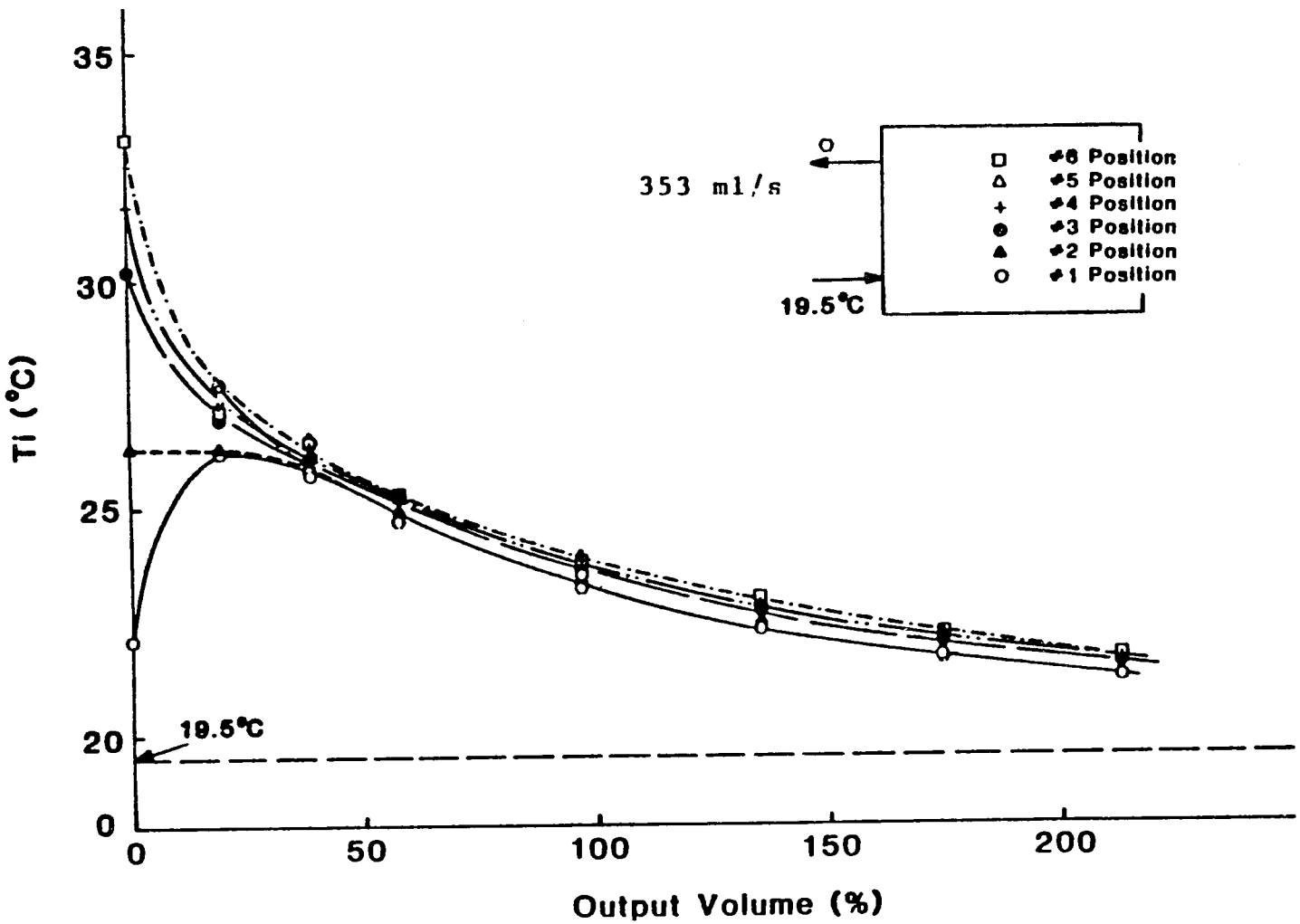

Fig. 6.4: Vertical Temperature History at Middle Probe for Continuous Output

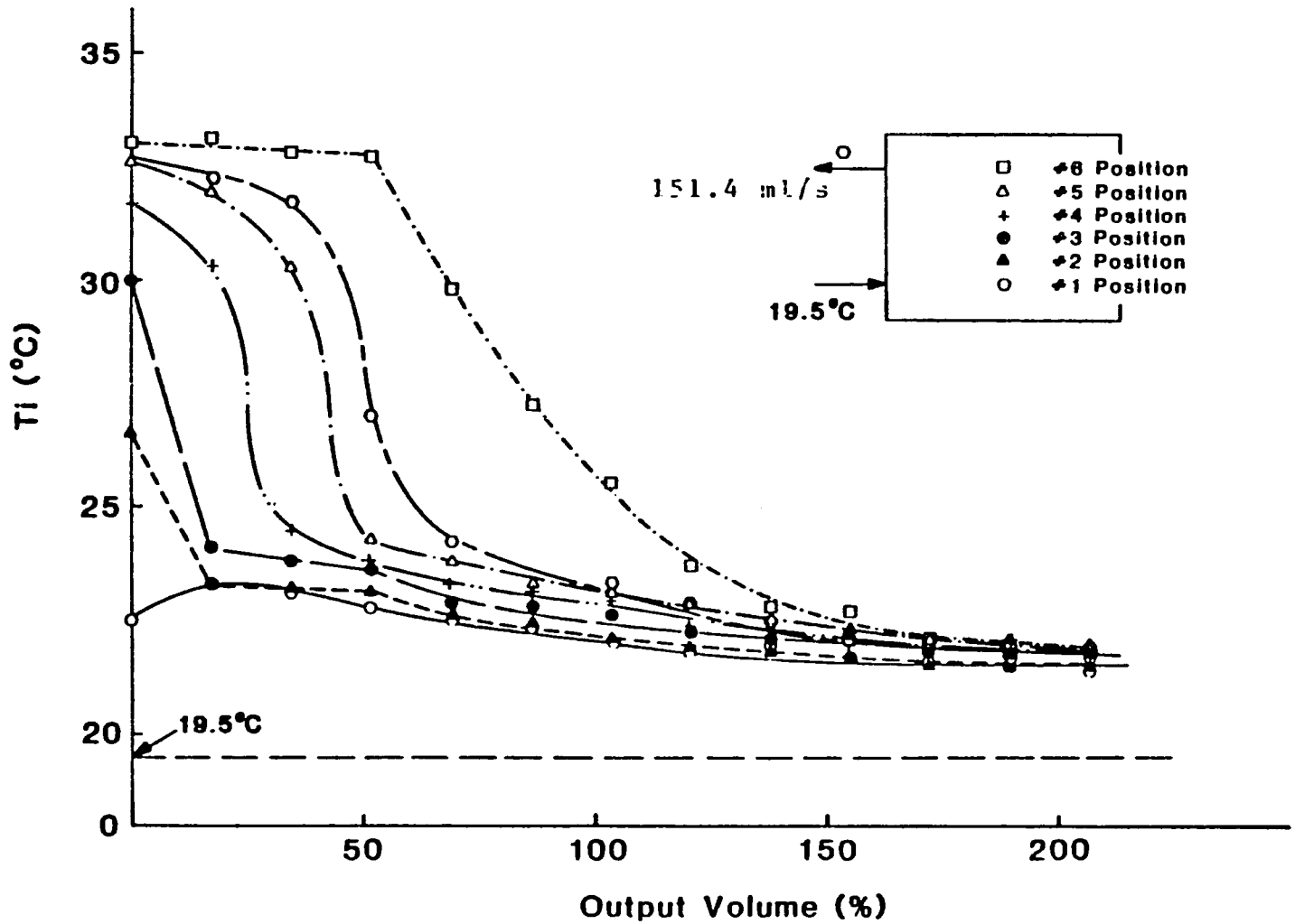

Fig. 6.5: Vertical Temperature History at Middle Probe for Continuous Output

of the tank tended to remain hot.

As more water was withdrawn, the water temperature in the mid-region fell continuously, and it is seen to approach the inlet temperature for output volume over 100%. The upper or the top region temperature remained high indicating that the simulated solar derived heat was sufficient to maintain this temperature.

The output water temperature was lower than the top region temperature but higher than the #5 position temperature; the output nozzle height is higher than the height of position #5. The output port should have been located nearer the top of the tank to assure that the hottest water in the tank can be utilized.

As the experiment was concluded, the temperature in the bottom and middle regions were only 0.3 to 0.7°C above the make-up water temperature; the top water temperature was constant also, about 3 to 4°C below the hot water inlet temperature from the heater. The temperature difference between the top and the bottom of the tank was about 18°C. At this time St = 8.4, and COEF = 4.2. Even though the output volume was over 240% and $T_{avg} - T_{makeup} = 1.6°C$, water was still being supplied to the load at 6°C above the make-up water temperature. The system had achieved a quasi-steady state. For this flow rate and for others less than 60 ml/s, the dominant factor determining the tank stratification is buoyance. The inertial forces do still affect the degree

of stratification, but the stratification is established. The larger the Grashoff number, the larger St and COEF become. The greater the inertial force (larger Reynolds number), the lower the top tank temperature and the higher the bottom temperature became. That is, the greater the Reynolds number, the lower the thermal stratification efficient, St, and the lower COEF. The inertial force plays an important part in suppressing thermal stratification. The higher the Reynolds number, the stronger the mixing effect.

6.1.2 Fully Mixed

The fully mixed condition ($\dot{m}$ > 200 ml/s) is shown in Fig 6.4 where the temperature history is for an output flow rate of about 353 ml/s.

Initially, the stratification was good, St = 14.2. After only 20% of the tank volume was withdrawn, the strong inertial force of the jet from the make-up water inlet was causing all water to circulate and mix strongly in the tank. The bottom region temperature rose, and the top region temperature fell. The temperature difference between the top and the bottom was only about 1.5°C; St = 1.75. After 40% of the tank volume was withdrawn, the temperature difference between the top and the bottom was about 0.8°C; St = 0.5; COEF = 1, and $(T_{avg} - T_{makeup})$ = 6.3°C. At that time, the tank was fully mixed. As the output flow continued, the temperature difference, St, and T_{avg} decreased further.

In this region, the dominant factor is the inertial

force. Buoyance is not a factor except in establishing the initial stratification. The greater the inertial force (Reynolds number), the faster the temperature difference decays, and the lower the thermal stratification coefficient, St, becomes. The COEF decreases to 1.0.

6.1.3 Transitional Condition

An example of the transitional region is shown in Fig. 6.5, where the temperature history is for an output flow rate of 151.4 ml/s (2.4 gpm).

Initially, the inertial force due to the make-up water injected into the tank from the inlet at the bottom was not large enough to cause all the tank water to circulate, but it did cause the water in the lower half of the tank to circulate and mix. As the output volume reached 17%, the mixing in the lower half had lowered the temperature at the positions #2 and #3 to within 0.8°C of the make-up water temperature while the temperatures at the top of the tank were unchanged. Thus the stratification coefficient, St, and COEF increased: St = 15.7, COEF = 1.63. As the output volume increased to 34%, the circulation was occuring at positions #1, #2, #3, and #4, and the St decreased because the cooler make-up water occupied part of the upper half of the tank. However, COEF was still increasing because the water temperature at the outlet decreased, even though the top temperatures were unchanged, and the average temperature of the tank was still decreasing. For the higher flow rates the circulation was more apparent and occurred earlier

resulting in lower values for St and COEF.

As the output volume increased to 120%, all of the water was circulating. The temperature difference between the top and bottom decreased to 1.9°C; St = 0.4 and COEF = 1.16. A fully mixed condition existed.

The experiment continued to an output volume of 224% when St = 0.07 and COEF = 1.11. This situation could be termed quasi-steady state.

In this range of flow rates, both the buoyant and inertial forces can be important. The larger the Reynolds number, the more quickly the system reaches the fully mixed condition, and correspondingly lower values of St and COEF exist.

6.2 Inlet and Outlet on the Opposite Sides, Continuous Load.

The results, St and COEF versus dimensionless output volume for each flow rate, are shown in Fig. 6.6 and 6.7. According to the same criterion developed in the previous section the curves in Fig. 6.6 divide the problem into three flow regions:

Full thermal stratification is achieved for flow rates up to 98.4 ml/s (1.56 gpm). This range corresponds to Re < 6270, slightly higher than observed in the case where inlet and outlet were on the same side.

The fully mixed condition is achieved for flow rates above 221 ml/s (3.5 gpm). For these flow rates the output volume exceeds 50%, that is, half the tank is replaced,

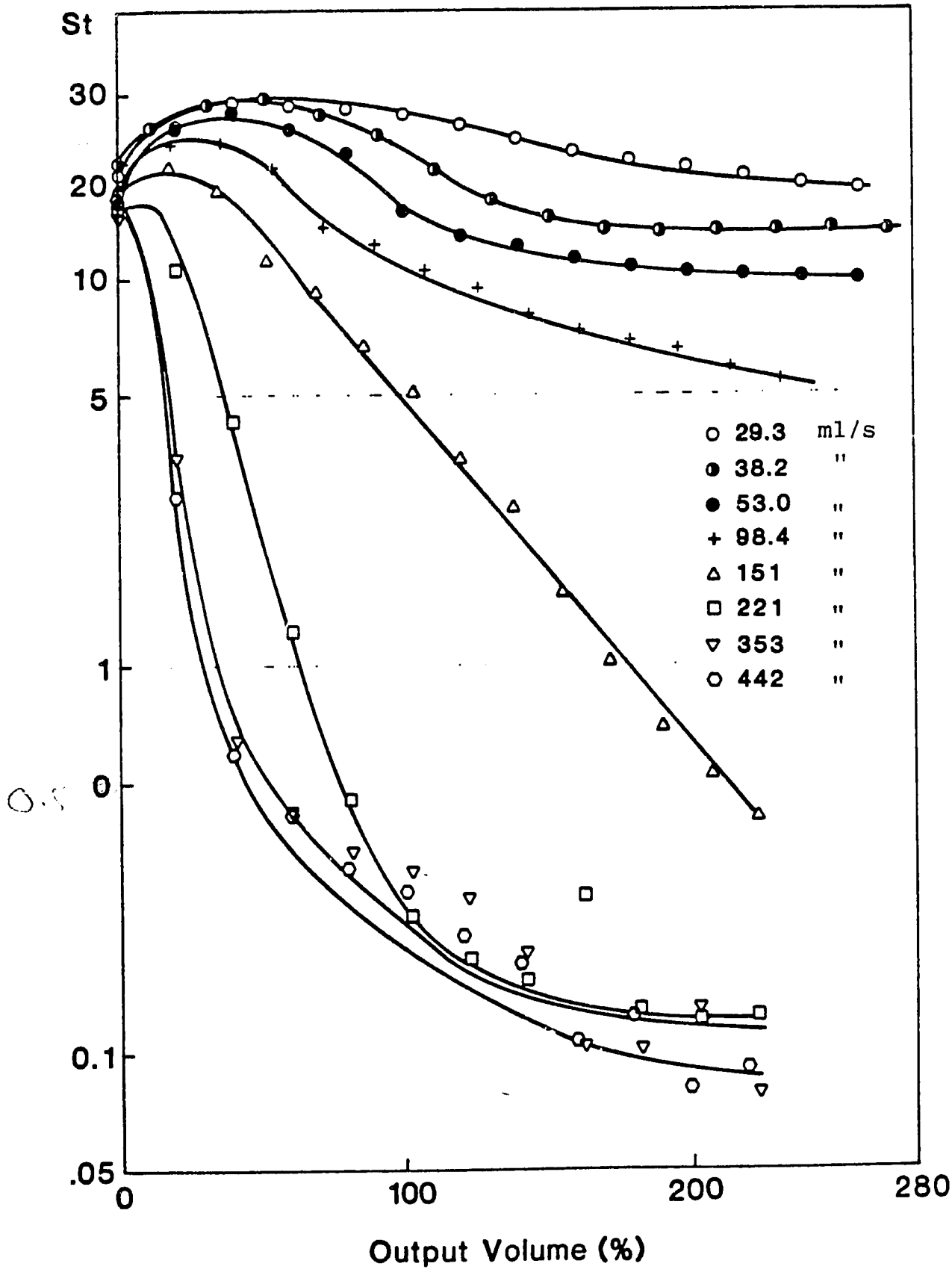

Fig. 6.6: Stratification Coefficient History for Opposite-side Configuration Continuous Output

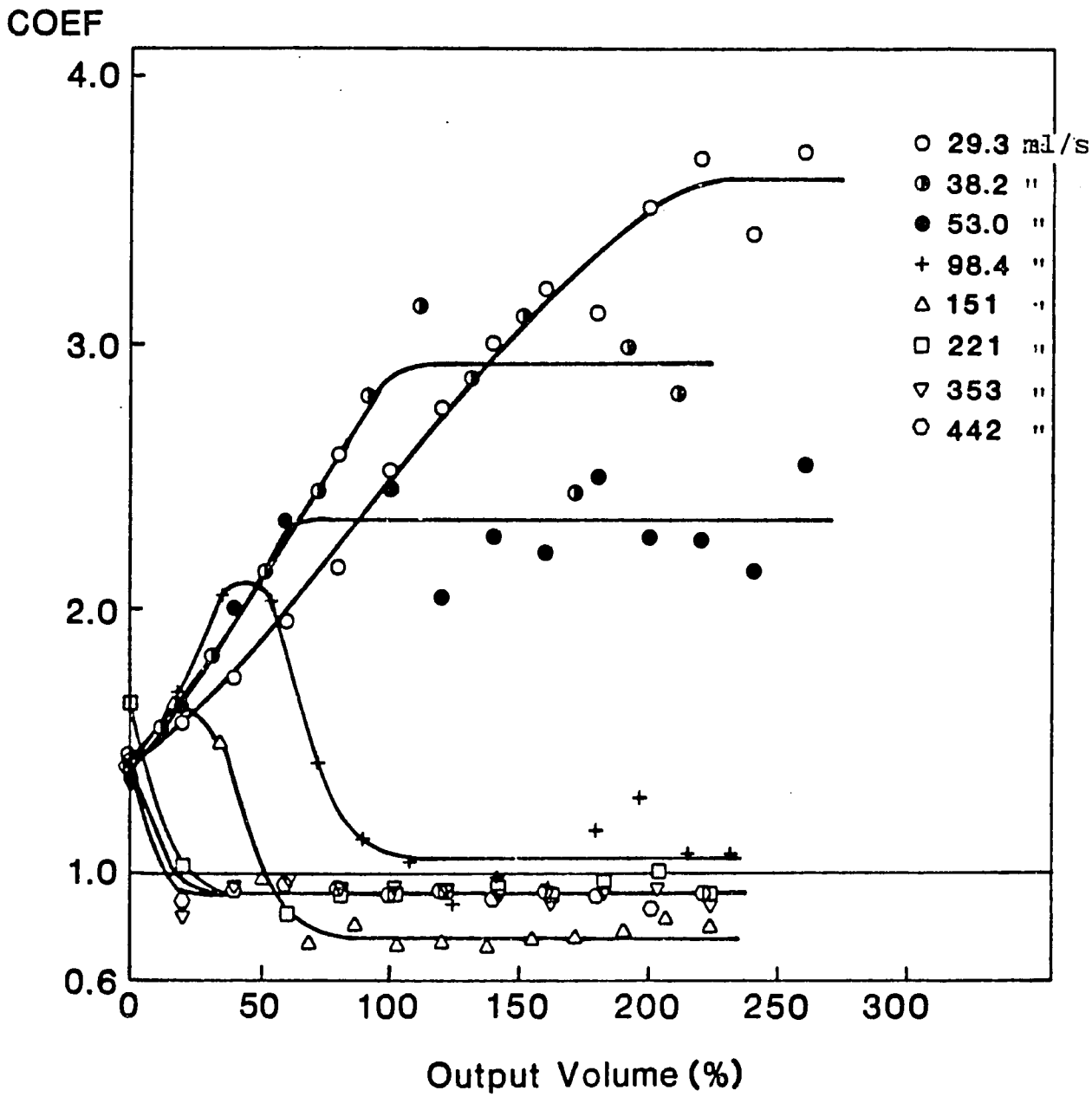

Fig. 6.7: Extraction Efficiency History for Opposite-side Continuous Output

before the tank is fully mixed. (St approximately equal to 1). Only the 151.4 ml/s (2.4 gpm) output flow rate resulted in the transitional condition.

In a comparison of Figs. 6.6 and 6.1, it is seen that the thermal stratification, St, of the opposite-side configuration is higher than the same-side configuration at the same flow rate and output volume. That is, the thermal stratification for the opposite-side configuration is better than for the same-side configuration.

A comparison of Figs. 6.7 and 6.2, indicates just the opposite for COEF. The extraction efficiency for the opposite-side configuration is lower than for the same-side configuration, even though the stratification coefficient for the opposite-side configuration is higher than the same-side configuration.

The output and vertical tank temperature histories at the middle section of the tank for flow rates representative of the three flow regimes are shown in Figs. 6.8, 6.9, and 6.10.

The results for the full thermal stratification are shown in Fig. 6.8, where the temperature history for a 38.2 ml/s (0.605 gpm) output flow rate is presented. It is almost the same as the same-side configuration, but the temperature difference between the top and bottom is 1.5°C more than for the same-side configuration. Thus the stratification coefficient, St, for the opposite-side configuration is higher than for the same-side configuration.

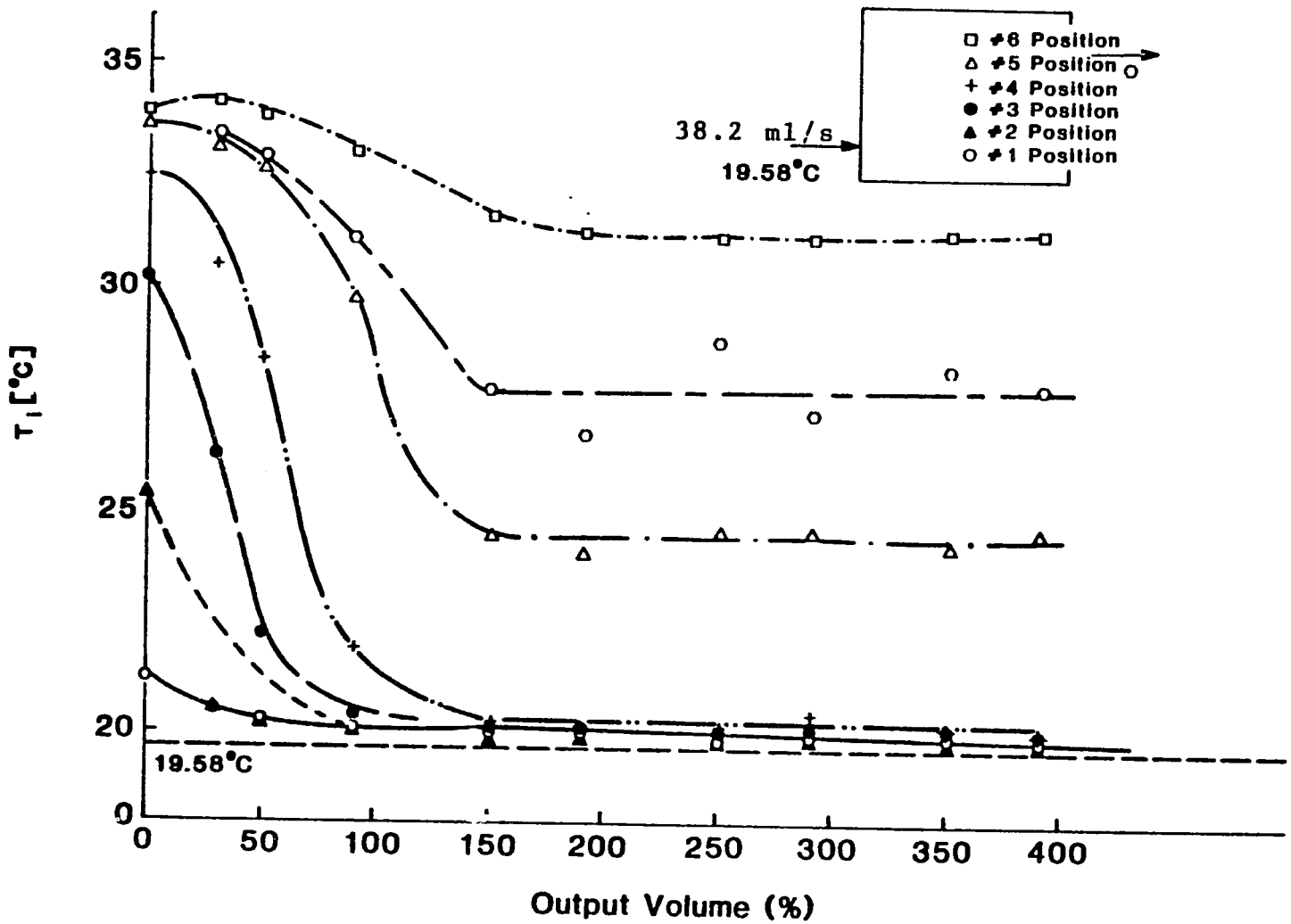

Fig. 6.8: Vertical Temperature History at Middle Probe for Continuous Output

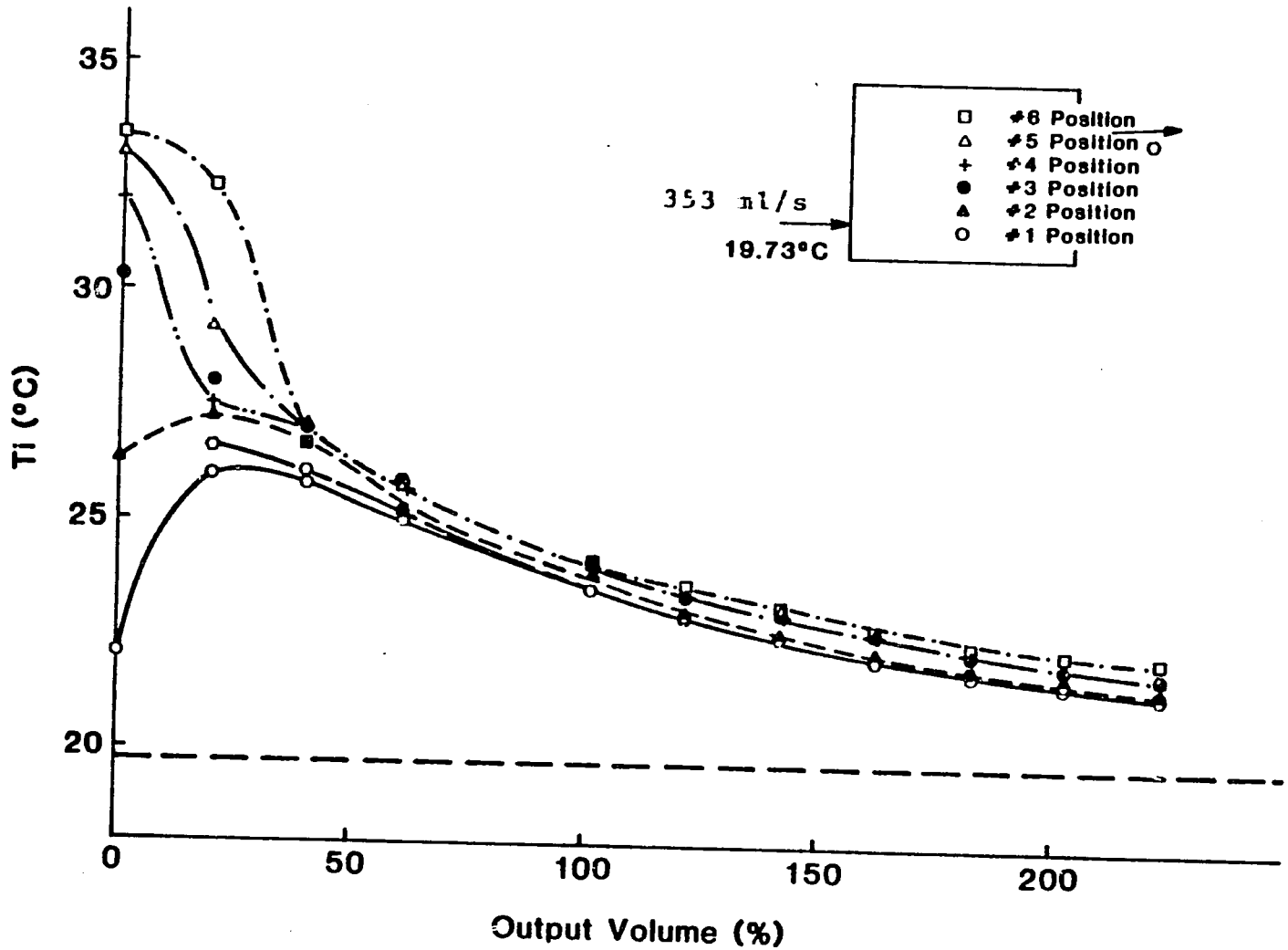

Fig. 6.9: Vertical Temperature History at Middle Probe for Continuous Output

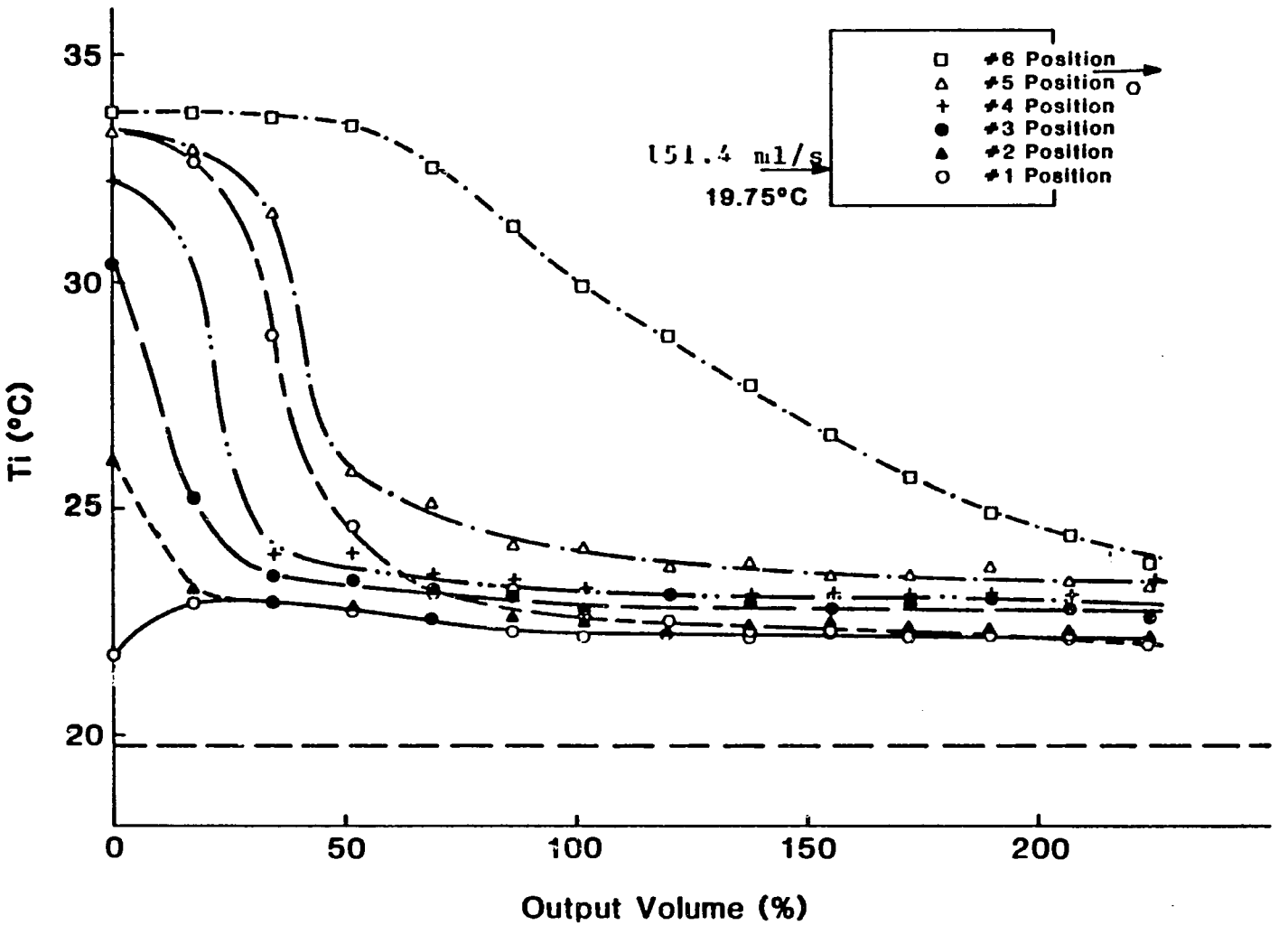

Fig. 6.10:Vertical Temperature History at Middle Probe for Continuous Output

A fluctuation of about 0.5 to 1.0°C in the output hot water temperature is seen in Fig. 6.8. Its amplitude decreases as time passes, and is due to the changes in the internal flow patterns in the tank.

The fully mixed condition is shown on Fig. 6.9, where the temperature history is for the 353 ml/s (5.6 gpm) output flow rate. In a comparison with Fig. 6.4, it is seen that it is almost the same as the same-side configuration. However, the decrease in the temperature difference takes place more slowly than for the same-side configuration. Thus it remains stratified to a greater degree.

The temperature histories for the transitional condition are shown in Fig. 6.10. The temperature histories are for the 151.4 ml/s (2.4 gpm) output flow rate. In a comparison with Fig. 6.5, it is seen that it is almost the same as the same-side configuration. However, the decrease in the temperature difference again takes place more slowly than for the same-side configuration. This it maintains its stratification to a higher degree than the same-side configuration.

The average tank temperature, T_{avg}, St, and COEF are plotted versus dimensionless output load for each of the above output flow rates and configurations in Figs. 6.11, 6.12, and 6.13. It is seen that the T_{avg} for the same-side configuration is lower than for the opposite-side configuration. This is a result of the better extraction efficiency of the same-side configuration. This result indicates that

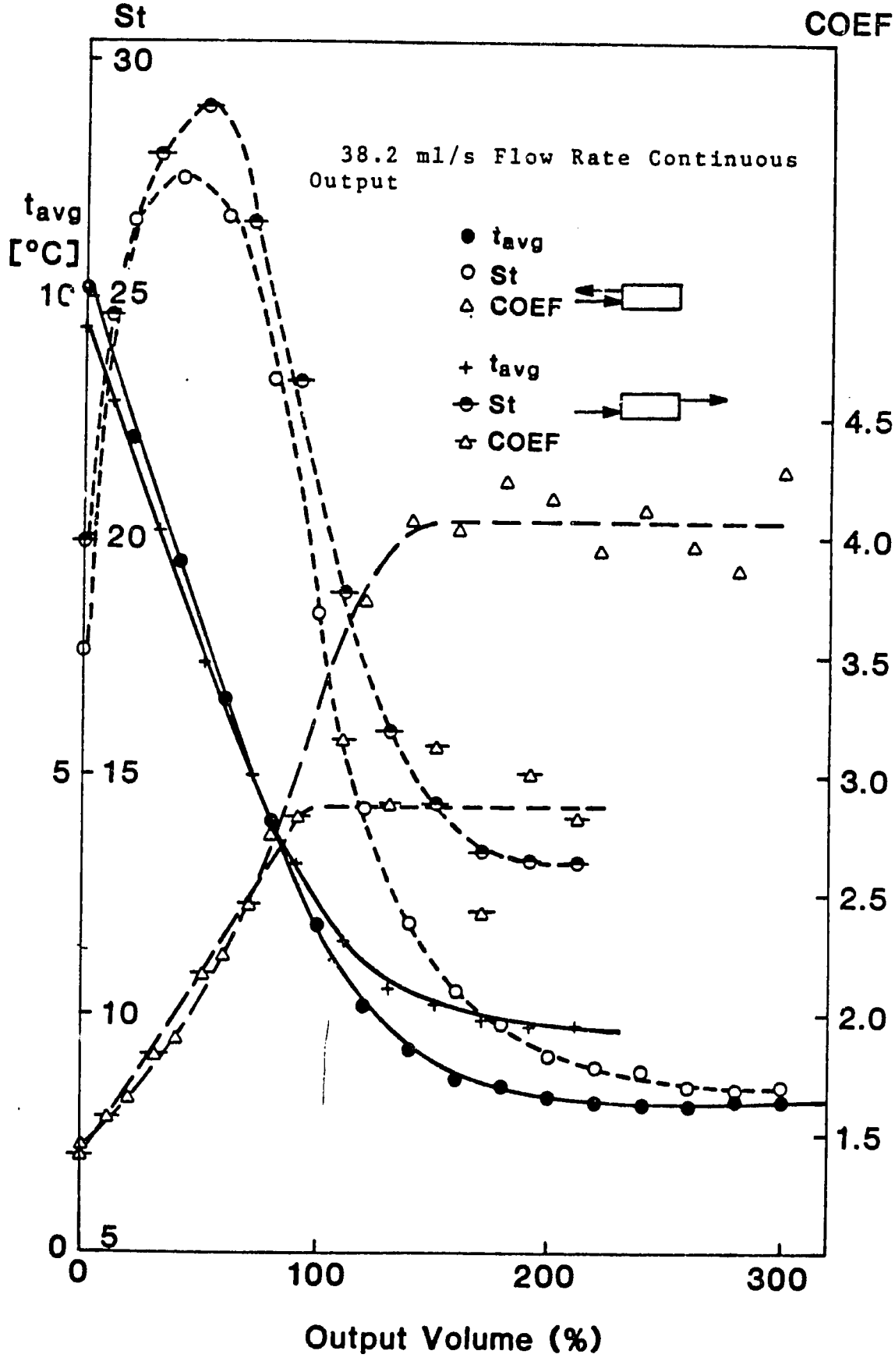

Fig. 6.11: A Comparison Between The Data for The Two Different Configuration

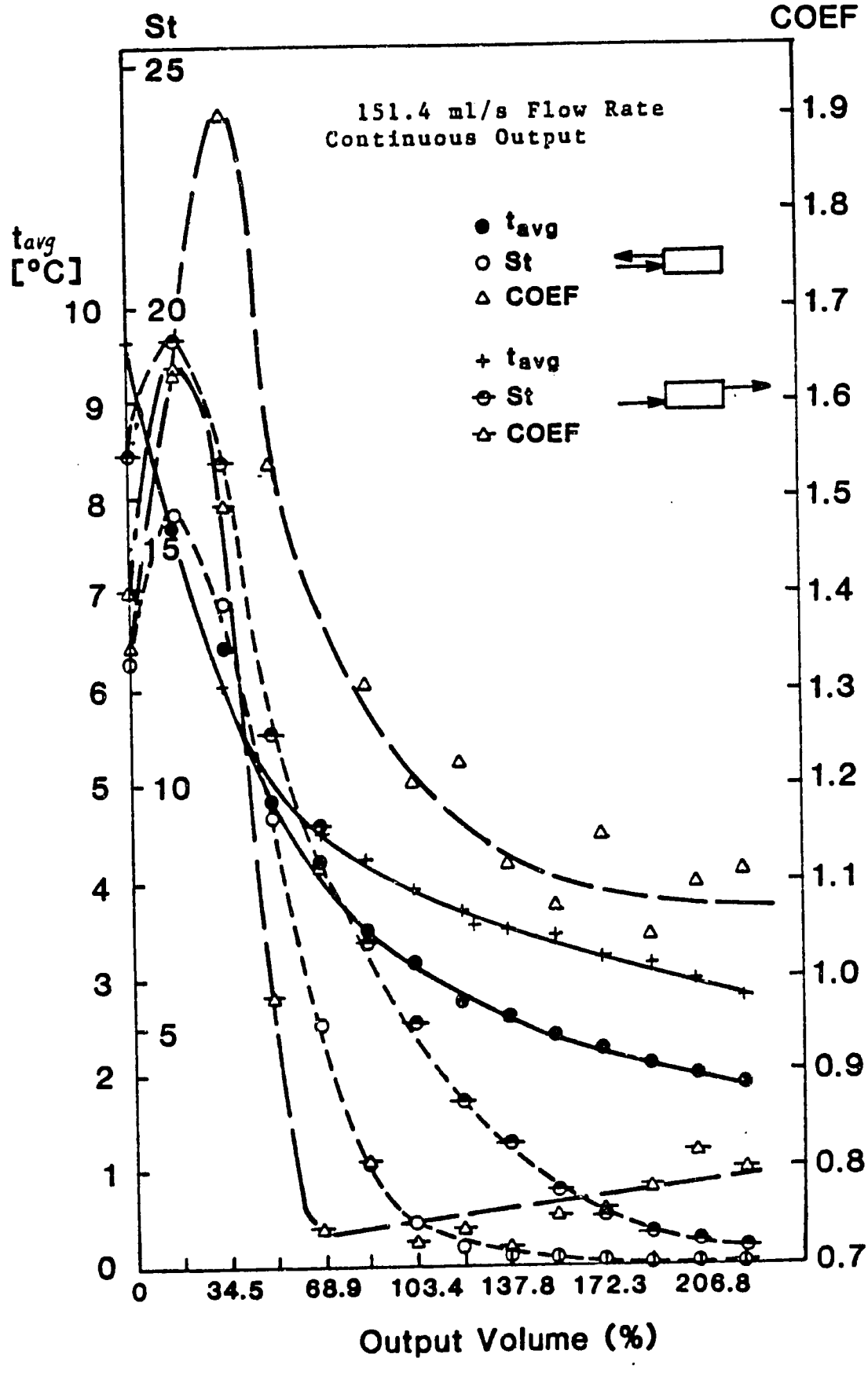

Fig. 6.12:A Comparison Between The Data for The Two Different Configuration

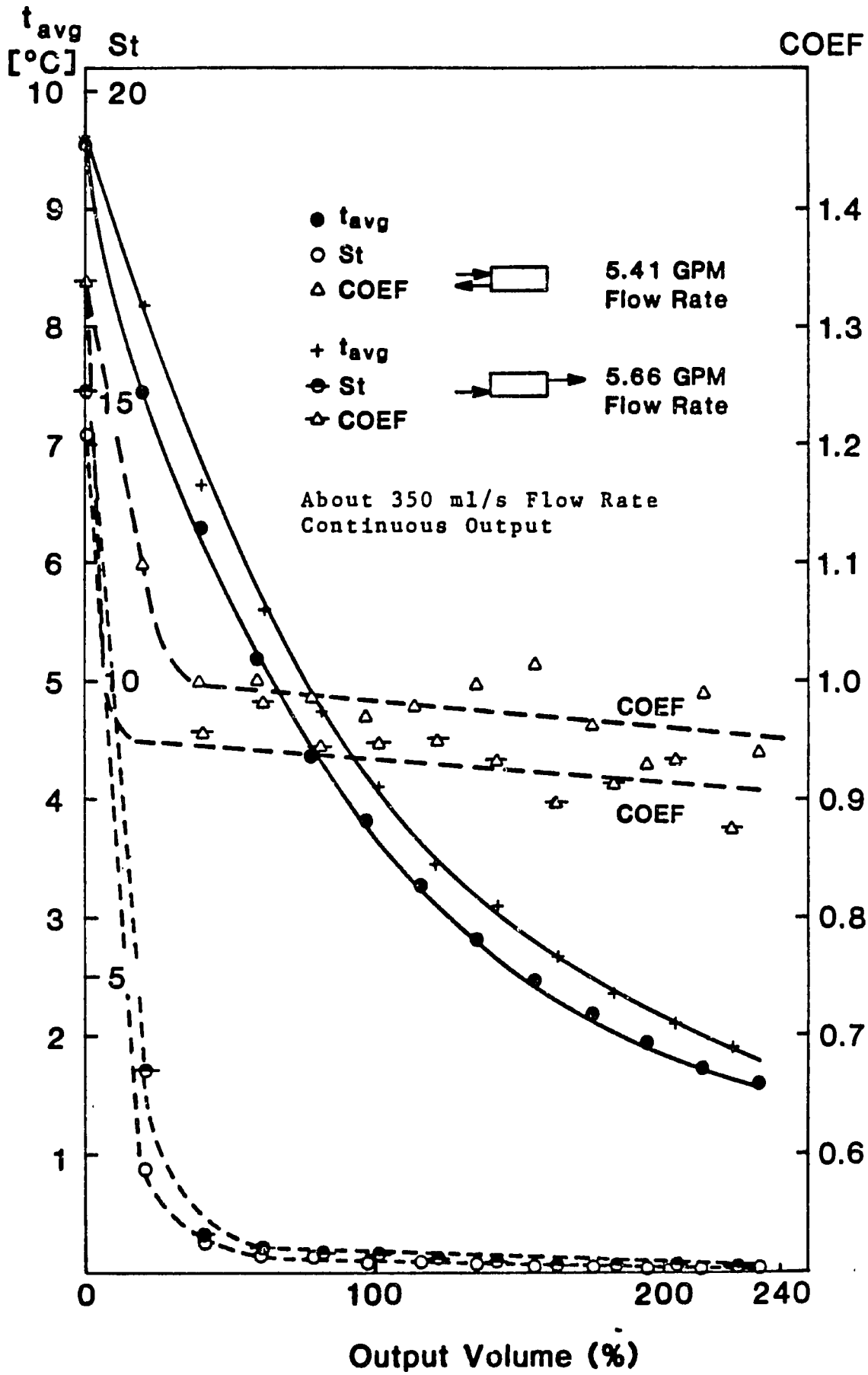

Fig. 6.13: A Comparison Between The Data for The Two Different Configuration

the output performance of the same-side configuration is better than the opposite-side configuration even though the thermal stratification for the opposite-side configuration is better than for the same-side configuration.

6.3 Discussion

Figures 6.14 through 6.19 illustrate the temperature distributions for each of the three defined flow rate regimes for the two inlet-outlet configurations and can be used to help explain the reason for the above phenomena.

Figs. 6.14 and 6.15 depict the temperature distributions for the continuous 38.2 ml/s output flow rate at about 100% output volume. For Fig. 6.14 the inlet and outlet nozzles are on the same side (same-side configuration); for Fig. 6.15, they are on opposite sides (opposite-side configuration). A comparison of Fig. 6.14 with Fig. 6.15, indicates that there is an additional warm fluid layer at the position #5 in the opposite-side configuration. For this output flow rate, it was previously pointed out that buoyance dominates the flow. The hotter water delivered from the heater rose to the top of the tank under the effect of buoyance and then flowed across the tank straight into the outlet in the same-side configuration; it formed a nearly straight streamline. For the opposite-side configuration, the hotter water also rose under the effect of buoyance, but then it reversed into the outlet. It formed a "U" shaped streamline. This "U" shaped flow caused the hotter water to occupy more volume in the tank than for the

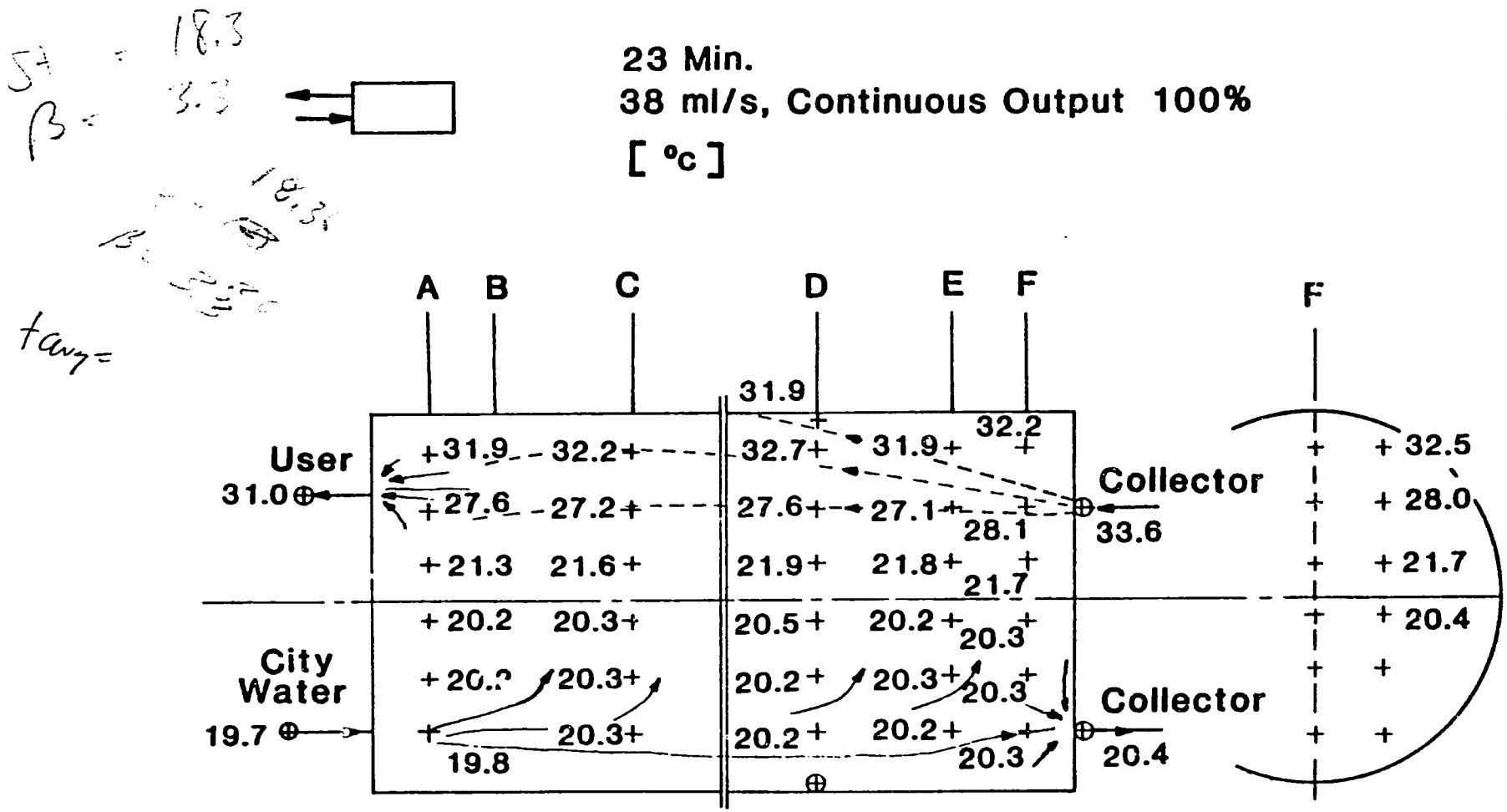

Fig. 6.14:The Temperature Distribution in The Tank

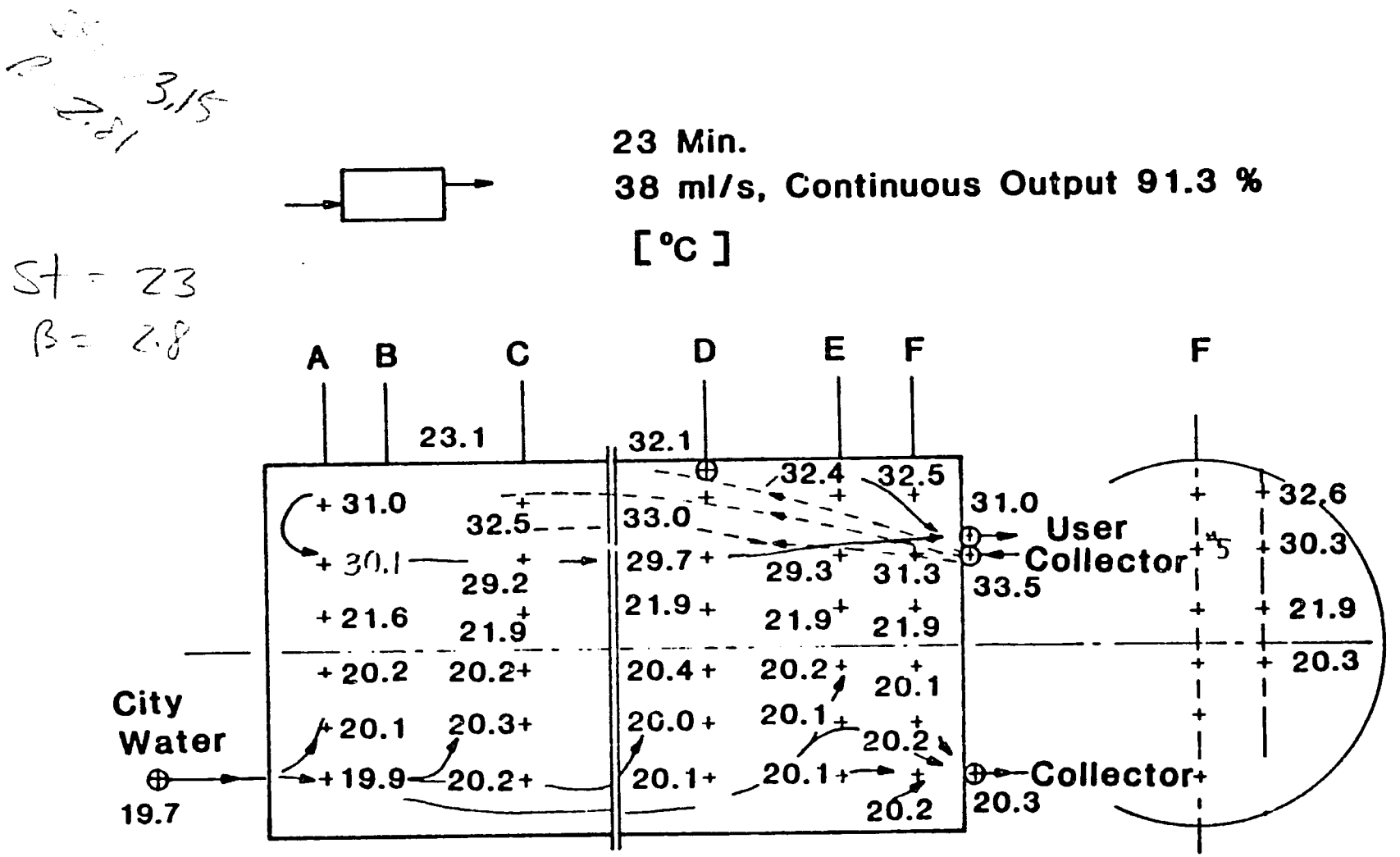

Fig. 6.15:The Temperature Distribution in The Tank

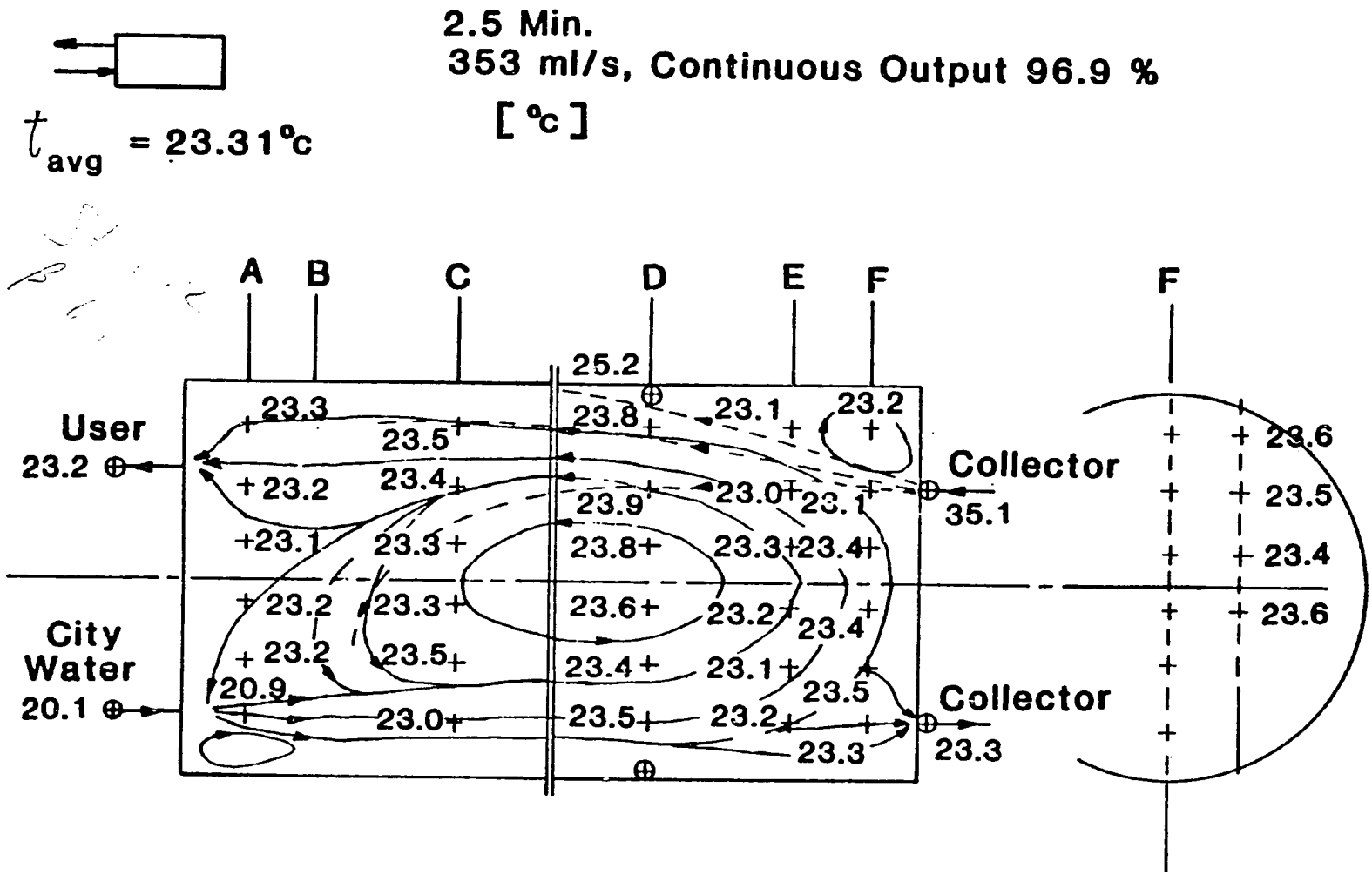

Fig.6.16: The Temperature Distribution in The Tank

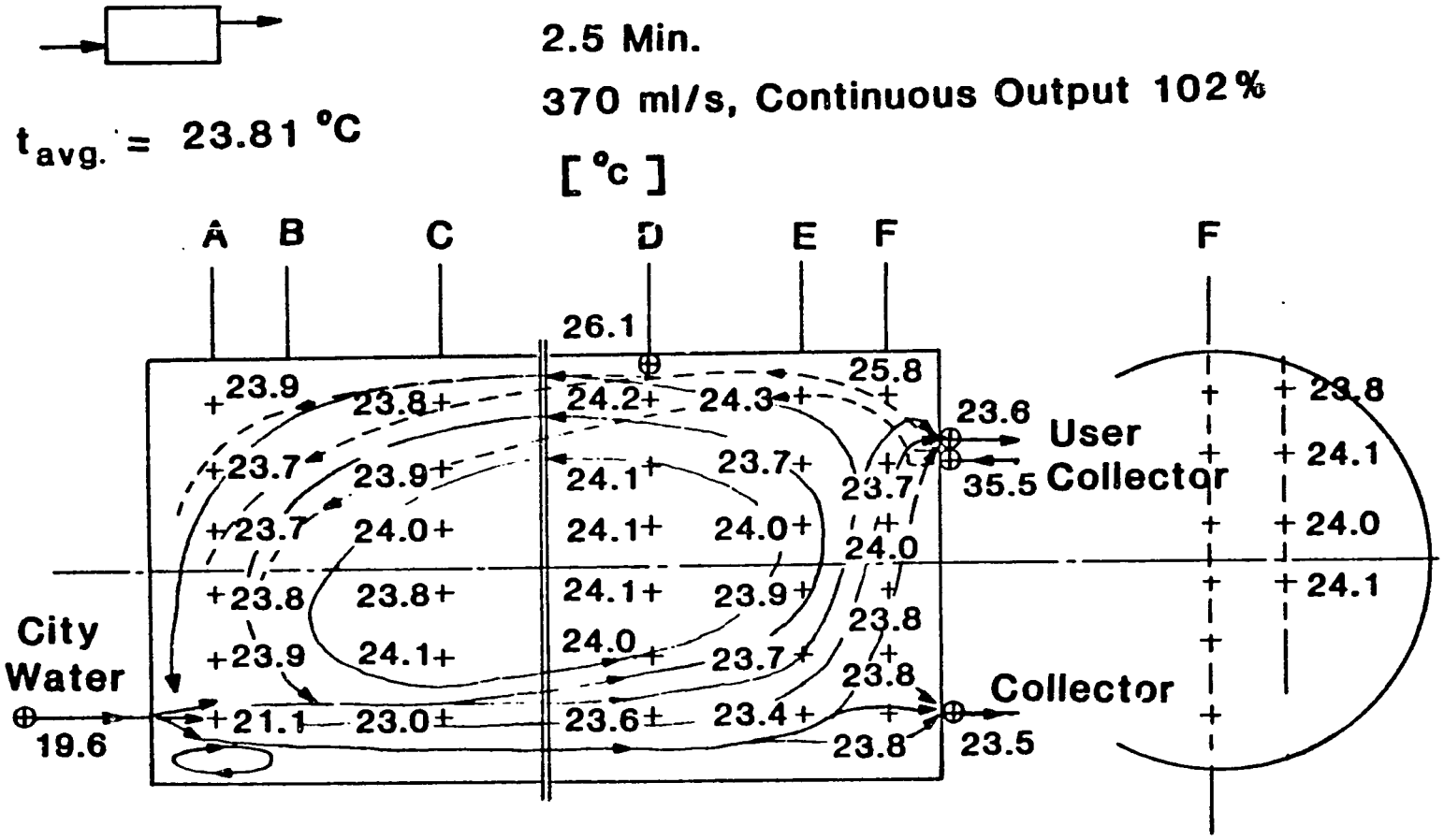

Fig. 6.17: The Temperature Distribution in The Tank

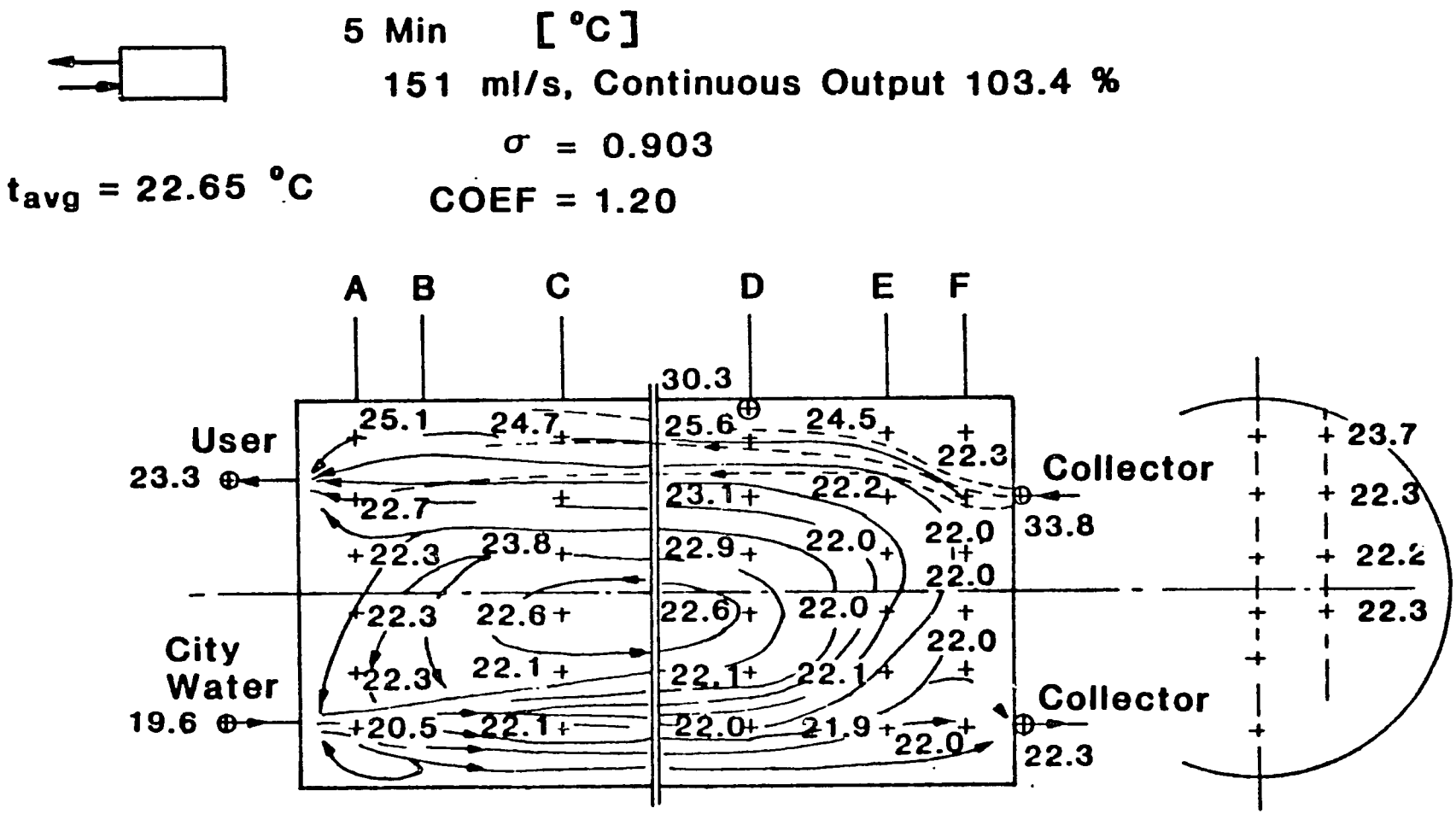

Fig. 6.18: The Temperature Distribution in The Tank

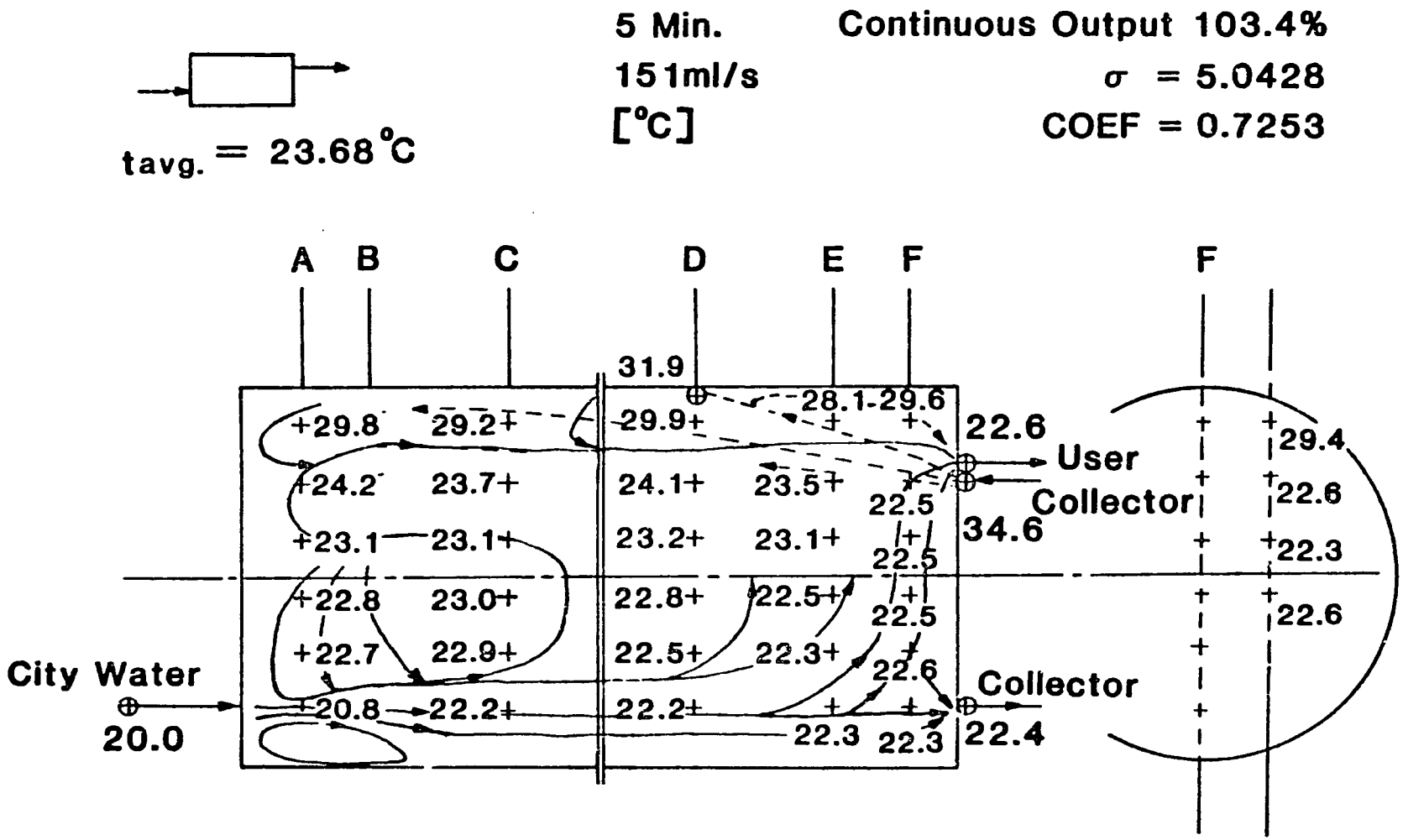

Fig. 6.19:The Temperature Distribution in The Tank

straight streamline flow. It is for this reason that the additional warm layer formed at the position #5 in the opposite-side configuration. This upper, warmer layer caused the stratification coefficient, St, to increase (St = 23.15 for the opposite-side configuration and St = 18.36 for the same-side configuration). Since the make-up water and the output hot water temperatures are the same for both configurations, the warmer layer, which increases the average temperature, reduces the value of COEF for the opposite-side configuration (2.81) compared to the same-side configuration (3.26), even though the stratification of the opposite-side configuration is higher.

Both Figs. 6.16 and 6.17 depict temperature distributions for a continuous 353 ml/s (5.5 gpm) output flow rate at about 100% output volume. Fig. 6.16 is for the same-side configuration for this output flow rate. The dominant factor is the make-up water inertial force, which causes all the water in the tank to circulate and mix strongly as previously shown. In comparing Figs. 6.16 and 6.17, it is noted that the make-up water in the opposite-side configuration appears to enter the outlet through a shorter mixing length (about the length of the tank plus the height of the tank). Thus the output water temperature in the opposite-side configuration is lower than the average temperature in the tank, and the COEF is less than 1.0. (The average value is 0.93.)

Since there is a longer mixing length (about two lengths of the tank plus the height of the tank) in the same-side

configuration, the mixing is increased and the stratification coefficient St decreases. Thus the St in the same-side configuration is lower than the opposite-side configuration, but both of them are very close to zero because of the strong circulation and mixing. The output water temperature in the same-side configuration is almost equal to the average temperature, and the COEF is close to 1.0. (The average value is 0.98.)

Figs. 6.18 and 6.19 depict temperature distributions for the continuous 151.4 ml/s output flow rate at 103% output volume. Fig. 6.18 is for the same-side configuration; Fig. 6.19 is for the opposite-side configuration. It was previously shown that both buoyant and inertial forces are important in establishing the temperature distribution for this flow rate. As the make-up water issues into the tank, it entrains the surrounding water which widens the jet. The jet boundary expands with distance from the inlet. In comparing Fig. 6.18 with Fig. 6.19, it is apparent that the make-up water in the same-side configuration passes through a longer "U" shaped path, about two lengths plus one height of the tank, before entering the outlet, while in the opposite-side configuration it passes through a shorter "L" shaped path, about one length plus one height of the tank. In the "U" shaped path, the make-up water inertial force causes the water inside the "U" shaped region to circulate forming a uniform temperature region which occupies almost

the entire tank. The top row of temperatures appears unaffected. The temperature drops abruptly to the second row and then decreases slowly to the bottom of the tank. In the shorter "L" shaped path, the inertia of make-up water is not sufficient to make all the water circulate. It entrains only the surrounding water which causes its own temperature to rise. Thus its temperature is lower than the surrounding temperature and closer to the bottom temperature. The hot water supplied from the heater rises to the top of the tank under the effect of the buoyance, and then reverses into the outlet, forming a "U" shaped path in the opposite-side configuration. In the same-side configuration the hot water simply flows across the top of the tank. The longer flow path causes the hot water to occupy more volume in the tank, thus increasing the stratification coefficient St, but decreasing the temperature at the outlet since the hot water loses more heat to the cooler water. Since the output water temperature is lower than the average temperature in the tank, its COEF should be lower than 1 (0.72 to 0.82 only), and lower than for the same-side configuration.

6.4 Correlation of Data for Continuous Flow

Figures 6.20 and 6.21 illustrate a plot of the stratification coefficient, St, against Grashof number with load flow rate as a parameter for two configurations. In determining the Grashof number, the temperature difference between make-up water and average tank water was used for the characteristic temperature difference:

$$Gr = g\,\beta\,D^3\,(T_{avg} - T_{makeup})/\nu^2 \qquad (6.1)$$

where

D = Diameter of the tank, 0.571 m

g = Acceleration due to gravity

ν = Kinematic viscosity

The thermal properties, ν and β, should be evaluated at the average of the mean temperature in the tank and the make-up water temperature. The characteristic dimension for the Gr is chosen as the tank diameter, D, since this is the mixing height and is commonly employed.

The output volume flow rate, $\dot{Q}$, and inlet pipe diameter, d, which affect the mixing intensity and the thickness of the mixing layer can be used to calculate a Reynolds number for the inlet flow:

$$Re = ud/\nu = 4\dot{Q}/\pi d\nu$$

where

$\dot{Q}$ = Output flow rate

d = Inlet pipe diameter for the make-up water

Partial least square fits of the data (except the fully mixed condition) yielded the correlations shown in Figs. 6.20 and 6.21 for each configuration. It can be seen that the curves fit the data reasonably well. The curves can be expressed mathematically as:

For the same-side configuration:

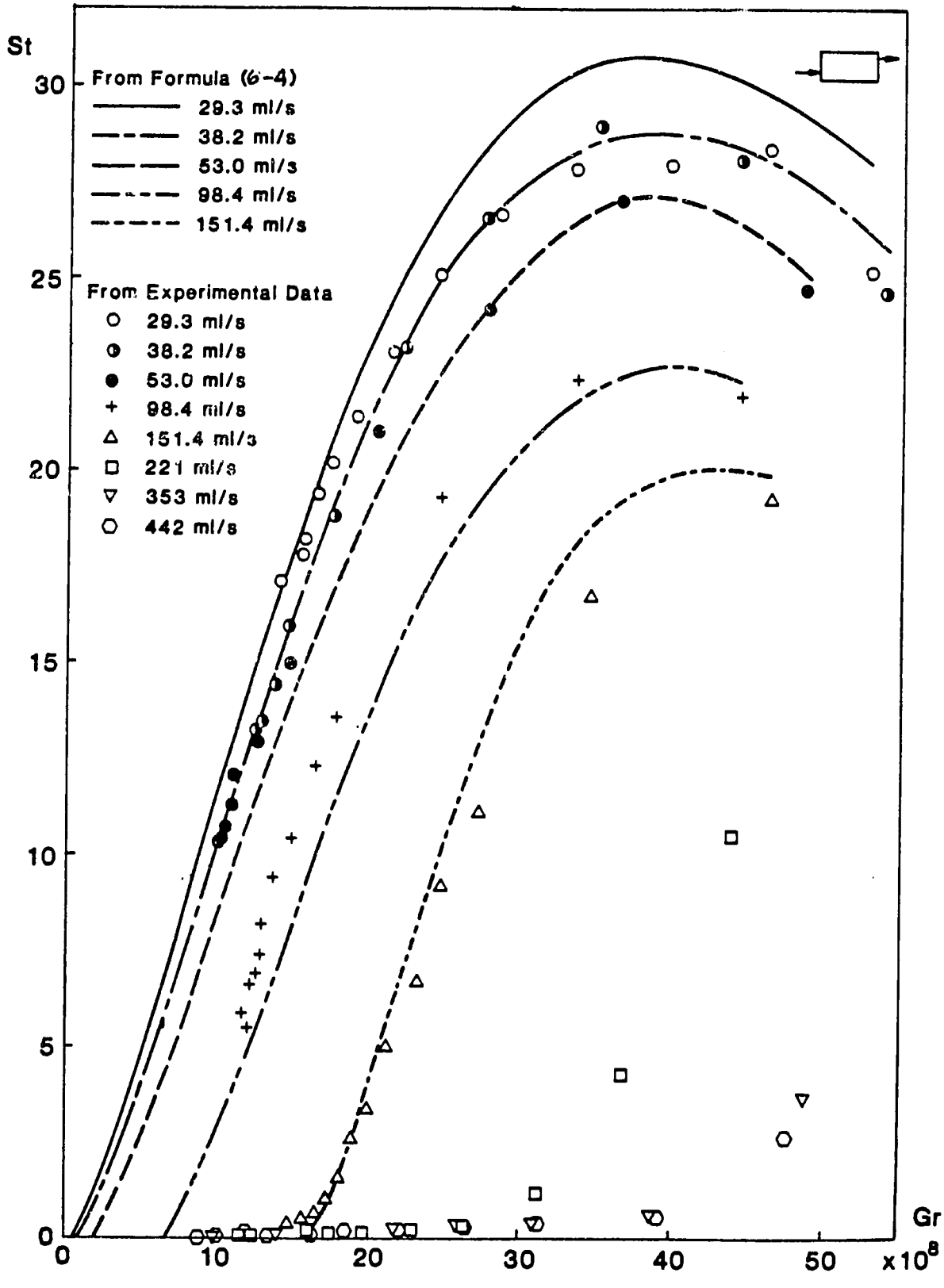

Fig. 6.20: Correlation of Stratification Coefficient St Data for Opposite-side Configuration Continuous Output

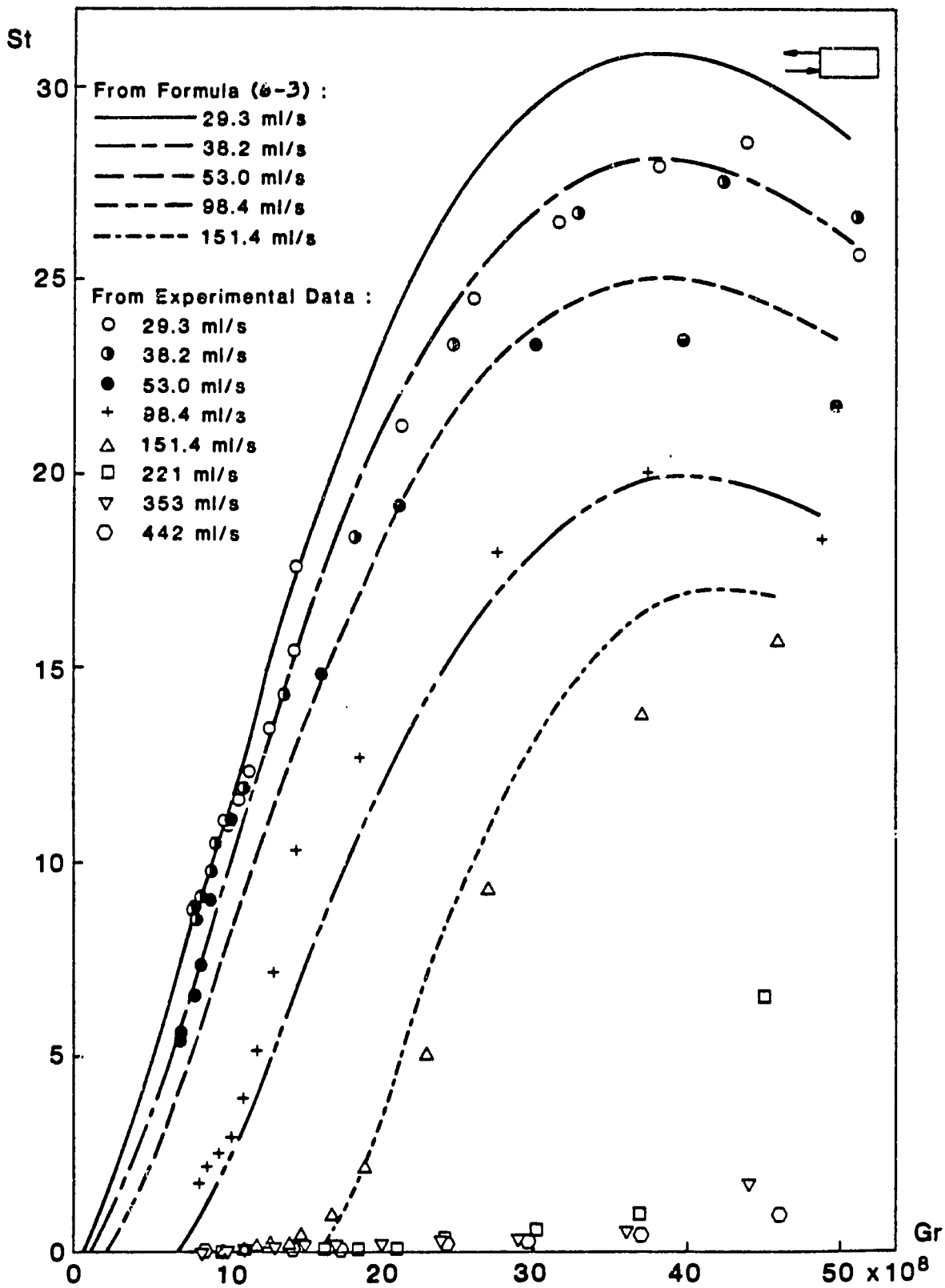

Fig. 6.21:Correlation of Stratification Coefficient St Data for Same-side Configuration Continuous Output

$$St = \left[\frac{1.906\times10^{-12}}{Re^{0.355}} \; \frac{(Gr-16.152Re^2)\; Gr_o}{Gr_o-16.52Re^2} \right]^{1.571} \cdot$$

$$\exp\left[-0.4057\times10^{-9} \; \frac{(Gr-16.152Re^2)\; Gr_o}{Gr_o-16.52Re^2} \right] \qquad (6.3)$$

where Gr_o is the value of Gr when the load flow begins. The mean deviation, Dev, = 12.3% where

$$Dev = \left[\frac{1}{n} \sum_{i=1}^{n} \left[\frac{St_{i,\ experiment} - St_{i,\ computation}}{St_{i,\ computation}} \right]^2 \right]^{\frac{1}{2}}$$

For the opposite-side configuration:

$$St = \left[\frac{0.869\times10^{-12}}{Re^{0.257}} \; \frac{(Gr-16.152Re^2)\; Gr_o}{Gr_o-16.152Re^2} \right]^{1.571} \cdot$$

$$\exp\left[-0.4057\times10^{-9} \; \frac{(Gr-16.152Re^2)Gr_o}{Gr_o-16.152Re^2} \right] \qquad (6.4)$$

The mean deviation is 10.3%.

From the above formulas, for $Gr < 16.152Re^2$, St is less than zero and no stratification occurs. That means that the inertial force is large enough to eliminate the effect of bouyancy. At that time it is the fully mixed condition. For $Gr > 16.152Re^2$, stratification exists.

In a comparison of Eqns. (6.3) and (6.4), it is seen

that the effect of make-up water inertial force is the same-side configuration ($Re^{-0.355}$) is greater than in the opposite-side configuration ($Re^{-0.257}$).

CHAPTER 7

RESULTS FOR PERIODIC LOAD FLOW

The experimentally determined stratification coefficient, St, and extraction efficiency, COEF, are plotted verse output volume in Figs. 7.1 to 7.4. As described in Chapter 4 the temperature distribution was determined just before the start of each flow and then at the end of each flow.

The criterion for stratification proposed for the continuous output was that the system was considered stratified if St > 5, mixed for St < 1 and in transition for 1 < St < 5. It is clear from Figs. 7.1 and 7.2 that for the six flows considered here only the stratified and transition regions exist. For the three flow rates up to 151.4 ml/s (2.4 gpm) in the same-side configuration and for the four flow rates up to 221 ml/s (3.54 gpm) for the opposite-side configuration the tank remains stratified. For the other flow rates up to 442 ml/s (7 gpm) St reaches a quasi-steady limit above 1, and hence the tank is not completely mixed.

In comparing Figs. 7.1 with 7.2, and 7.3 with 7.4, it is seen that they all follow the same trend as the continuous output: 1) The higher the output flow rate, the lower stratification coefficient, St; 2) The extraction efficiency, COEF, in the same-side cofiguration is higher than the opposite-side configuration for the corresponding output flow rate, even though the St for the same-side configuration is lower than for the opposite-side configuration.

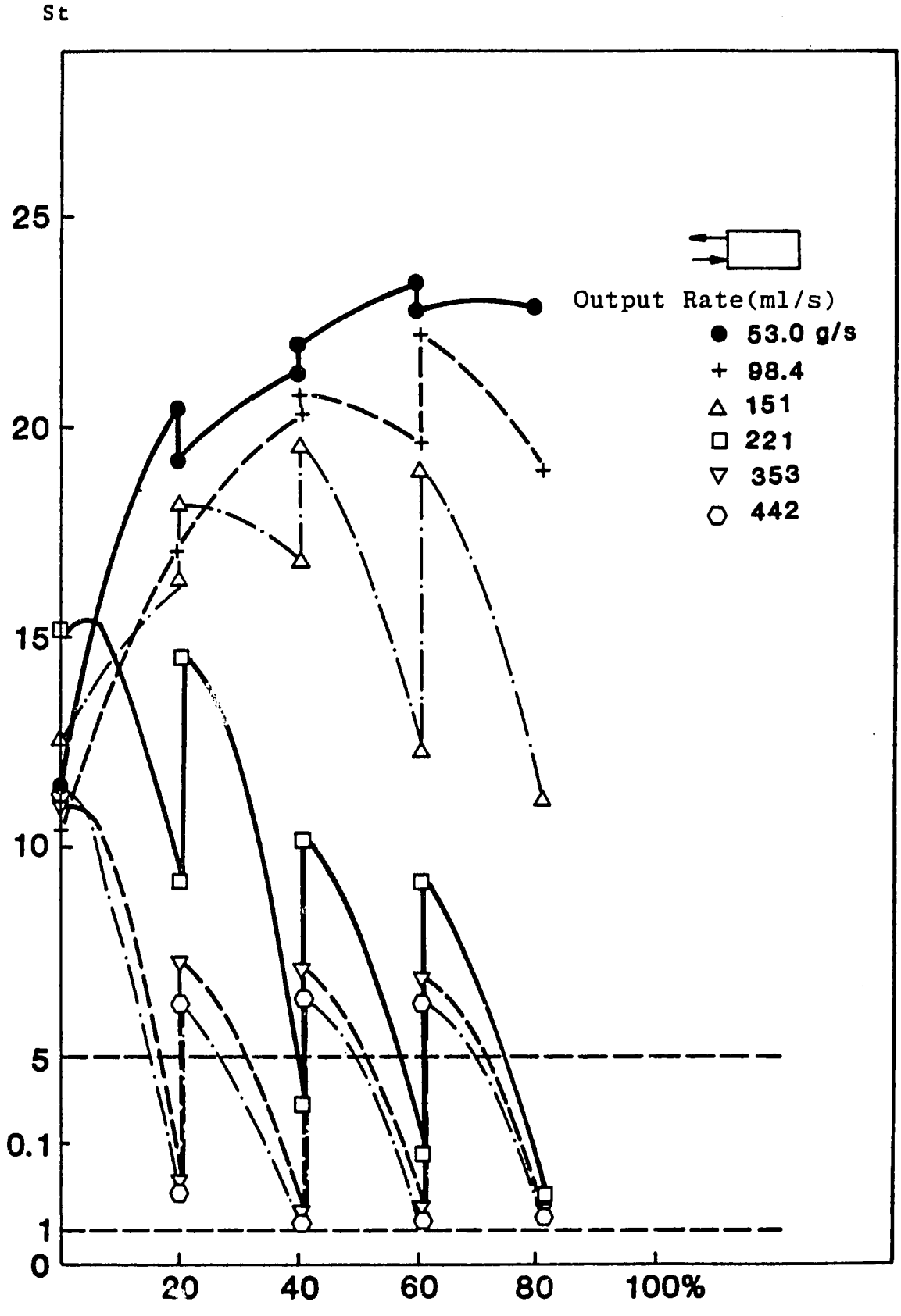

Fig.7.1 Stratification Coefficient History for Periodic Output

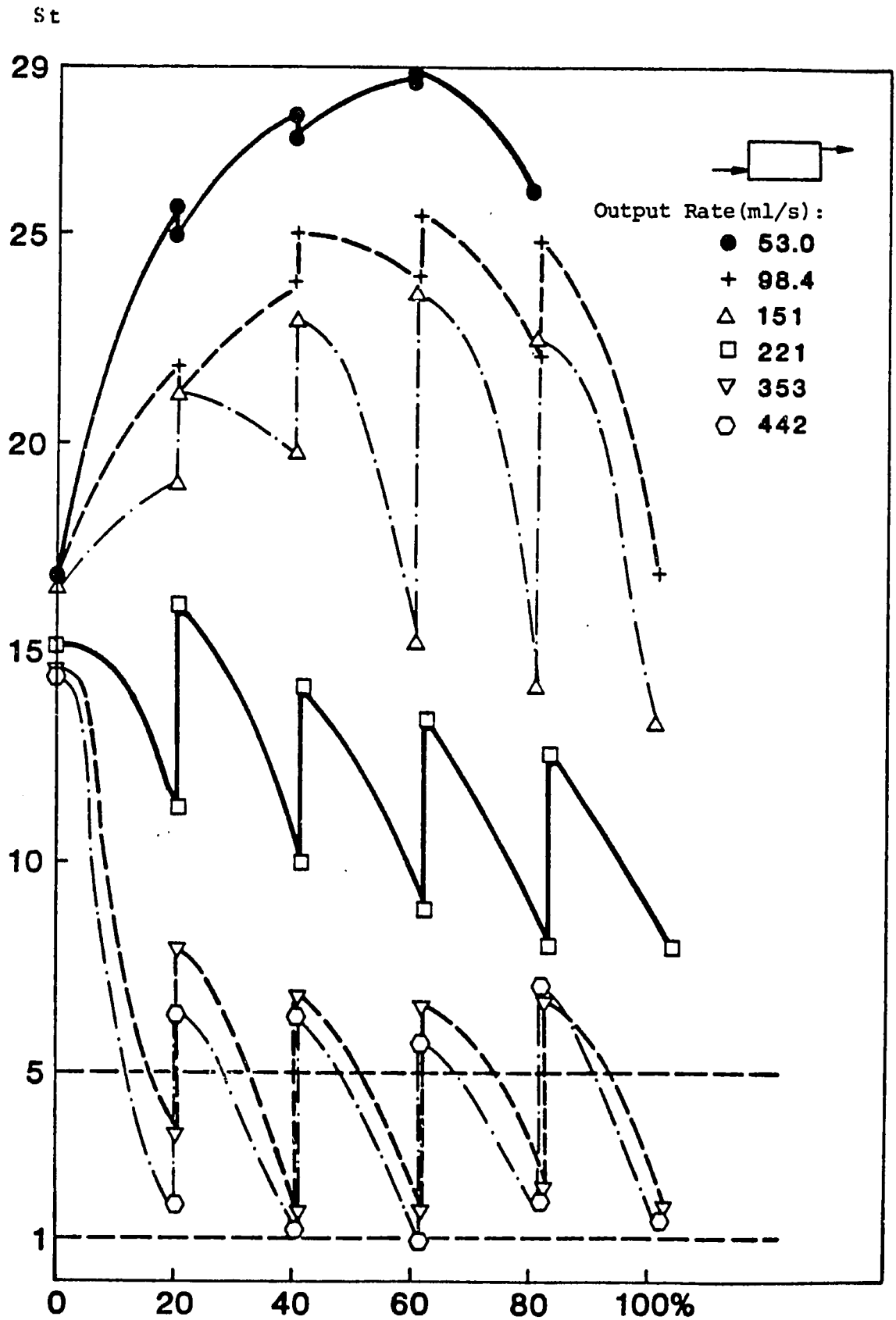

Fig. 7.2: Stratification Coefficient History for Periodic Output

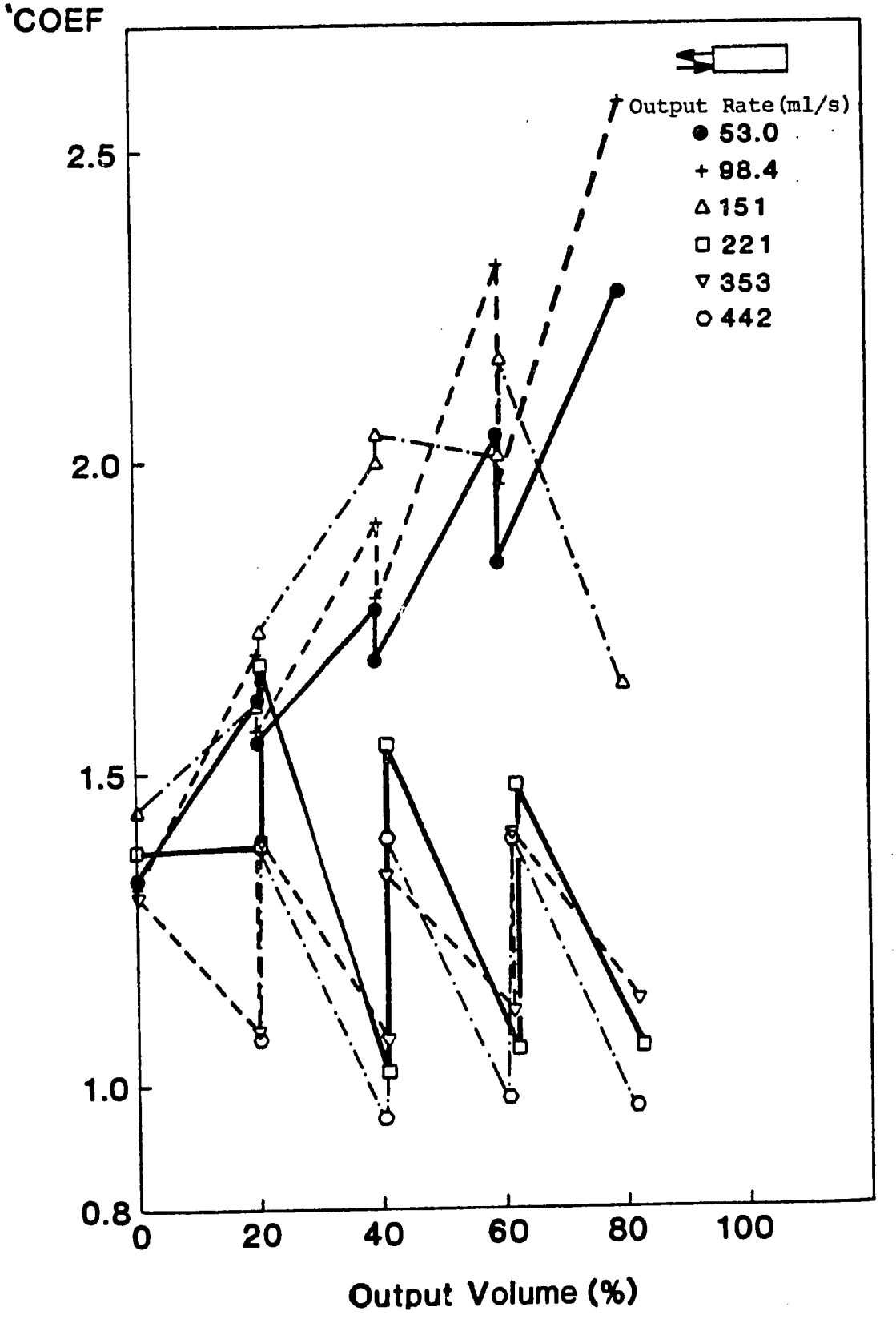

Fig. 7.3: Extraction Coeficient History for Periodic Output

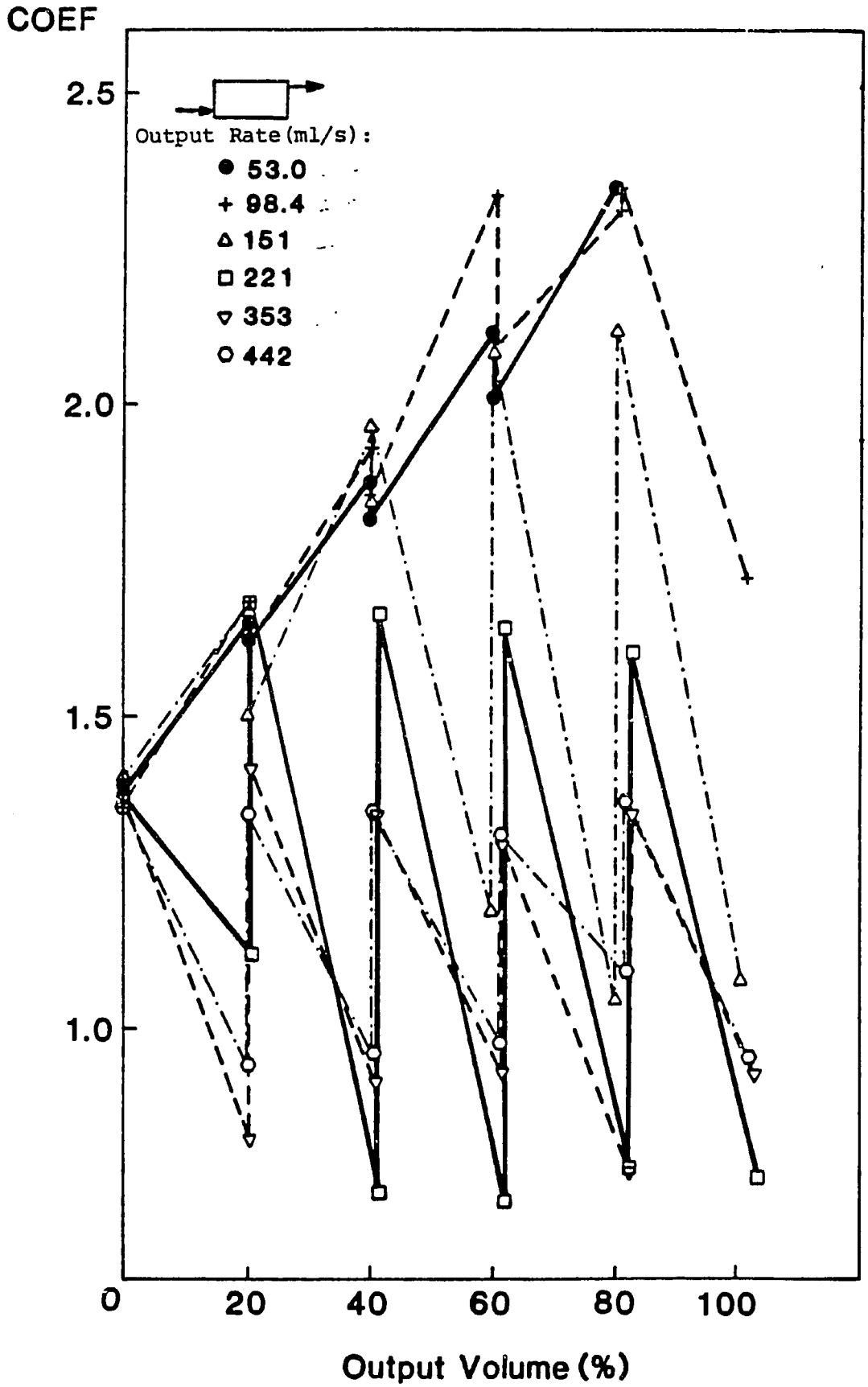

Fig. 7.4: Extraction Coeficient History for Periodic Output

Because the output is periodic, the water in the tank recovers a measure of thermal stratification between drains. Hence the St of periodic output is higher than for the continuous output. In the Figs. 7.1, and 7.2, the St is always greater than 1.

In Fig. 7.5, the stratification coefficient is plotted as a function of Grashof number for both the periodic output and the continuous output for the same-side configuration. The two results are very close. The mean deviation is less than 10%. It is also compared with the correlating equation for the continuous flow. The curve fits the data well; the mean deviation is 7.2%.

The same information is plotted in Fig. 7.6 but for the opposite-side configuration. The results are again very close with the same magnitude of mean deviation as the above (less than 10% for data, 6.3% for the equation). These results indicate that the continuous flow correlations can be used for the corresponding periodic flow. The values of St from periodic output are usually a little higher at the same value of Gr than for the continuous output.

The average water temperature in the tank, the extraction efficiency, COEF, the stratification coefficient, St, for two different configurations at the output flow rates of 53.0, 151.4 and 353 ml/s (0.84, 2.33 and 5.6 gpm) are shown in Figs. 7.7, 7.8 and 7.9, respectively. A better understanding of why these curves have their particular shapes can be gained by studying the transient behavior of the tem-

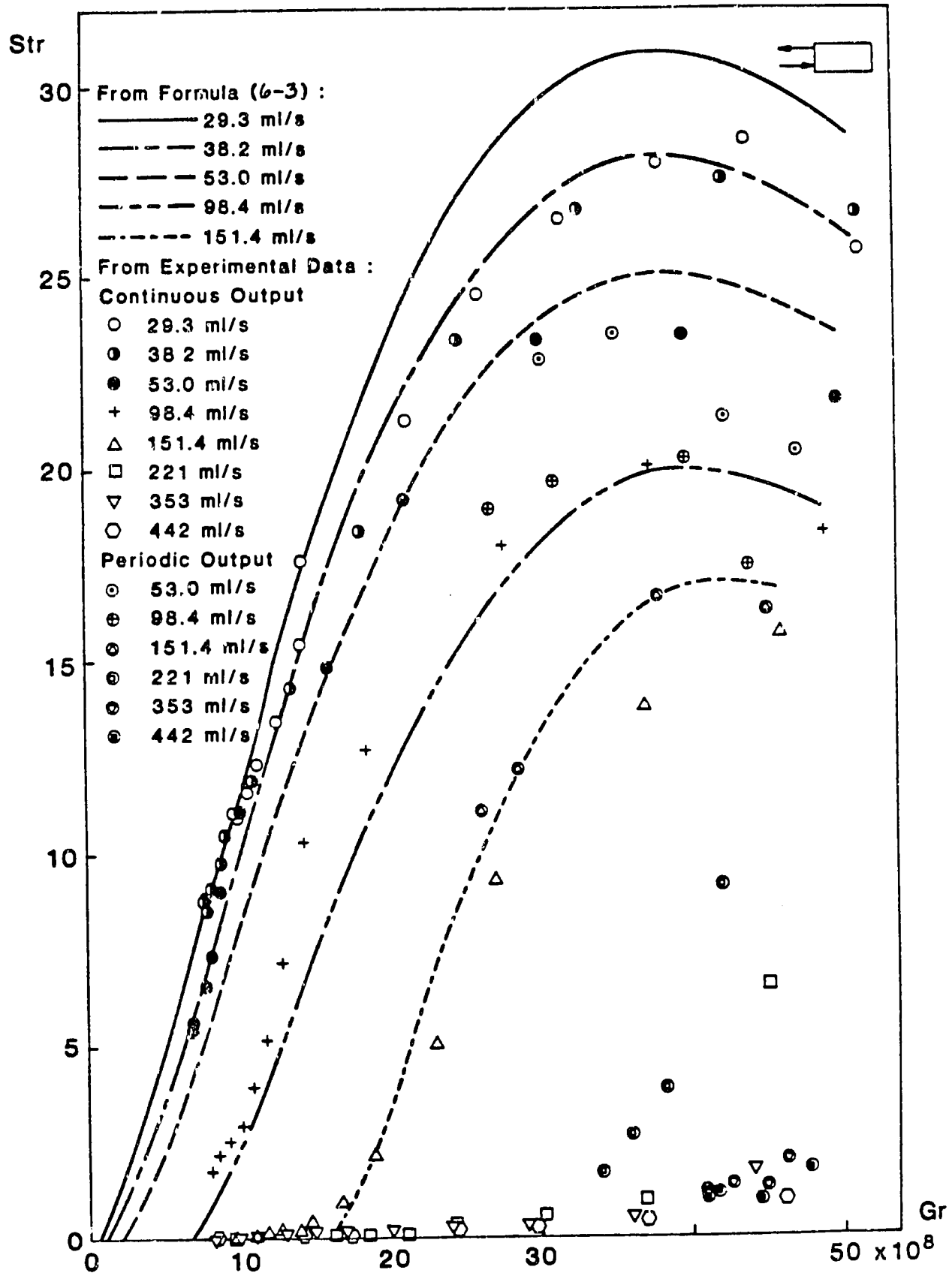

Fig. 7.5: Correlation of Stratification Coefficient St Data for Same-side Configuration Continuous and Periodic Output

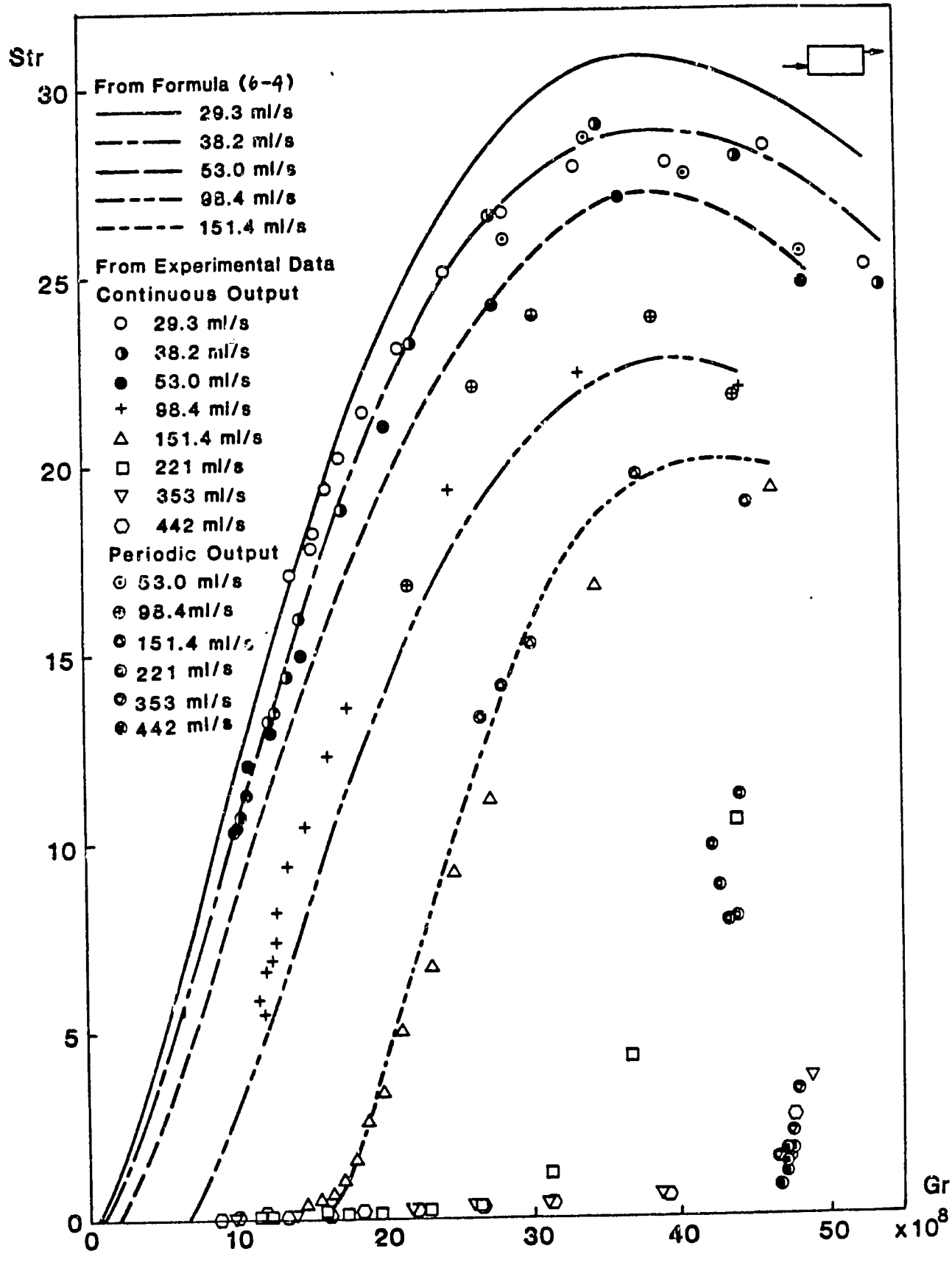

Fig. 7.6: Correlation of Stratification Coefficient St Data for Opposite-side Configuration Continuous and Periodic Output

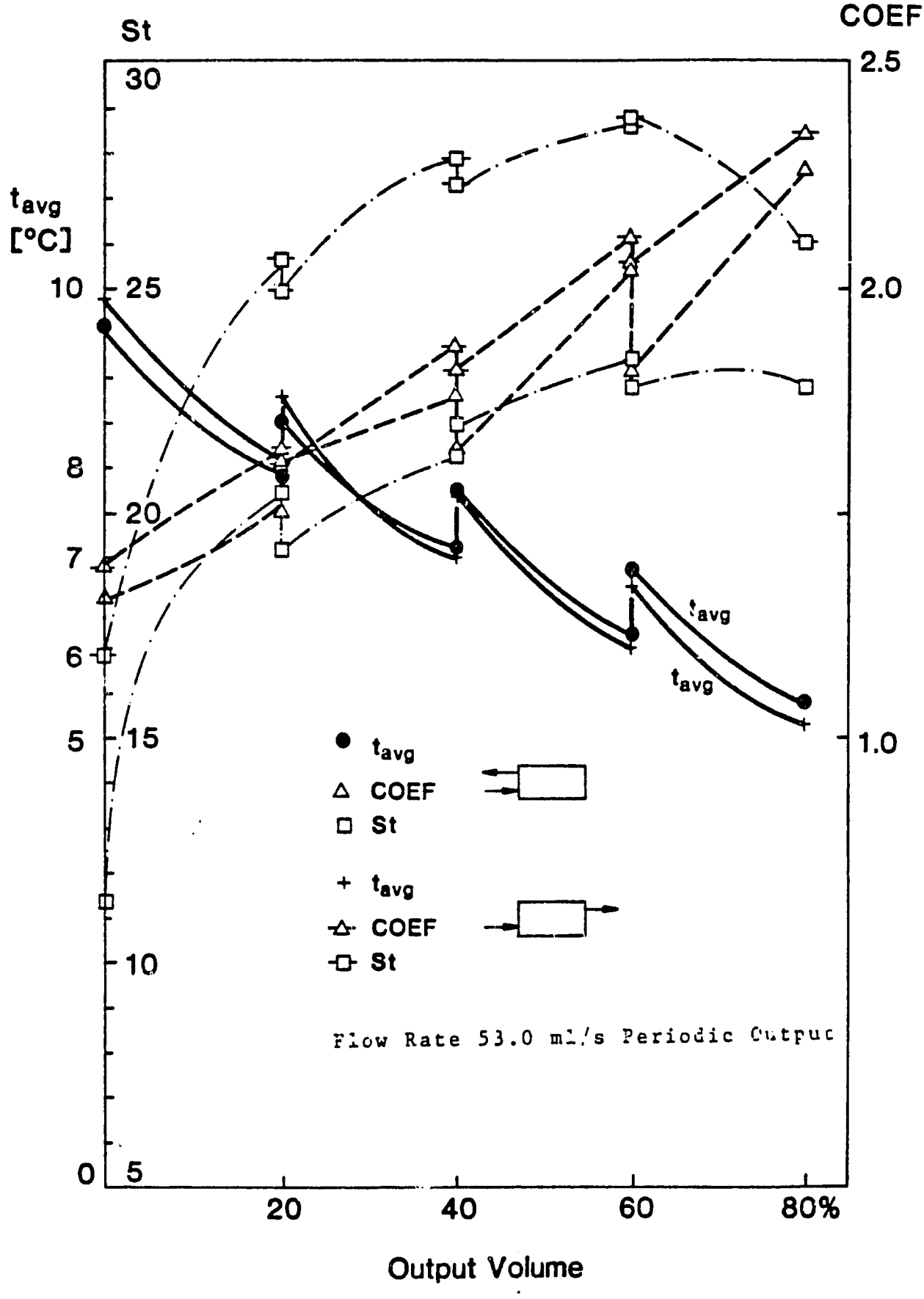

Fig. 7.7: A Comparison Between The Data for The Two Different Configurations

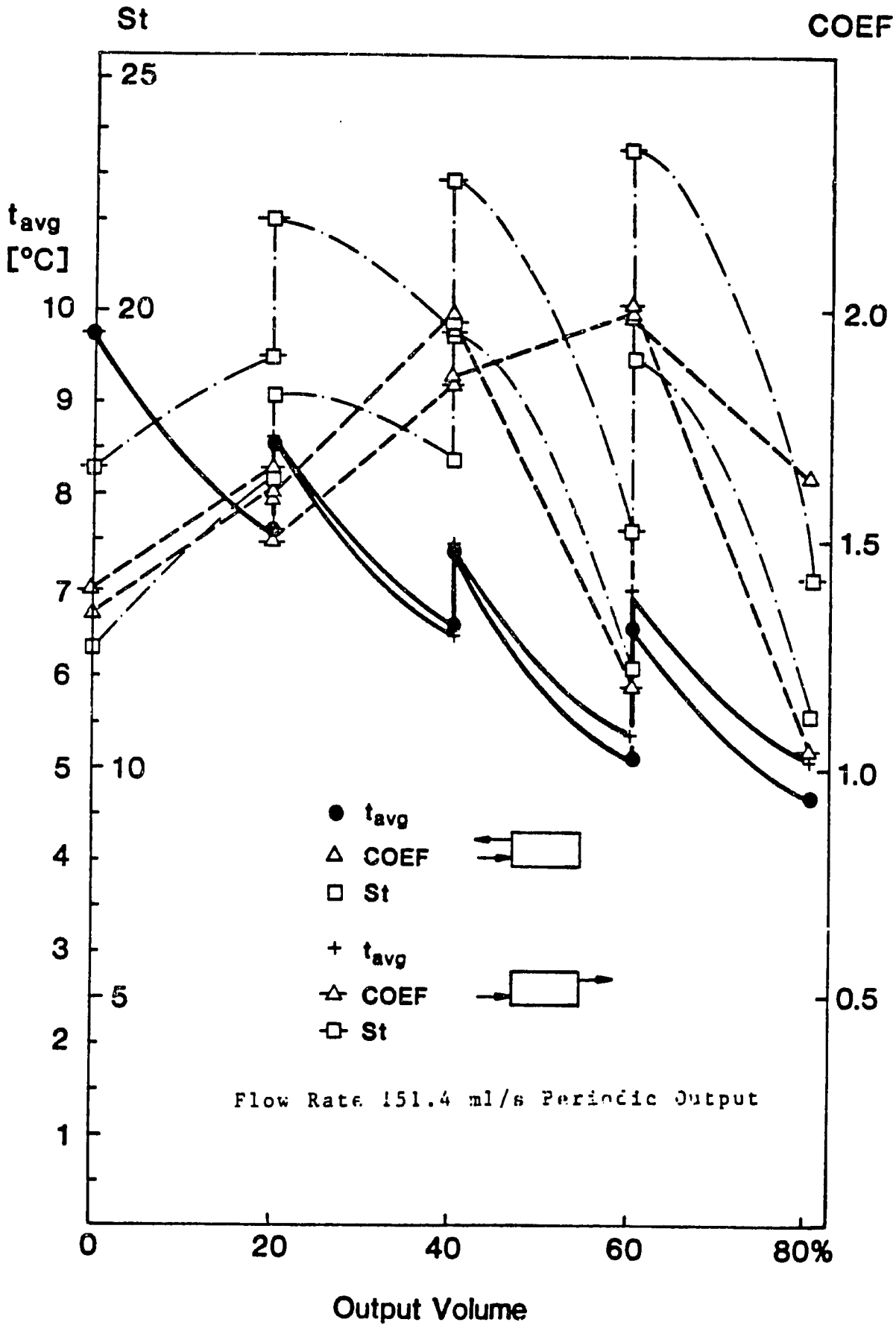

Fig. 7.8: A Comparison Between The Data for The Two Different Configurations

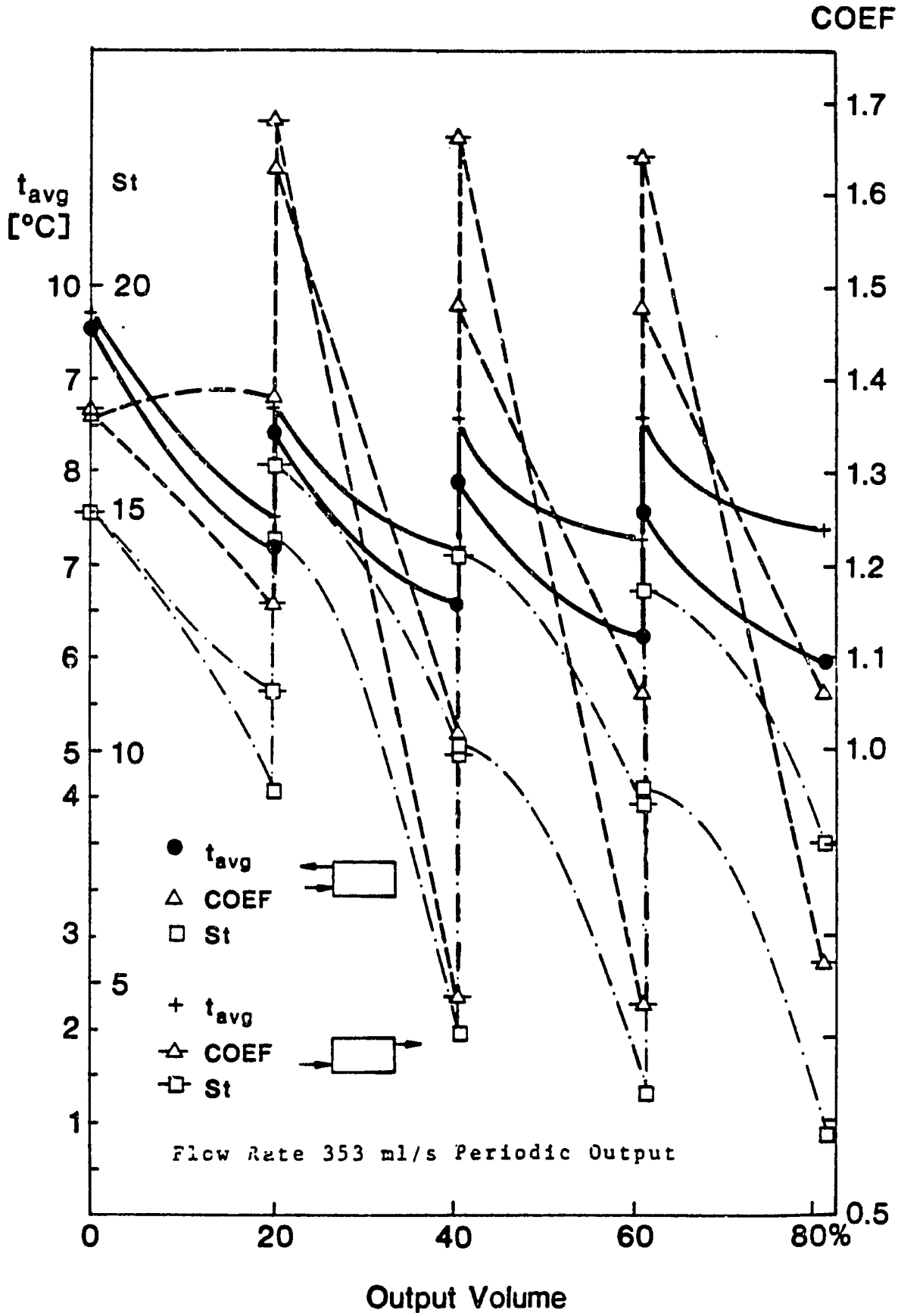

Fig. 7.9: A Comparison Between The Data for The Two Different Configurations

perature distributions.

Figures 7.10 through 7.17 depict the temperature distributions at different times for the 151.4 ml/s (2.3 gpm) output flow rate for both geometric configurations. From Figs. 7.10 and 7.14, it is seen that the initial temperature distributions for both configurations are almost the same. At the end of 20% volume output, from Figs. 7.11 and 7.15, it can be seen that the thermal stratification was still well-maintained at the beginning of the drain. Because the make-up cool water entered the bottom of the tank, the average temperature decreased, but the temperatures at the bottom and at the top remained almost unchanged. In fact, the thermal stratification improved. The values of St and COEF increased (Fig. 7.8). The temperature near the outlet in the opposite-side configuration was higher than for the same-side configuration.

The stratification recovery is shown in Figs. 7.12 and 7.16. Because of the entrainment (or mixing) effect of the make-up water jet, the temperatures at the bottom increased from 0.5 to 1.1°C, and the temperatures at the top increased accordingly. However, the average temperature decreased about 1.2°C from the beginning of the experiment. Thus a large portion of the bottom part of the tank became essentially isothermal and the value of St was higher (Fig. 7.8).

The Figs. 7.13 and 7.17 give the temperature distributions at the end of 40% volume output. From these figures the following can be concluded:

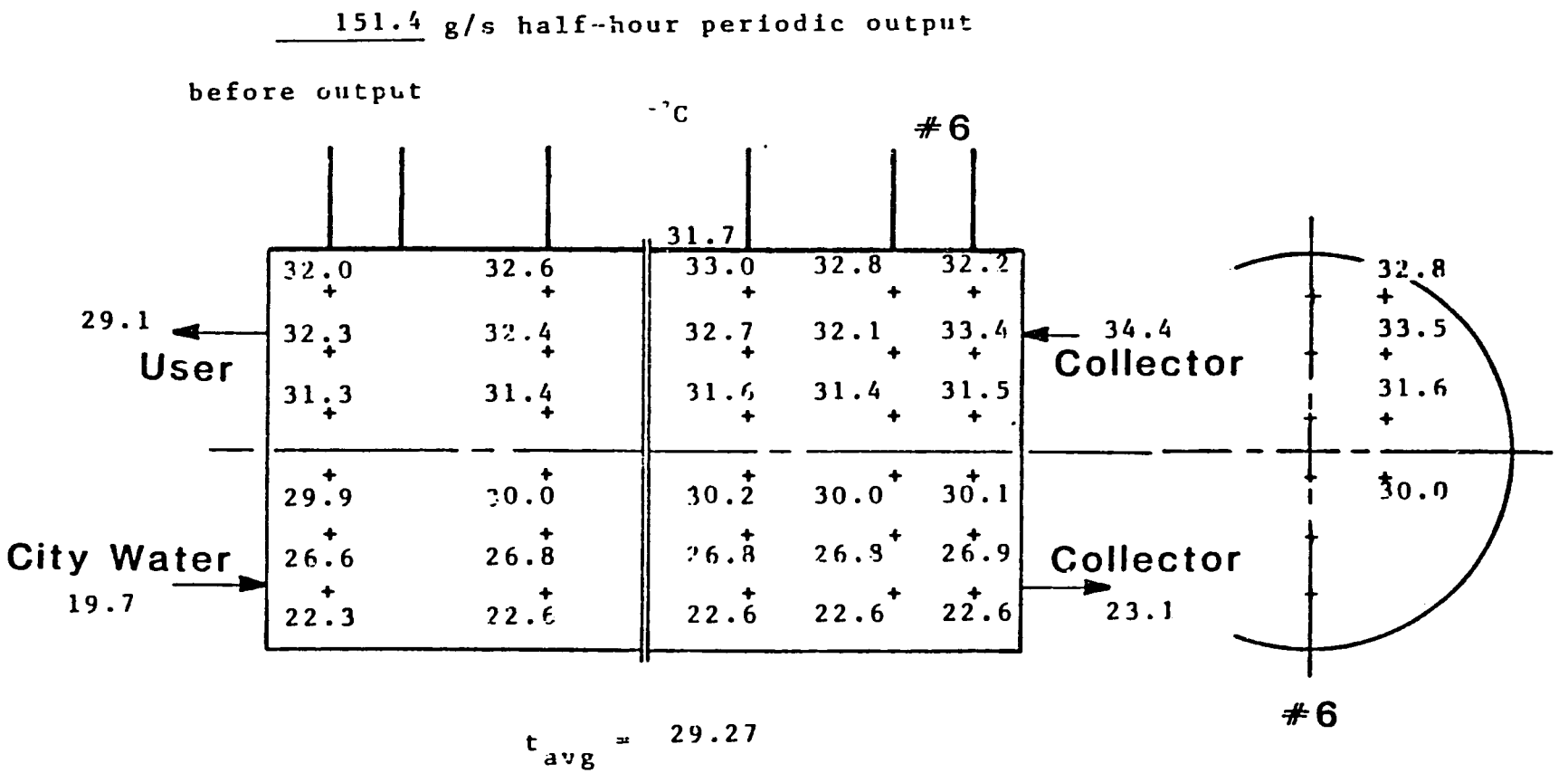

Fig. 7.10: The Temperature Distribution in The Tank

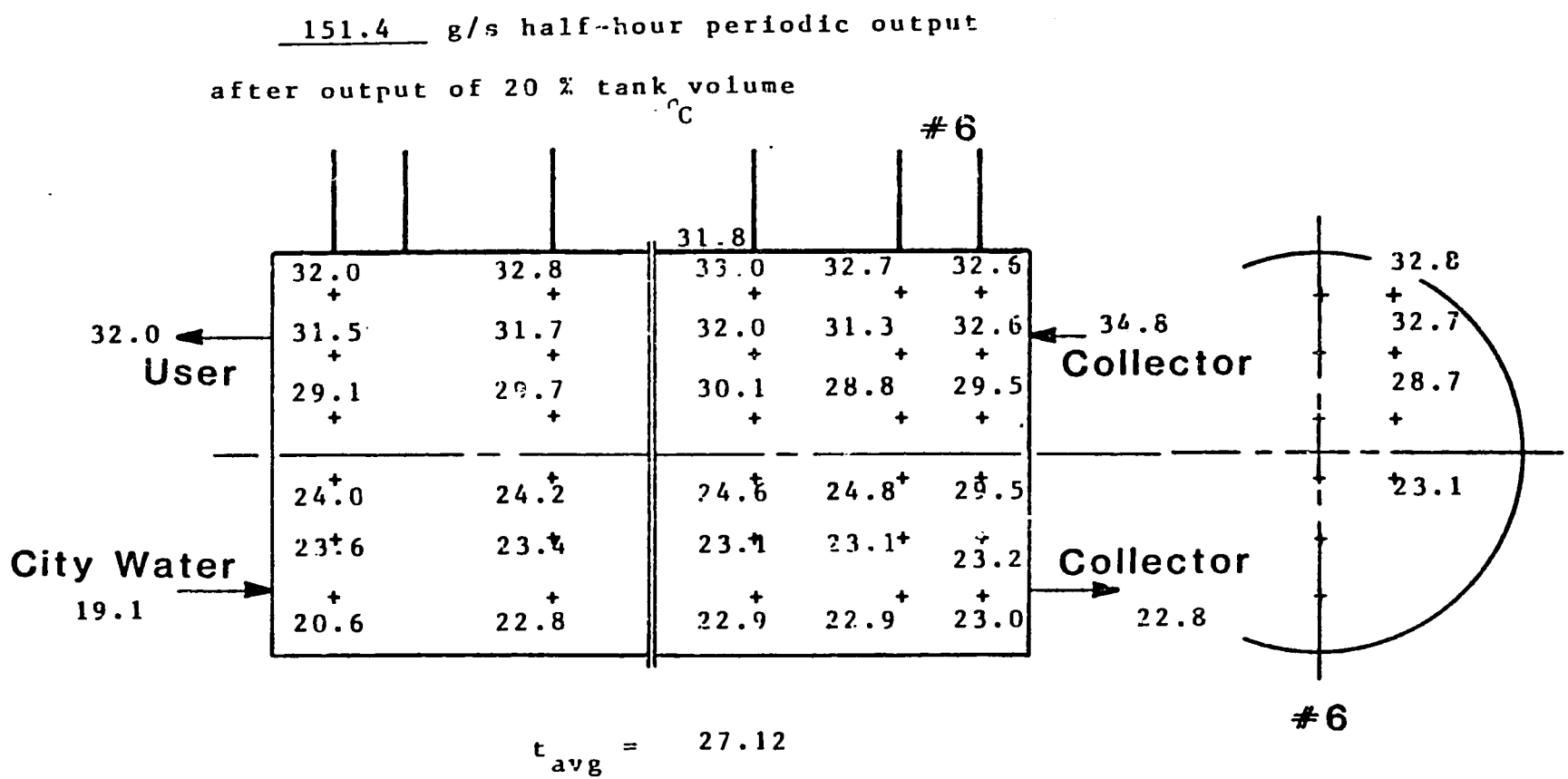

Fig. 7.11: The Temperature Distribution in The Tank

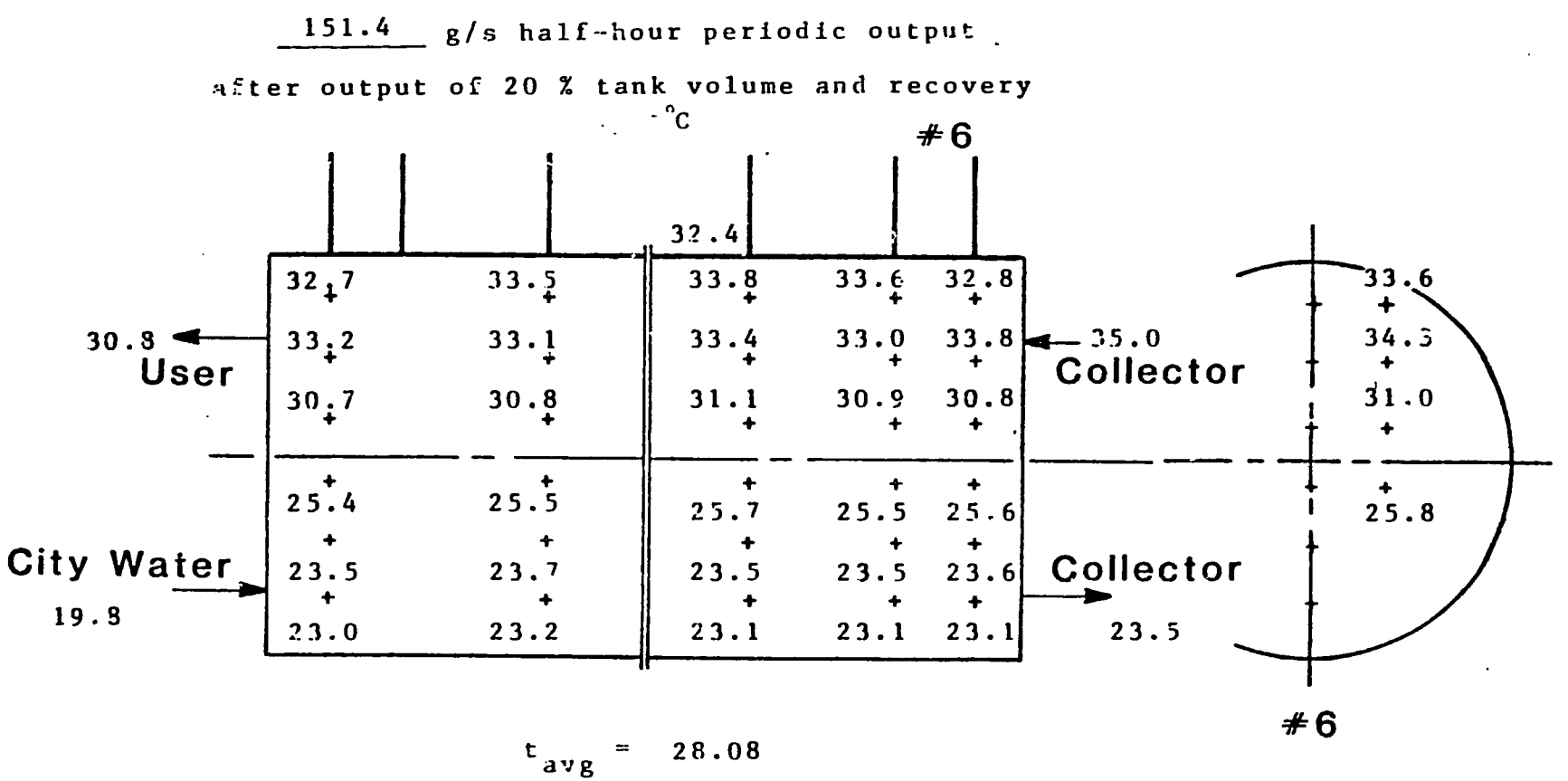

Fig. 7.12: The Temperature Distribution in The Tank

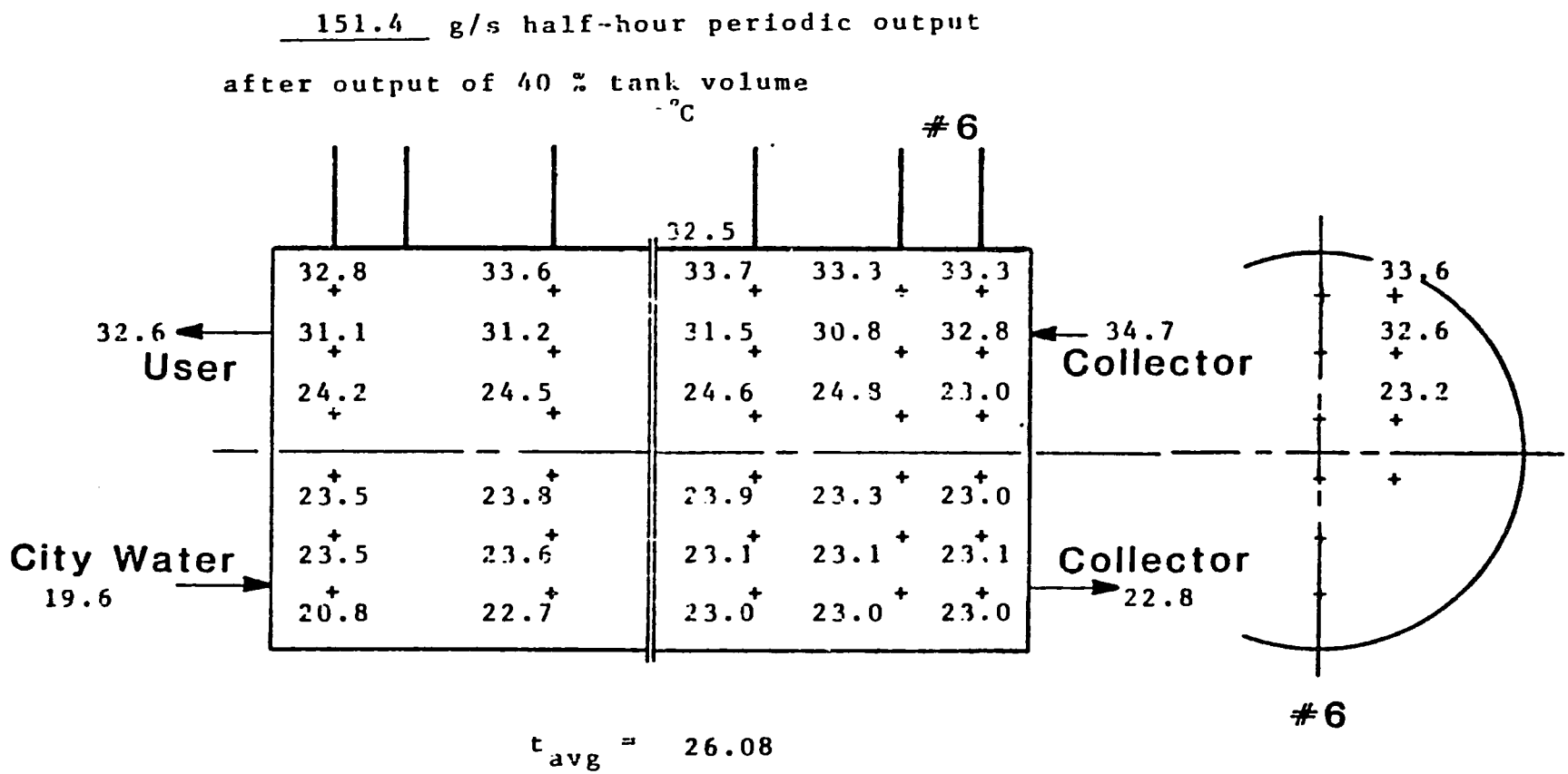

Fig. 7.13: The Temperature Distribution in The Tank

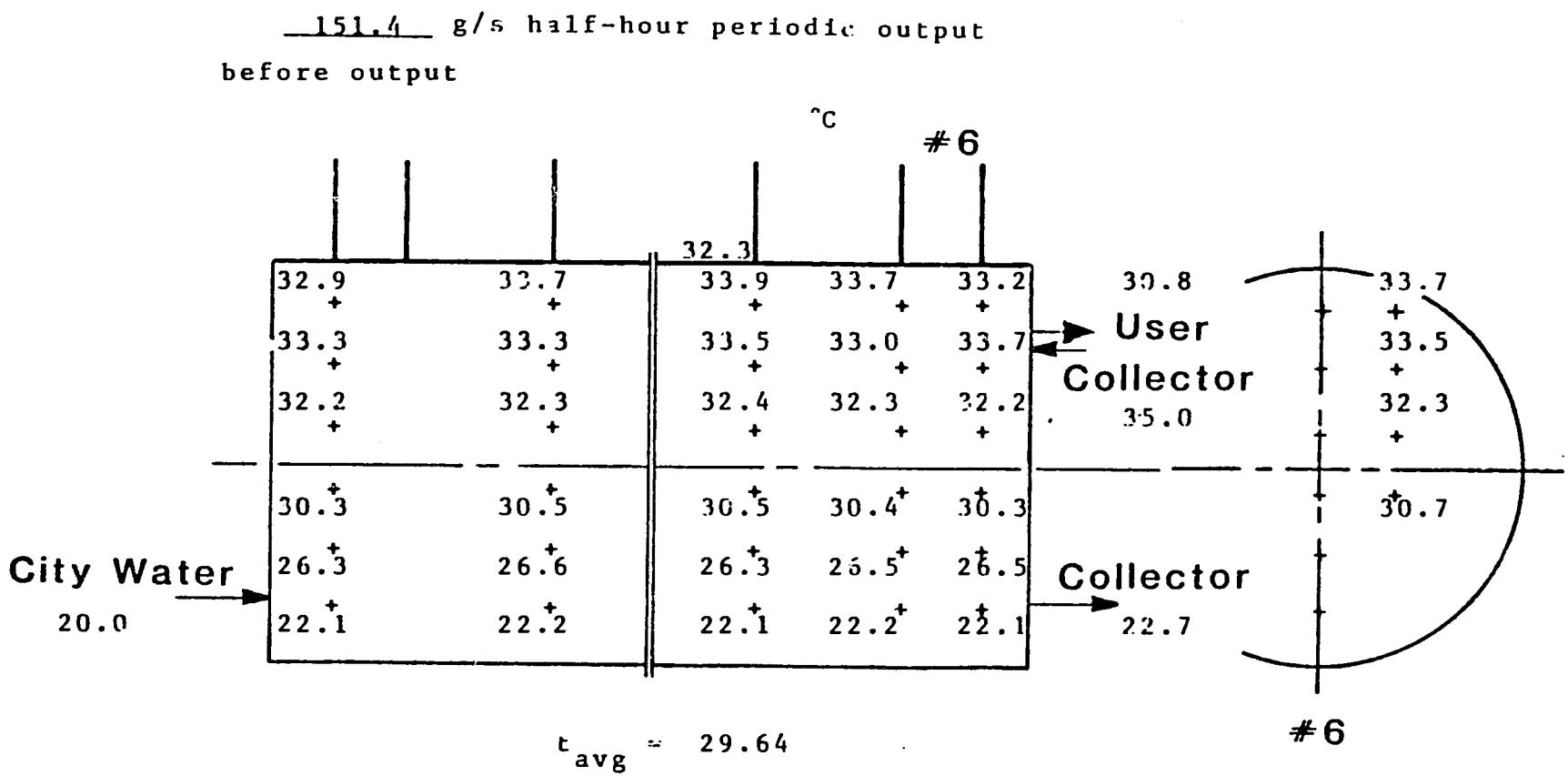

Fig. 7.14: The Temperature Distribution in The Tank

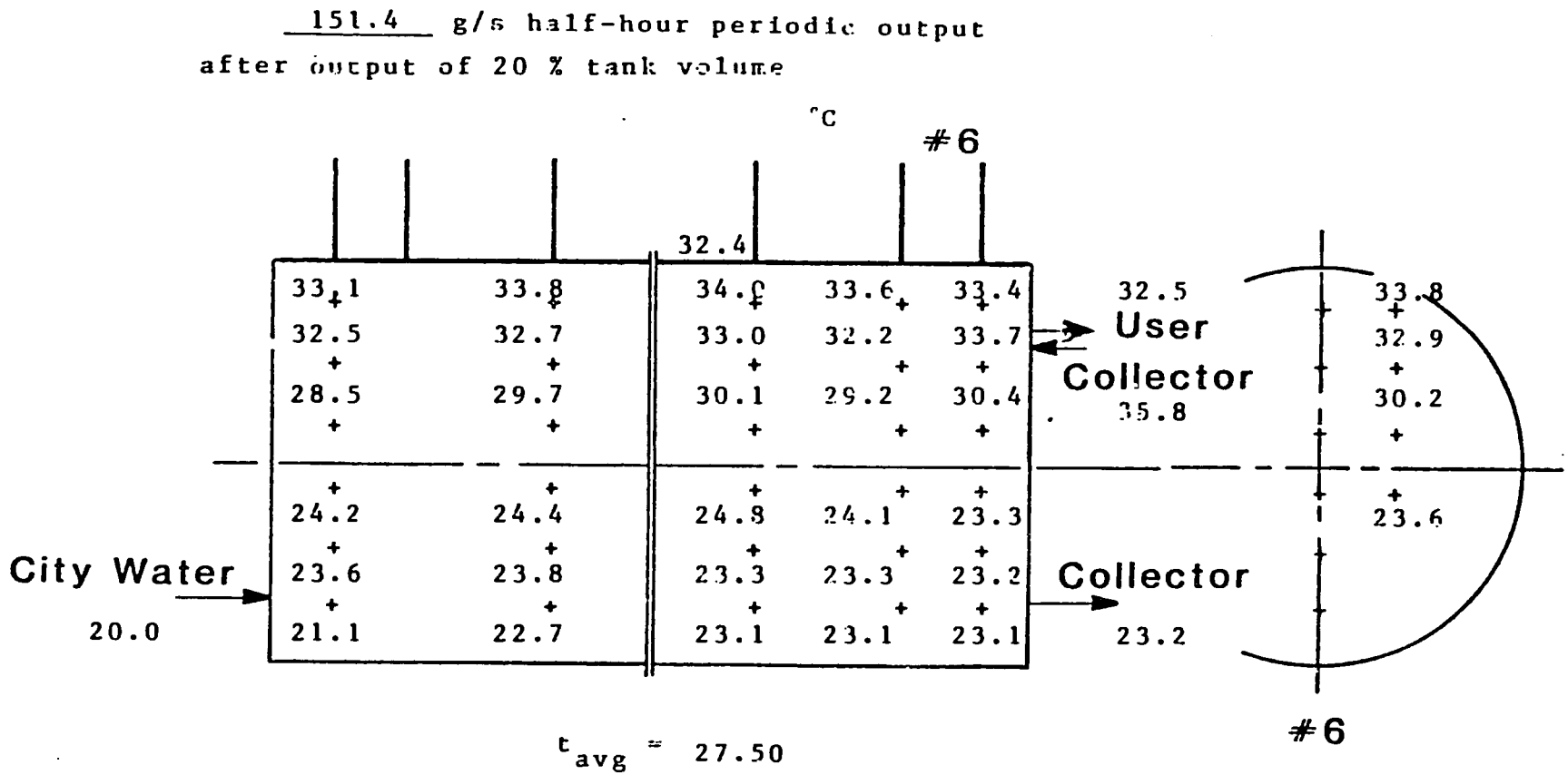

Fig. 7.15: The Temperature Distribution in The Tank

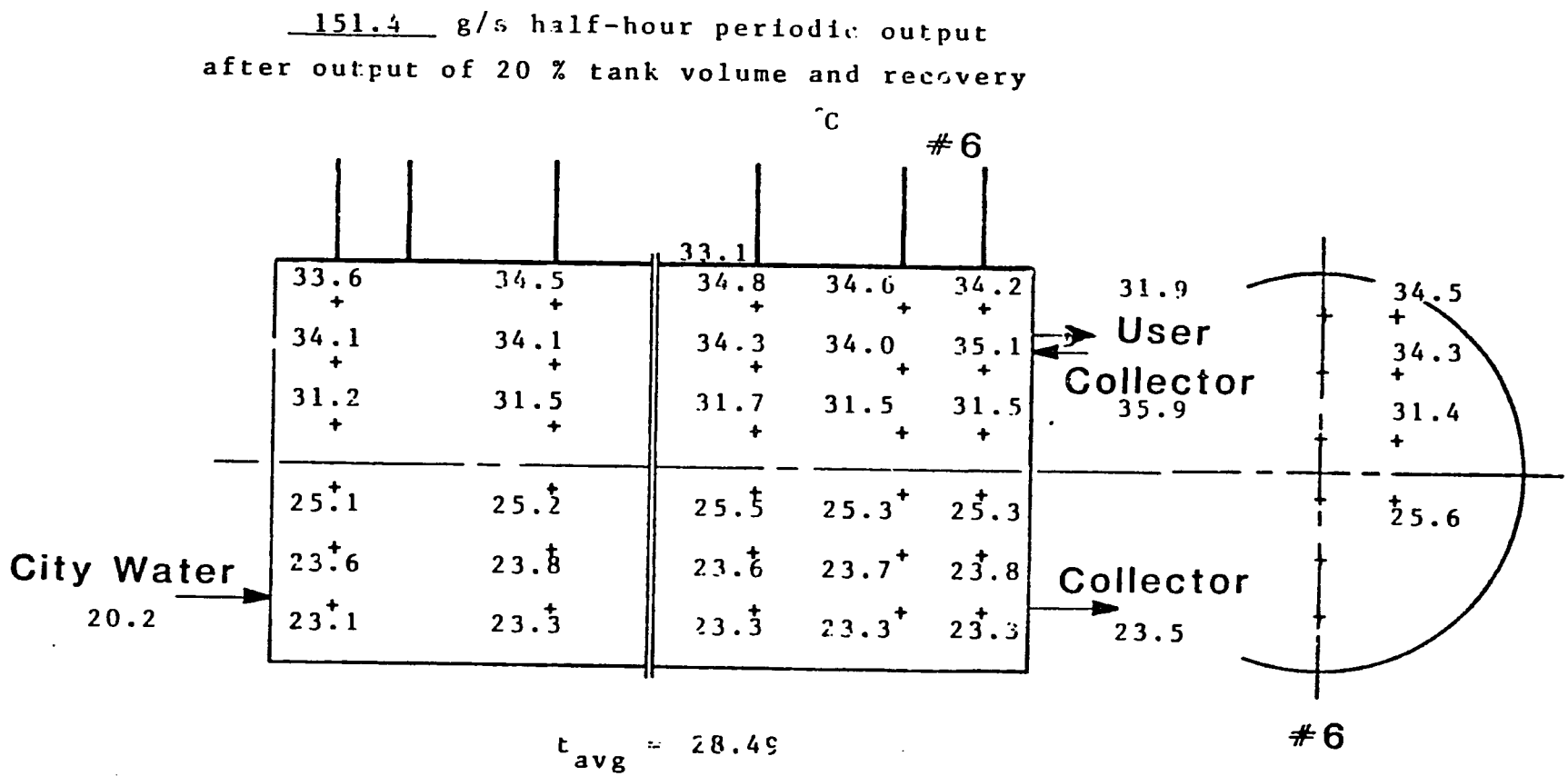

Fig. 7.16: The Temperature Distribution in The Tank

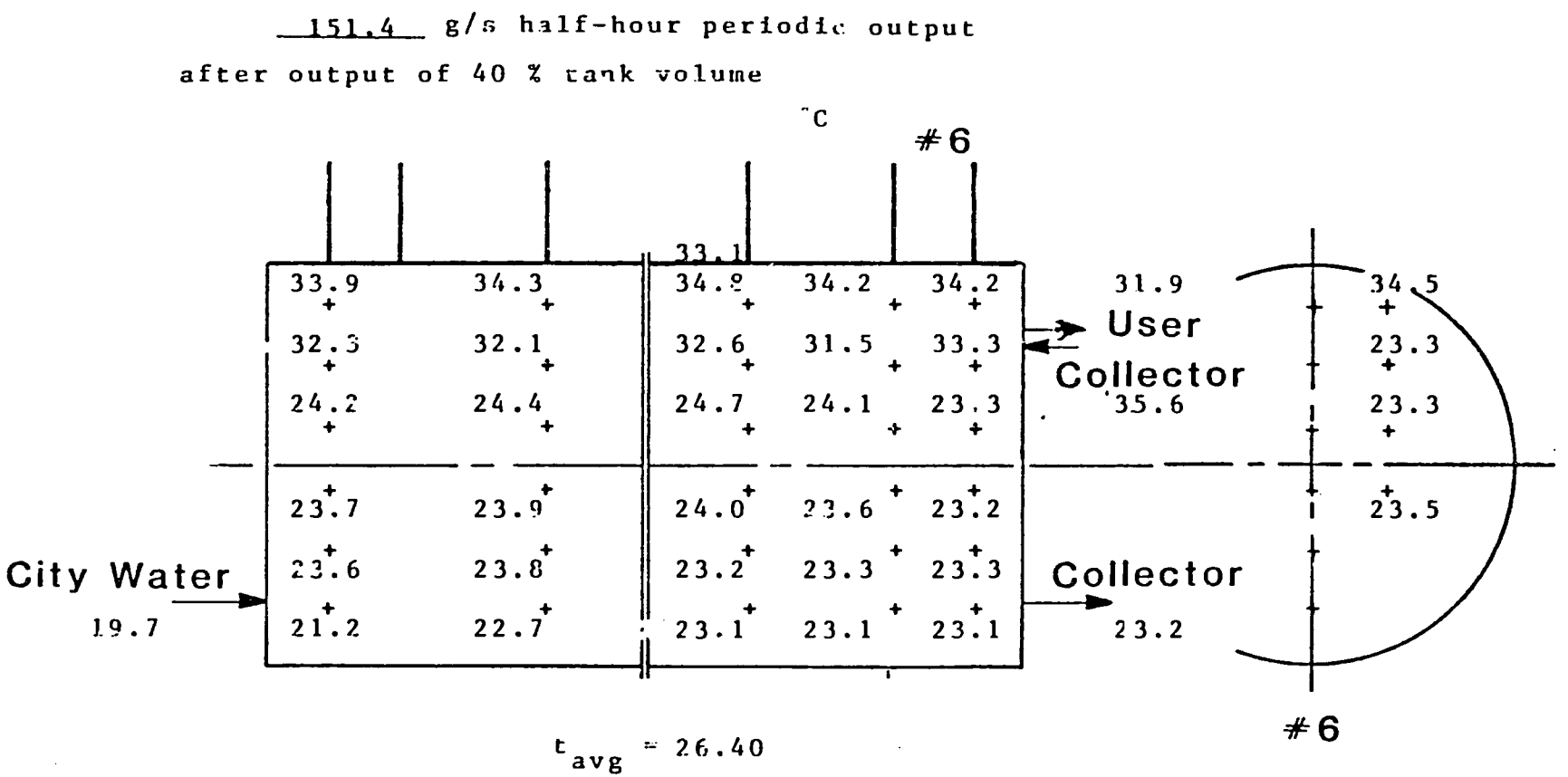

Fig. 7.17: The Temperature Distribution in The Tank

The stratification was well-maintained because no strong circulation or mixing occurred.

The cool make-up water at the time occupied over half the tank, and the temperature in this part was nearly uniform and close to the average temperature in the tank. Thus the stratification coefficient began to decrease. The region affected by the cool make-up water flow had reached the hot water outlet of the opposite-side configuration but remained far from the hot water outlet of the same-side configuration. Thus the temperature of the output hot water in the opposite-side configuration was lower than for the same-side configuration COEF in the opposite-side configuration dropped below that of the same-side configuration and remained so until the end of this experiment (Fig. 7.8).

Figures 7.18 to 7.23 give the temperature distributions in the same-side and opposite-side configurations at different times for the 353 ml/s (5.6 gpm) output flow rate.

Figures 7.22 and 7.23 give the temperature distributions before and after 20% of the tank volume has been exchanged. The temperature distributions for both configurations are almost the same. Both are approaching a uniform temperature distribution, since the make-up water formed a strong circulation and caused significant mixing.

As the make-up water issued into the tank, it entrained the surrounding water. In the initial region, the local temperature was close to the make-up water temperature. The jet boundaries expanded with the distance from the nozzle

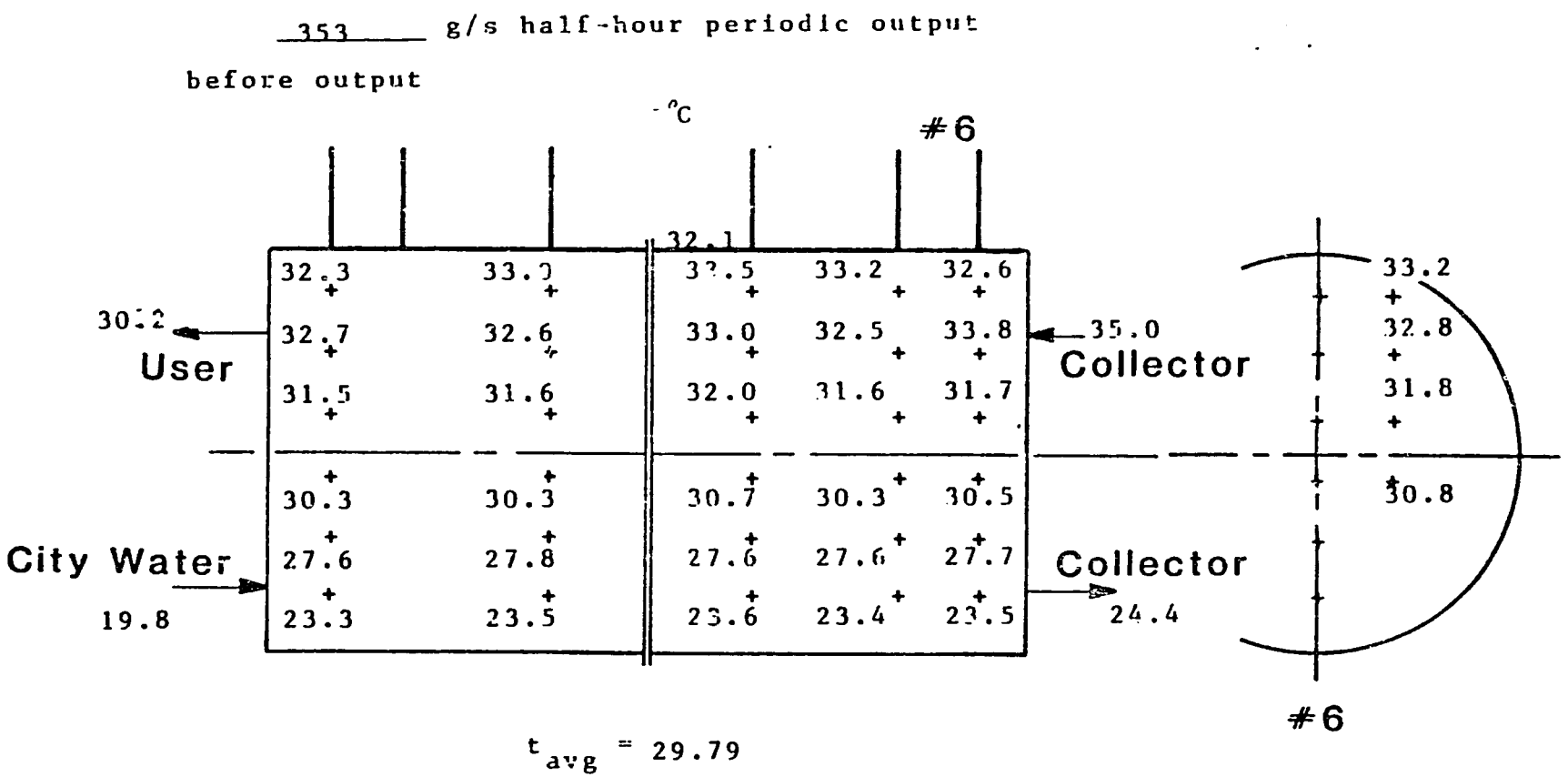

Fig. 7.18: The Temperature Distribution in The Tank

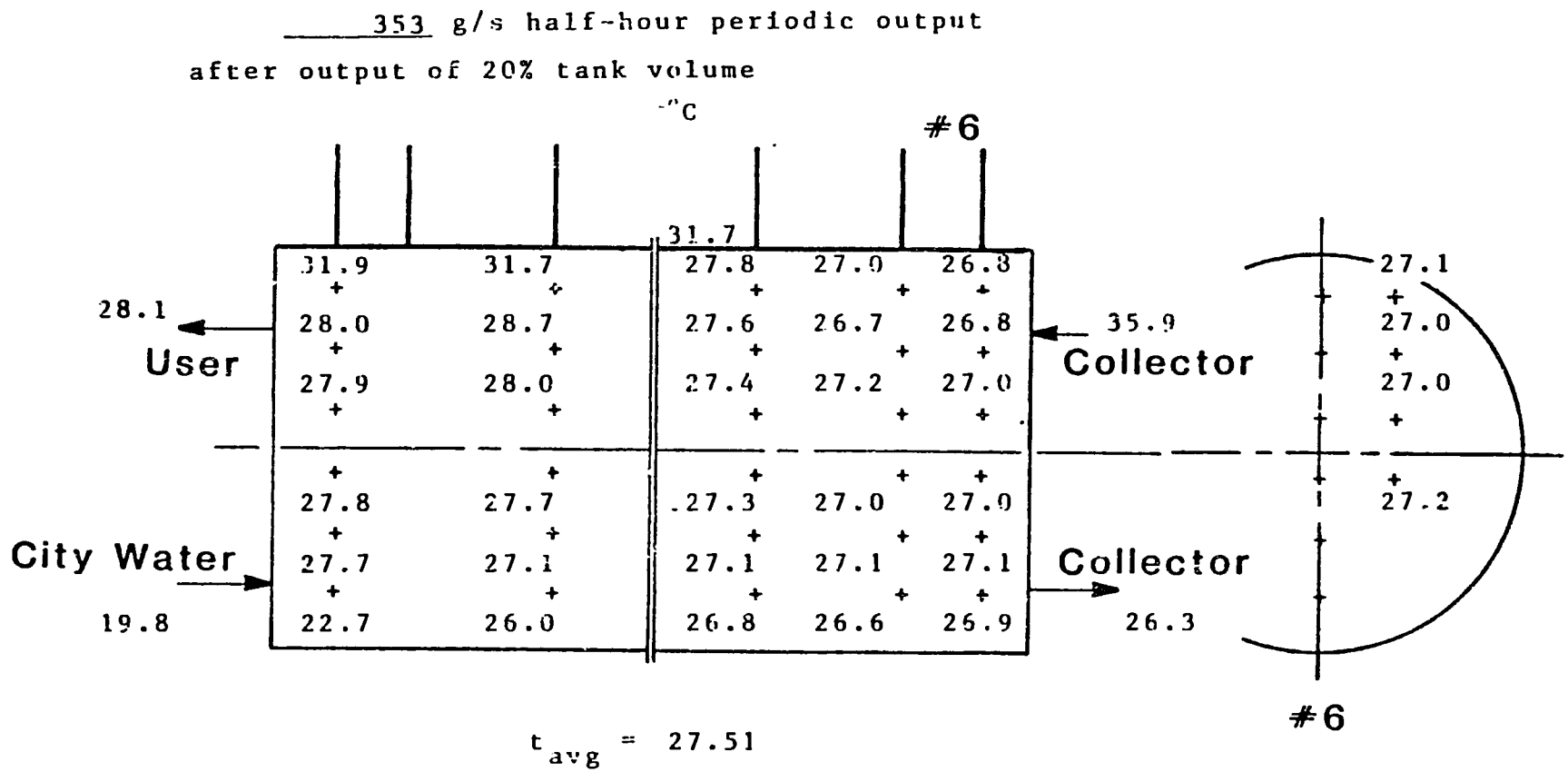

Fig. 7.19: The Temperature Distribution in The Tank

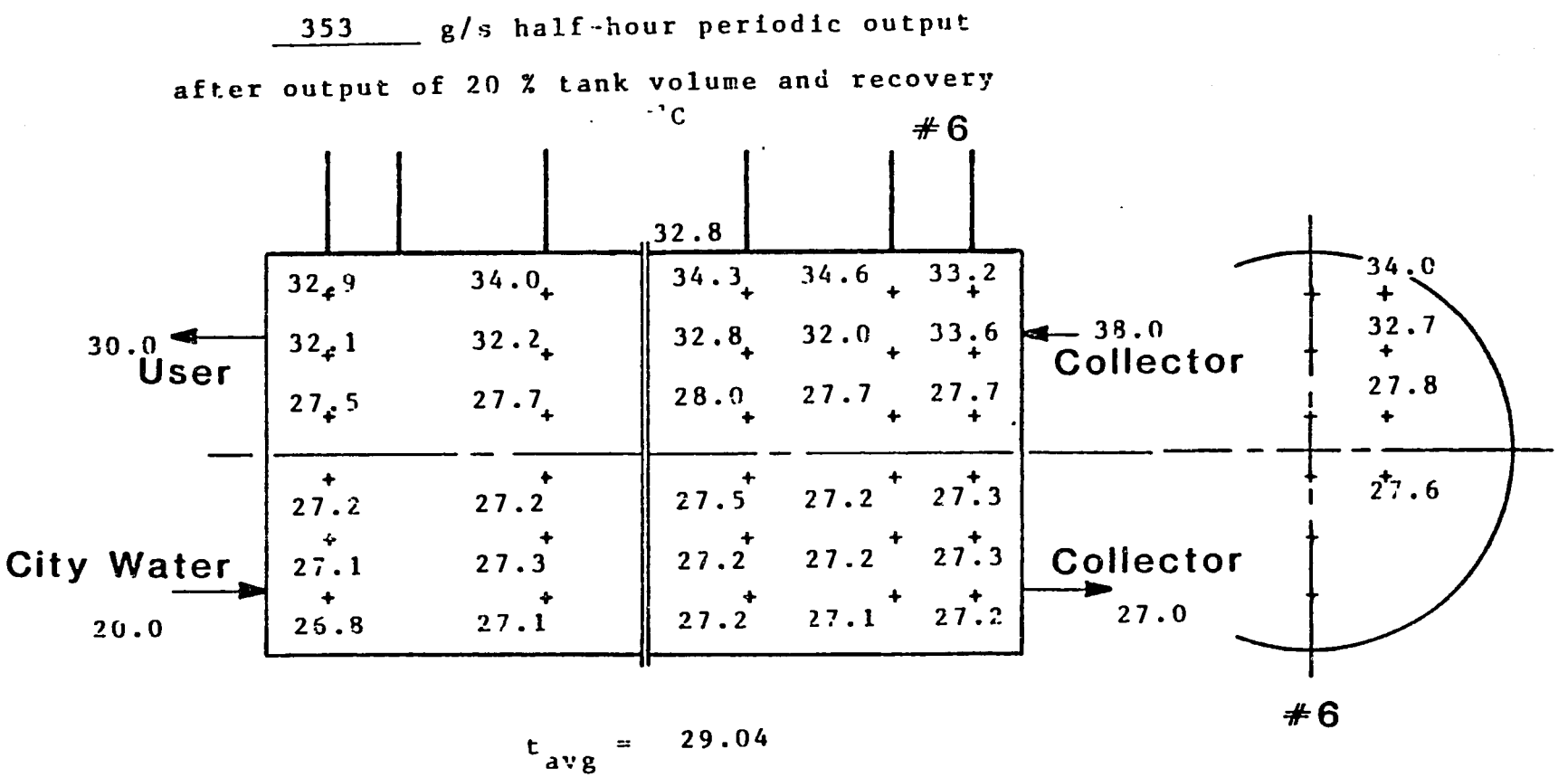

Fig. 7.20: The Temperature Distribution in The Tank

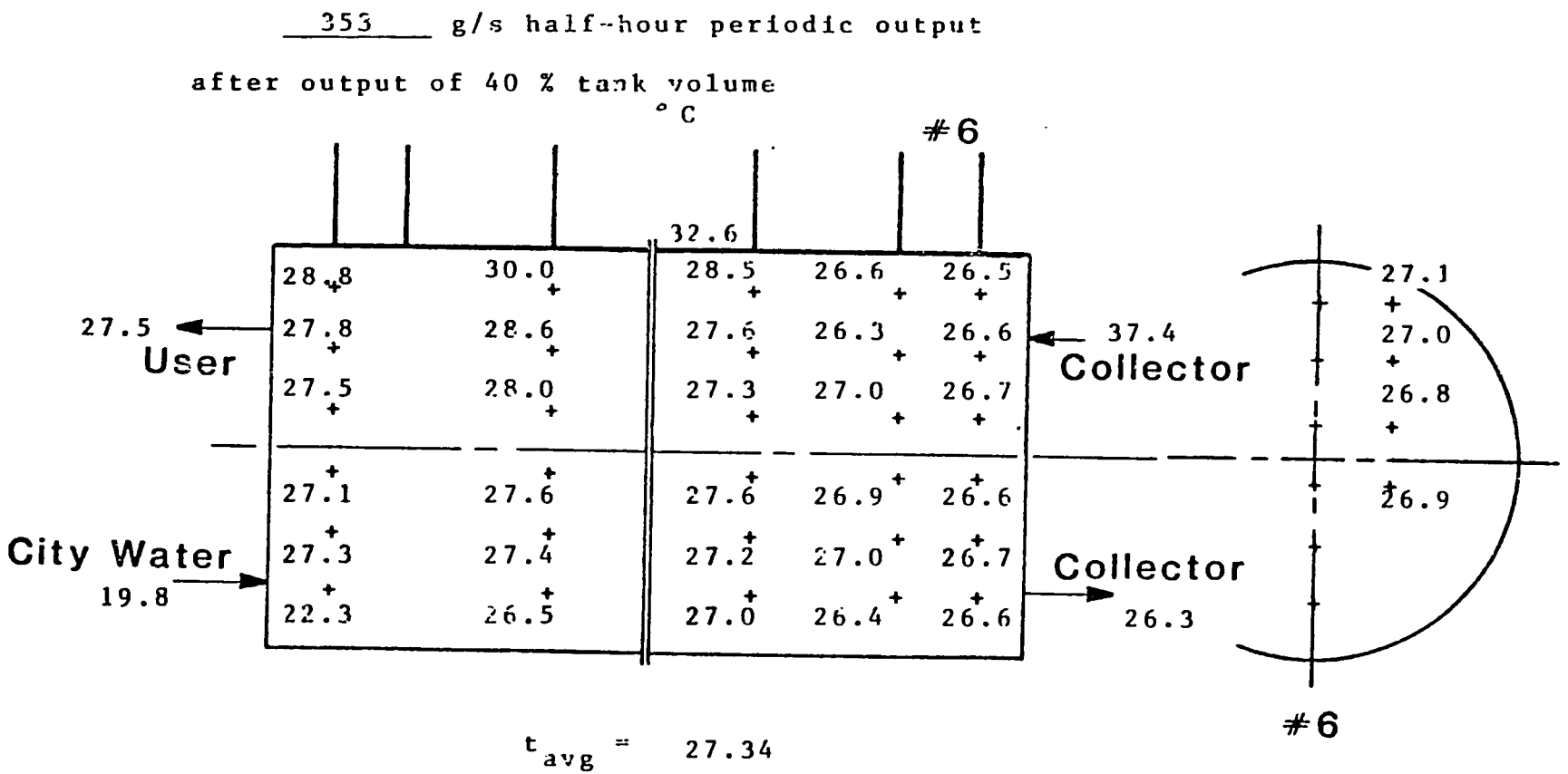

Fig. 7.21: The Temperature Distribution in The Tank

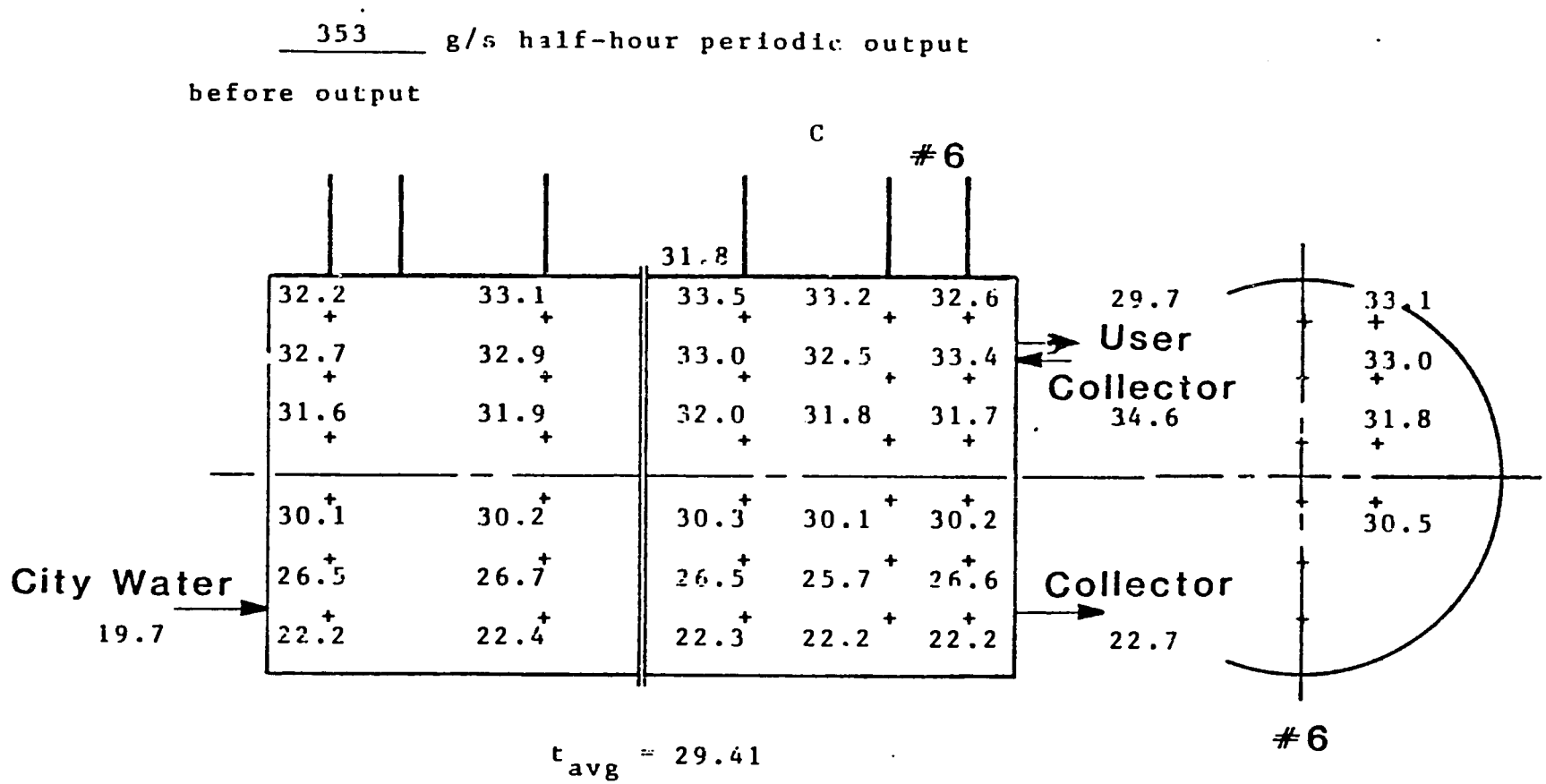

Fig. 7.22: The Temperature Distribution in The Tank

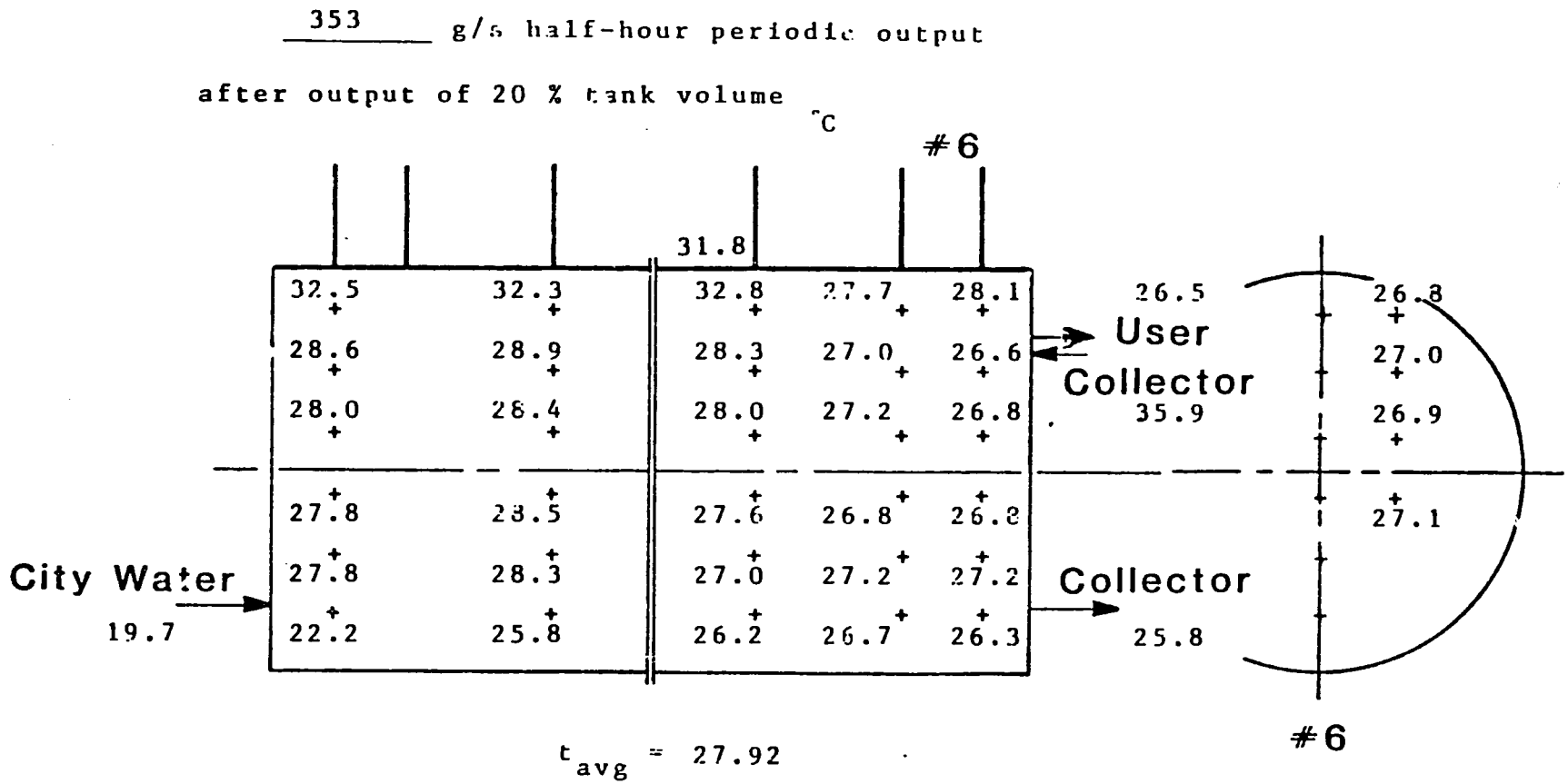

Fig. 7.23: The Temperature Distribution in The Tank

until the water in the tank began to circulate. In the right top region there was strong mixing with the input hot water, and its temperature increased.

The make-up water appears to pass through an "L" shaped path, and then to enter the outlet before mixing with the input hot water in the opposite-side configuration. At that time, there was a dead region with a higher temperature at the top. In the same-side configuration the make-up water appears to pass through an "U" shaped path after mixing with the input hot water before entering the outlet.

The output temperature for the opposite-side configuration ("L" path) should be lower than the average temperature in the tank, and lower than the output water temperature of the same-side configuration ("U" path). Thus the value of COEF for the opposite-side configuration should be less than 1, and also less than the same-side value.

The circulating and mixing strength of the opposite-side configuration ("L" path) should be less than the same-side configuration ("U" path) which give rise to a dead region with higher temperature. Thus the stratification coefficient, St, of the opposite-side configuration ("L" path) should be a little higher than than the same-side configuration ("U" path).

CHAPTER 8

CONCLUSIONS

The thermal stratification in a horizontal storage tank driven by a simulated solar thermosyphon water heater has been investigated experimentally. The different tank plumbing configuration (inlet and outlet on the same side and on the opposite sides of the tank) were evaluated. Two different output patterns (continuous and periodic) at eight different load flow rates (from 29.3 ml/s to 442 ml/s), and at different temperature levels were investigated.

The thermal stratification was characterized by a stratification coefficient, St, defined as

$$\sum_i [m_i (T_i - T_{avg})^2] / M_{total}$$

It represents the mass weighted average of the square of the temperature deviation in the tank. The experimental results were also given in terms of an extraction efficiency, COEF, defined as

$$(T_{output} - T_{makeup}) / (T_{avg} - T_{makeup})$$

As the hot water was withdrawn, axial temperature gradients were observed and temperature differences of 2 to 5°C were noted indicating that a two-dimensional treatment was necessary.

Stratification was improved (that is, the stratification coefficient, St, increased), as (T_{avg}-T_{makeup}) increased and as make-up water flow rate decreased.

Based on the stratification coefficient, St, three stratification regimes: stratified (St > 5), fully mixed (St < 1), and transition (1 < St < 5) were identified. In turn, the stratification coefficient, St, was correlated with inlet flow Reynolds number and hence divided the withdrawal operation into different regimes corresponding to different Reynolds numbers. Similar results were identified for the extraction efficiency, COEF, but the trends were not so clearly established.

The tank plumbing configuration affects the energy extraction and stratification. The same-side configuration improved the extraction efficiency, COEF, due to the change in the internal path, even though the stratification coefficient, St, was lower than for the opposite-side configuration.

The data were correlated with the stratification coefficient, St, in terms of make-up water inlet flow Reynolds number, and a pseudo Grashof number based on the tank diameter. Two formulas, one for the same-side configuration and another for the opposite-side configuration, were obtained.

The half-hour periodic output pattern improved the stratification coefficient, St, and extraction efficiency, COEF, due to stratification recovery between flows in comparison with the continuous output pattern for the same flow

rates. The correlation formulas for the continuous flow also fit the data for half-hour periodic output pattern.

REFERENCES

1. Young, M. F. and Bergquam, J. B., "Performance Characteristics of a Thermosyphon Solar Domestic Hot Water System," ASME Journal of Solar Energy Engineering, 103, 1981, pp. 193-200.

2. Lavan, Zalman and Thompson, James, "Experimental Study of Thermally Stratified Hot Water Storage Tanks," Solar Energy, 19, 1977, pp. 519-524.

3. Sliwinski, B. J., Mech, A. R. and Shih, T. S., "Stratification in Thermal Storage During Charging," Sixth International Heat Transfer Conference, Toronto, 4, 1978, pp. 149-154.

4. Phillips, W. F. and Dave, R. N., "Effects of Stratification on the Performance of Liquid-Based Solar Heating Systems," Solar Energy, 29, 1982, pp. 111-120.

5. Young, M. F. and Baughn R., "An Investigation of Thermal Stratification in Horizontal Storage Tanks," ASME Journal of Solar Energy Engineering,103, November, 1981, pp. 286-290.

6. Firl, G. G., Schmitt, B. J. and Young, M. F., "An Experimental Study of the Use of Flow Diffusers in Horizontal Solar Storage Tanks," Proceedings of the ASME Solar Energy Division Sixth Annual Conference, Las Vagas, April, 1984, pp. 380-384.

7. Morrison, G. L. and Ranatunga, D. B. J., " Thermosyphon Circulation in Solar Collectors," Solar Energy,24, 1980 pp. 191-198.

8. Holman, J. P., Heat Transfer, McGraw-Hill, Inc., 1976, p. 253.

9. Ibid., p.509.

APPENDIX A

AN ESTIMATE OF THERMAL LOSSES FROM THE "THERMAL FLOWMETER"

The "thermal flowmeter" can be modeled as a cylinder, as shown in Fig. A.1, to estimate the thermal losses. The "thermal flowmeter" was operated in the following condition:

Environmental temperature, T_∞: 24±3°C

Power supply: 10 amps and 102±0.5 volts

$T_2 = T_1 + 12°C$, $19.5 < T_1 < 27 \pm C$

For $T_\infty = 21°C$ and $T_1 = 27°C$, the maximum heat loss from the "thermal flowmeter" wall to the environment would result. For this situation the average temperature of the water in the flowmeter T_{in} is $(T_1 + T_2)/2$ or 33°C. This neglects the thermal resistance between the water and the inner surface of the pipe.

The conduction from the inner to the outer surface of the meter is:

$$Q_{cond} = 2(3.1416)kL(T_{in}-T_{out})/\ln(R_{out}/R_{in})$$
$$= 2(3.1416)0.05(0.42)(33-T_{out})/\ln(0.080/0.046)$$
$$= 0.2384(33-T_{out}) \text{ Watts}$$

The convection from T_{out} to T_∞:

$$Q_{conv} = Ah(T_{out}-T_\infty)$$

The convective heat transfer coefficient is calculated in the clasic way assuming natural convection. First, the Grashof-Prandtl number product is determined. Then the appropriate constants for h are selected from the table in Reference 8. The properties of air are evaluated at the film temperature.

$$T_f = (T_{out}+T_\infty)/2.$$

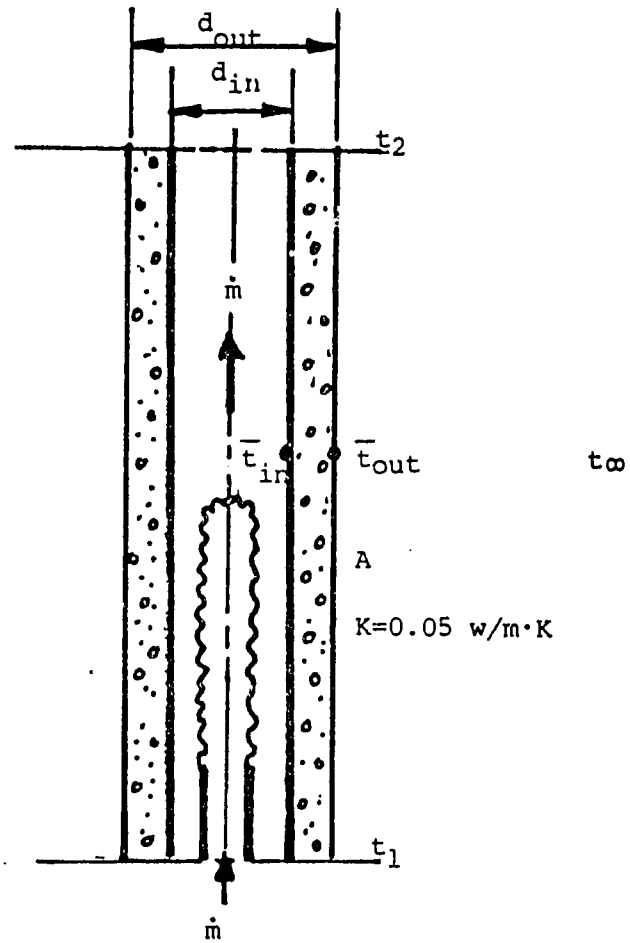

Fig. A.1 Thermal Flowmeter Model for Estimating the Thermal Losses

For $T_{out} = 25°C$

$T_f = (25+21)/2 = 23\,°C = 296K$

$\beta = 1/T_f = 1/296 = 3.378 \times 10^{-3}\ K^{-1}$

$\nu = 15.6 \times 10^{-6}$ m/s

$Pr = 0.71$

$$GrPr = \beta\ (T_{out} - T_\infty)\ L^3\ Pr/\nu^2$$
$$= 9.8 \times 3.378 \times 10^{-3} \times 4 \times (0.42)^3 \times 0.71/(15.6\times10^{-6})^2$$
$$= 28.6\times10^6.$$

For a vertical cylinder with laminar flow:

$$h = 1.42[(T_{out}-T_\infty)/L]^{\frac{1}{4}}$$
$$A = \pi\ D_{out}\ L$$
$$= 3.1416 \times 0.08 \times 0.42$$
$$= 0.1055\ m^2$$
$$Q_{conv} = Ah(T_{out} - T_\infty)$$
$$= 0.1055 \times 1.42 \times (T_{out} - T_\infty)^{1\frac{1}{4}}/\ 0.42^{\frac{1}{4}}$$
$$= 0.1861 \times (T_{out} - T_\infty)^{1\frac{1}{4}}$$

The radiation from T_{out} to T_∞ :

$$Q_{rad} = \varepsilon\sigma\ A(T_{out}^4 - T_\infty^4)$$

For the aluminum surface of the tape the emissivity

$\varepsilon = 0.4$ [9]

$\sigma = 5.6697 \times 10^{-8}\ W/m^2\ K^4$

$$Q_{rad} = o.4 \times 5.6697\times10^{-8} \times 0.01055(T_{out}^4 - T_\infty^4)$$

The heat conducted to the outer surface of the meter must be dissipated by convection and radiation in steady state. To determine this heat loss, a value for T_{out} must be determined by iteration that satisfies this balance.

For $T_{out} = 24.8 + 273 = 297.8K$

$T_{\infty} = 21 + 273 = 294K$

$$Q_{rad} = 0.2393\ (2.978^4 - 2.94^4) = 0.9424 \text{ Watts}$$

$$Q_{conv} = 0.1861\ (24.8 - 21)^{1\frac{1}{4}} = 0.9873 \text{ Watts}$$

$$Q_{rad} + Q_{conv} = 0.9424 + 0.9873 = 1.93 \text{ Watts}$$

$$Q_{cond} = 0.2384\ (33 - 24.8) = 1.955 \text{ Watts.}$$

The difference between Q_{cond} and the sum of Q_{rad} and Q_{conv} is about 1% so the assumed value of 24.8°C for T_{out} is very close and

$$Q_{loss} = Q_{cond} = Q_{rad} + Q_{conv} = 1.95 \text{ Watts}$$

Therfore, the heat loss under the most severe condition (maximum water temperature, lowest ambient temperature) is estimated to be about 1.95 Watts.

From an energy balance

$$Q_{elect} - Q_{loss} = c\,\dot{m}\,(T_2 - T_1)$$

For the heater,

$$Q_{elect} = 10 \text{ amps} \times 102 \text{ volts} = 1020 \text{ Watts}$$

Since Q_{loss} is only 1.95 Watts the heat loss is less than 0.2% of the heat from the heater and $(Q_{elect} - Q_{loss})$ can be considered as a constant. That is,

$$(Q_{elect} - Q_{loss})/\ c = \dot{m}\ (T_2 - T_1) = \text{constant}$$

and a measurement of $(T_2 - T_1)$ can be used to determine $\dot{m}$ directly.

APPENDIX B

TABULATED DATA

The same side configuration 29.3 g/s output continuously
Interval 30 minutes, Tavg,o = 19.649 °C, Tmakeup = 19.65 °C.

No.	Voutput %	Tavg - Tmakeup °C	Toutput - Tmakeup °C	ST	COEF
1	0	9.670	14.45	19.7179	1.4943
2	20.0	8.558	14.05	25.7145	1.6417
3	40.0	7.493	13.75	28.4955	1.8350
4	60.0	6.599	13.55	27.9441	2.0534
5	80.0	5.607	13.05	26.5186	2.3273
6	100.0	4.737	12.75	24.4783	2.6916
7	120.0	3.928	12.65	21.2268	3.2202
8	140.0	3.276	11.35	17.5757	3.4648
9	160.0	2.748	10.55	15.4230	3.8389
10	180.0	2.408	10.05	13.4002	4.1732
11	200.0	2.209	9.95	12.3342	4.5047
12	220.0	2.090	9.55	11.6066	4.5690
13	240.0	1.919	9.45	11.0065	4.9243
14	260.0	1.997	8.95	10.9411	4.4812
15	280.0	1.958	9.35	10.7775	4.7754
16	300.0	1.952	9.25	10.6448	4.7375
17	320.0	1.906	9.45	10.8623	4.9590

The same side configuration 38.2 g/s output continuously

Interval 23 minutes, Tavg,o = 19.84 °C, Tmakeup = 19.81 °C.

No.	Voutput %	Tavg - Tmakeup °C	Toutput - Tmakeup °C	ST	COEF
1	0	10.107	14.69	17.6177	1.4534
2	20	8.523	13.99	26.6189	1.6415
3	40	7.237	13.69	27.5193	1.8916
4	60	5.800	12.99	26.6990	2.2396
5	80	4.514	12.39	23.3294	27.445
6	100	3.431	11.19	18.3637	3.2615
7	120	2.598	9.69	14.3382	3.7304
8	140	2.135	8.69	11.8576	4.0692
9	160	1.811	7.29	10.4728	4.0255
10	180	1.746	7.39	9.7636	4.2315
11	200	1.633	6.79	9.1321	4.1580
12	220	1.570	6.19	8.8762	3.9414
13	240	1.554	6.39	8.7986	4.1127
14	260	1.563	6.19	8.4784	3.9597
15	280	1.605	6.19	8.4198	3.8563
16	300	1.609	6.89	8.4990	4.2822

The same side configuration 53.0 g/s output continuously

Interval 16.5 minutes, Tavg,o = 19.68 °C, Tmakeup = 19.70 °C.

No.	Voutput %	Tavg - Tmakeup °C	Toutput - Tmakeup °C	ST	COEF
1	0	9.725	12.9	13.3462	1.3265
2	13.87	8.364	13.2	21.6687	1.5781
3	33.77	6.813	12.9	23.3969	1.8934
4	53.67	5.394	12.3	23.2862	2.2803
5	73.58	3.911	11.5	19.1697	2.9401
6	93.47	3.015	9.9	14.7731	3.2839
7	113.4	2.003	8.1	11.0465	4.0435
8	133.3	1.751	7.6	9.0548	4.3406
9	153.2	1.646	7.0	7.3533	4.2534
10	173.1	1.555	7.3	6.5551	4.6937
11	193.0	1.522	6.8	5.8258	4.4680
12	212.9	1.392	6.9	5.5749	4.9576
13	232.8	1.369	6.5	5.4245	4.7466

The same side configuration 98.4 g/s output continuously
interval 8 minutes, Tavg,o = 19.75 °C, Tmakeup = 19.75 °C.

No.	Voutput %	Tavg - Tmakeup °C	Toutput - Tmakeup °C	ST	COEF
1	0	10.154	13.05	11.6605	1.2852
2	17.9	8.222	13.25	18.3032	1.6114
3	35.8	6.509	12.85	19.9531	1.9741
4	53.8	4.837	11.95	17.9453	2.4705
5	71.7	3.438	9.25	12.7250	2.6900
6	89.6	2.767	5.35	10.2807	1.9332
7	107.5	2.466	5.45	7.2192	2.2103
8	125.4	2.278	4.95	5.1945	2.1731
9	143.4	2.107	4.85	4.0059	2.3018
10	161.3	1.988	3.75	2.9607	1.8867
11	179.2	1.848	4.25	2.5948	2.2996
12	197.1	1.703	4.45	2.2183	2.2182
13	215.0	1.587	3.55	1.8176	2.2373

The same side configuration 151.4 g/s output continuously

Interval 5 minutes, Tavg,o = 19.46 °C, Tmakeup = 19.5 °C.

No.	Voutput %	Tavg - Tmakeup °C	Toutput - Tmakeup °C	ST	COEF
1	0	9.659	13.0	12.600	1.3458
2	17.23	7.776	12.7	15.694	1.6332
3	34.46	6.436	12.2	13.824	1.8955
4	51.69	4.878	7.5	9.346	1.5374
5	68.93	4.217	4.7	5.066	1.1145
6	86.16	3.515	4.6	2.167	1.3087
7	103.39	3.155	3.8	0.903	1.2046
8	120.62	2.774	3.4	0.435	1.2256
9	137.85	2.592	2.9	0.231	1.1189
10	155.08	2.416	2.6	0.193	1.0759
11	172.31	2.258	2.6	0.148	1.1513
12	189.55	2.108	2.2	0.095	1.0438
13	206.78	1.998	2.2	0.078	1.1010
14	224.01	1.887	2.1	0.071	1.1128

The same side configuration 221 g/s output continuously

Interval 4 minutes, $T_{avg,o}$ = 19.62 °C, Tmakeup = 19.52 °C.

No.	Voutput %	Tavg - Tmakeup °C	Toutput - Tmakeup °C	ST	COEF
1	0	9.930	12.98	12.4595	1.3071
2	20.39	7.635	9.18	6.5945	1.2023
3	40.78	6.371	6.88	0.9905	1.0798
4	61.17	5.368	5.58	0.5714	1.0394
5	81.56	4.444	4.58	0.2875	1.0306
6	101.95	3.851	3.98	0.1344	1.0366
7	122.34	3.435	3.48	0.1584	1.0131
8	142.73	3.071	3.08	0.0963	1.0029
9	163.12	2.730	2.78	0.1205	1.0184
10	183.51	2.254	2.28	0.1438	1.0117
11	203.91	1.877	1.78	0.0783	0.9481

The same side configuration 353 g/s output continuously

Interval 2.5 minutes, Tavg,0 = 19.65 °C, Tmakeup = 19.5 °C.

No.	Voutput %	Tavg - Tmakeup °C	Toutput - Tmakeup °C	ST	COEF
1	0	9.611	12.9	14.2050	1.3422
2	19.4	7.454	8.2	1.7473	1.1000
3	38.8	6.296	6.3	0.5066	1.0007
4	58.2	5.197	5.2	0.3092	1.0063
5	77.5	4.362	4.2	0.2676	0.9858
6	96.9	3.813	3.7	0.1730	0.9703
7	116.3	3.272	3.2	0.1700	0.9781
8	135.7	2.810	2.8	0.1490	0.9965
9	155.1	2.466	2.5	0.0936	1.0136
10	174.5	2.184	2.1	0.0931	0.9614
11	193.8	1.935	1.8	0.0831	0.9303
12	213.2	1.718	1.7	0.0649	0.9900
13	232.6	1.599	1.5	0.0675	0.9380

The same side configuration 442 g/s output continuously

Interval 2 minutes, $T_{avg,o}$ = 19.67 °C, Tmakeup = 19.6 °C.

No.	Voutput %	Tavg - Tmakeup °C	Toutput - Tmakeup °C	ST	COEF
1	0	9.839	13.0	13.1206	1.3213
2	20	7.748	8.0	1.0159	1.0325
3	40	6.480	6.4	0.4698	0.9877
4	60	5.299	5.3	0.3096	1.0001
5	80	4.417	4.4	0.2365	0.9962
6	100	3.729	3.7	0.1917	0.9923
7	120	3.223	3.2	0.1275	0.9929
8	140	2.756	2.7	0.0909	0.9797
9	160	2.415	2.5	0.0753	1.0353
10	180	2.125	2.1	0.0580	0.9881
11	200	1.868	1.9	0.0481	1.0170
12	220	1.679	1.6	0.0542	0.9530

Opposite side configuration 29.3 g/s output continuously

Interval 30 minutes, Tavg,o = 19.746 °C, Tmakeup = 19.74 °C.

No.	Voutput %	Tavg - Tmakeup °C	Toutput - Tmakeup °C	ST	COEF
1	0	9.777	13.86	18.4747	1.4176
2	20	8.728	13.66	25.1997	1.5651
3	40	7.780	13.56	28.4185	1.7430
4	60	6.792	13.26	27.9988	1.9523
5	80	5.876	12.66	27.9023	2.1547
6	100	5.106	12.86	26.5963	2.5187
7	120	4.464	12.26	25.1368	2.7464
8	140	3.930	11.76	23.1226	2.9922
9	160	3.535	11.36	21.4353	3.2134
10	180	3.266	10.16	20.1934	3.1103
11	200	3.122	10.96	19.3575	3.5108
12	220	2.943	10.86	18.1932	3.6904
13	240	2.917	9.96	17.7986	3.4149
14	260	2.866	10.66	17.0685	3.7189

Opposite side configuration 38.2 g/s output continuously

Interval 23 minutes, Tavg,o = 19.64°C, Tmakeup = 19.575 °C.

No.	Voutput %	Tavg - Tmakeup °C	Toutput - Tmakeup °C	ST	COEF
1	0	9.672	14.025	19.8900	1.4500
2	11.3	8.887	13.825	24.6630	1.5556
3	31.3	7.529	13.725	28.0907	1.8229
4	51.3	6.159	13.225	28.9920	2.1472
5	71.3	4.997	12.225	26.6095	2.4462
6	91.3	4.070	11.425	23.1528	2.8070
7	111.3	3.253	10.225	18.8343	3.1427
8	131.2	2.759	7.925	15.8822	2.8727
9	151.2	2.585	8.025	14.4083	3.1042
10	171.2	2.443	5.925	13.3897	2.4252
11	191.2	2.358	7.025	13.1742	2.9795
12	211.2	2.355	6.625	13.2125	2.8131

Opposite side configuration 53.0 g/s output continuously

Interval 16.5 minutes, Tavg,o = 19.77 °C, Tmakeup = 19.80 °C.

No.	Voutput %	Tavg - Tmakeup °C	Toutput - Tmakeup °C	ST	COEF
1	0	9.817	13.50	15.6546	1.3751
2	20.0	8.134	13.30	24.7570	1.6350
3	40.0	6.325	12.70	27.0587	2.0077
4	60.0	5.020	11.70	24.1653	2.3306
5	79.9	3.753	9.70	20.9999	2.5845
6	99.9	2.767	6.80	14.9667	2.4576
7	119.9	2.397	4.90	12.8976	2.0442
8	139.9	2.114	4.80	12.0954	2.2707
9	159.9	2.121	4.70	11.1945	2.2162
10	179.9	2.039	5.10	10.6939	2.5013
11	199.8	1.990	4.50	10.4208	2.2612
12	219.8	1.986	4.50	10.3011	2.2657
13	239.8	2.005	4.30	10.0161	2.1446
14	259.8	2.048	5.20	9.9294	2.5394

Opposite side configuration 98.4 g/s output continuously

Interval 8.0 minutes, Tavg,o = 19.78 °C, Tmakeup = 19.80 °C.

No.	Voutput %	Tavg - Tmakeup °C	Toutput - Tmakeup °C	ST	COEF
1	0	9.564	13.30	15.7952	1.3905
2	17.9	7.544	12.70	22.0202	1.6834
3	35.8	5.912	12.10	22.4047	2.0467
4	53.8	4.490	9.00	19.3382	2.0229
5	71.7	3.318	4.70	13.5600	1.4165
6	89.6	3.094	3.50	12.2849	1.1310
7	107.5	2.801	2.90	10.3857	1.0352
8	125.4	2.612	2.30	9.4121	0.8805
9	143.4	2.468	2.40	8.1732	0.9725
10	161.3	2.468	2.30	7.3585	0.9320
11	179.2	2.417	2.80	6.8886	1.1585
12	197.1	2.337	3.00	6.6143	1.2836
13	215.0	2.248	2.40	5.8693	1.0674
14	233.0	2.259	2.40	5.5209	1.0626

Opposite side configuration 151.4 g/s output continuously

Interval 5.0 minutes, Tavg,o = 19.75 °C, Tmakeup = 19.76 °C.

No.	Voutput %	Tavg - Tmakeup °C	Toutput - Tmakeup °C	ST	COEF
1	0	9.634	13.54	16.9409	1.4055
2	17.2	7.841	12.84	19.2864	1.6375
3	34.5	6.049	9.04	16.7502	1.4943
4	51.7	4.926	4.84	11.1113	0.9825
5	68.9	4.513	3.34	9.1724	0.7401
6	86.2	4.254	3.44	6.7113	0.8087
7	103.4	3.916	2.84	5.0428	0.7253
8	120.6	3.702	2.74	3.4263	0.7402
9	137.8	3.524	2.54	2.5689	0.7207
10	155.1	3.368	2.54	1.5692	0.7541
11	172.3	3.208	2.44	1.0430	0.7606
12	189.5	3.121	2.44	0.6985	0.7817
13	206.8	2.970	2.44	0.5204	0.8216
14	224.0	2.797	2.44	0.4051	0.8009

Opposite side configuration 221 g/s output continuously

Interval 4.0 minutes, Tavg,o = 19.68 °C, Tmakeup = 19.70 °C.

No.	Voutput %	Tavg - Tmakeup °C	Toutput - Tmakeup °C	ST	COEF
1	0	9.604	13.3	15.1739	1.6452
2	20.4	7.461	7.7	10.4929	1.0320
3	40.7	6.377	5.1	4.3129	0.7997
4	61.1	5.538	4.7	1.2246	0.8486
5	81.4	4.776	4.4	0.4457	0.9212
6	101.8	4.223	3.9	0.2456	0.9235
7	122.1	3.673	3.5	0.1746	0.9530
8	142.5	3.257	3.1	0.1524	0.9518
9	162.8	2.976	2.7	0.2537	0.9073
10	183.2	2.374	2.3	0.1303	0.9688
11	203.6	2.275	2.3	0.1225	1.1011
12	223.9	2.056	2.0	0.1251	0.9240

Opposite side configuration 353 g/s output continuously

Interval 2.5 minutes, Tavg,o = 19.78 °C, Tmakeup = 19.73 °C.

No.	Voutput %	Tavg - Tmakeup °C	Toutput - Tmakeup °C	ST	COEF
1	0	9.606	12.87	14.9120	1.3398
2	20.3	8.178	6.87	3.4434	0.8401
3	40.6	6.663	6.37	0.6575	0.9561
4	60.9	5.580	5.47	0.4171	0.9802
5	81.3	4.727	4.47	0.3365	0.9456
6	101.6	4.087	3.87	0.2906	0.9469
7	121.9	3.446	3.27	0.2466	0.9490
8	142.2	3.079	2.87	0.1831	0.9321
9	162.5	2.659	2.37	0.1046	0.8913
10	182.9	2.342	2.17	0.1017	0.9267
11	203.2	2.110	1.97	0.1339	0.9335
12	223.5	1.907	1.67	0.0805	0.8758

Opposite side configuration 442 g/s output continuously

Interval 2.0 minutes, Tavg,o = 19.61 °C, Tmakeup = 19.58 °C.

No.	Voutput %	Tavg - Tmakeup °C	Toutput - Tmakeup °C	ST	COEF
1	0	9.540	13.32	15.8923	1.3962
2	20.1	7.960	7.12	2.6971	0.8945
3	40.2	6.752	6.52	0.5891	0.9659
4	60.3	5.571	5.32	0.4104	0.9549
5	80.4	4.771	4.52	0.3021	0.9475
6	100.5	4.059	3.72	0.2622	0.9165
7	120.6	3.430	3.22	0.2024	0.9389
8	140.7	3.021	2.72	0.1698	0.9004
9	160.8	2.568	2.42	0.1076	0.9423
10	180.9	2.297	2.12	0.1237	0.9230
11	201.0	1.980	1.72	0.0814	0.8688
12	221.1	1.743	1.62	0.0914	0.9295

The same side configuration 53.0 g/s output periodically, In each 30 minutes output interval 16.5 minutes, Tavg,0 = 20.0 °C, Tmakeup = 20.0 °C.

No.	Voutput %	Tavg - Tmakeup °C	Toutput - Tmakeup °C	ST	COEF
1	0	9.575	12.5	11.323	1.3055
	19.98	7.921	12.8	20.423	1.6159
2		8.521	12.8	19.125	1.5020
	39.97	7.211	12.7	21.238	1.7613
3		7.736	12.7	21.917	1.6418
	59.96	6.137	12.5	23.424	2.0367
4		6.868	12.5	22.771	1.8200
	79.94	5.483	12.2	22.780	2.2666

The same side configuration 98.4 g/s output periodically, In each 30 minutes output interval 9 minutes, Tavg,0 = 19.57 °C, Tmakeup = 19.6 °C.

No.	Voutput %	Tavg - Tmakeup °C	Toutput - Tmakeup °C	ST	COEF
1	0	9.583	12.4	10.3858	1.2940
	20	7.462	12.6	17.4128	1.6886
2		8.577	12.9	17.3299	1.5041
	40	6.828	13.0	20.2265	1.9038
3		7.580	13.0	20.7374	1.7149
	60	5.492	12.7	19.6190	2.3126
4		6.693	12.7	22.1832	1.8975
	80	4.824	12.4	18.9158	2.5705

The same side configuration 151 g/s output periodically, In each 30 minutes output interval 6 minutes, Tavg,0 = 19.52 °C, Tmakeup = 19.52 °C.

No.	Voutput %	Tavg - Tmakeup °C	Toutput - Tmakeup °C	ST	COEF
1	0	9.749	13.08	12.5534	1.3417
	20	7.601	12.18	16.3361	1.6025
2		8.561	13.68	18.1649	1.5979
	40	6.560	13.08	16.7551	1.9940
3		7.396	13.78	19.4797	1.8633
	60	5.130	10.28	12.2173	2.0066
4		6.566	13.08	18.9676	1.9920
	80	4.690	7.68	11.1332	1.6378

The same side configuration 221 g/s output periodically, In each 30 minutes output interval 4 minutes, Tavg,0 = 19.57 °C, Tmakeup = 19.6 °C.

No.	Voutput %	Tavg - Tmakeup °C	Toutput - Tmakeup °C	ST	COEF
1	0	9.546	13.0	15.1364	1.3619
	20.4	7.167	9.9	9.1119	1.3813
2		8.410	13.7	14.4974	1.6290
	40.7	6.570	6.7	3.8661	1.0198
3		7.899	11.7	10.1047	1.4812
	61.1	6.222	6.6	2.6119	1.0608
4		7.577	11.2	9.1624	1.4781
	81.4	5.939	6.3	1.6729	1.0608

The same side configuration 353 g/s output periodically, In each 30 minutes output interval 2.5 minutes, Tavg,0 = 19.75 °C, Tmakeup = 19.75 °C.

No.	Voutput %	Tavg - Tmakeup °C	Toutput - Tmakeup °C	ST	COEF
1	0	10.038	12.95	10.8895	1.2901
	20.3	7.760	8.35	2.0307	1.0760
2		9.288	12.35	7.1817	1.3279
	40.6	7.587	8.05	1.2503	1.0611
3		8.908	11.85	7.0420	1.3303
	61.0	7.212	8.05	1.3172	1.1161
4		8.515	11.35	6.8417	1.3329
	81.3	6.917	7.85	1.1590	1.1349

The same side configuration 442 g/s output periodically, In each 30 minutes output interval 2 minutes, Tavg,0 = 20.0 °C, Tmakeup = 20.0 °C.

No.	Voutput %	Tavg - Tmakeup °C	Toutput - Tmakeup °C	ST	COEF
1	0	9.688	12.6	11.2378	1.3006
	20.2	7.936	8.5	1.7364	1.0711
2		9.070	11.8	6.2643	1.3009
	40.4	7.512	7.1	0.9831	0.9452
3		8.749	11.3	6.3901	1.2916
	60.7	7.068	6.9	1.0851	0.9762
4		8.411	11.0	6.2372	1.3078
	80.9	6.958	6.7	1.0507	0.9629

Opposite side configuration 53.0 g/s output periodically, In each 30 minutes output interval 16.5 minutes, $T_{avg,o}$ = 19.83 °C, Tmakeup = 19.85 °C.

No.	Voutput %	Tavg - Tmakeup °C	Toutput - Tmakeup °C	ST	COEF
1	0	9.870	13.65	16.8018	1.3830
	20	8.156	13.45	25.6184	1.6491
2		8.771	14.15	24.9029	1.6133
	40	7.019	13.15	27.3646	1.8734
3		7.725	14.05	27.2804	1.8188
	60	6.021	12.75	28.6482	2.1172
4		6.673	13.75	28.8137	2.0607
	80	5.134	12.05	26.0477	2.3472

Opposite side configuration 98.4 g/s output periodically, In each 30 minutes output interval 9 minutes, Tavg,o = 19.735 °C, Tmakeup = 19.70 °C.

No.	Voutput %	Tavg - Tmakeup °C	Toutput - Tmakeup °C	ST	COEF
1	0	9.652	12.9	14.4440	1.3744
	20	7.491	12.6	21.8232	1.6819
2		8.642	13.6	21.2106	1.6045
	40	6.686	12.9	23.9194	1.9293
3		7.542	13.6	25.0205	1.8517
	60	5.437	12.7	23.9981	2.3359
4		6.617	13.4	25.4801	2.0950
	80	4.802	11.1	22.1304	2.3114
5		5.703	10.8	24.9080	2.3114
	100	4.058	7.0	16.8255	1.7250

Opposite side configuration 151 g/s output periodically, In each 30 minutes output interval 6 minutes, Tavg,o = 19.90 °C, Tmakeup = 19.9 °C.

No.	Voutput %	Tavg - Tmakeup °C	Toutput - Tmakeup °C	ST	COEF
1	0	9.739	13.6	16.5249	1.3964
	20	7.597	12.6	18.9732	1.6586
2		8.595	12.9	21.9879	1.5009
	40	6.502	12.0	19.7594	1.8456
3		7.484	14.7	22.8824	1.9642
	60	5.407	6.4	15.2246	1.1837
4		6.918	14.4	23.5582	2.0814
	80	5.079	5.3	14.1486	1.0435
5		6.607	14.0	22.5117	2.1188
	100	4.837	5.2	13.3808	1.0751

Opposite side configuration 221 g/s output periodically, In each 30 minutes output interval 4 minutes, Tavg,o = 19.93 °C, Tmakeup = 19.9 °C.

No.	Voutput %	Tavg - Tmakeup °C	Toutput - Tmakeup °C	ST	COEF
1	0	9.714	13.3	15.1317	1.3691
	20.4	7.522	8.7	11.2314	1.1566
2		8.741	14.7	16.1122	1.6816
	40.7	7.198	5.3	9.9546	0.7363
3		8.608	14.3	14.1306	1.6613
	61.1	7.296	5.3	8.8421	0.7265
4	[illegible]	8.594	14.1	13.3914	1.6406
	81.4	7.390	5.7	7.9659	0.7713
5		8.679	13.9	12.5919	1.6016
	101.8	7.463	5.7	7.9921	0.7638

Opposite side configuration 353 g/s output periodically, In each 30 minutes output interval 2.5 minutes, $T_{avg,o}$ = 19.82 °C, T_{makeup} = 19.85 °C.

No.	Voutput %	Tavg - Tmakeup °C	Toutput - Tmakeup °C	ST	COEF
1	0	9.565	12.85	14.4748	1.378
	20.3	8.067	6.65	3.4251	0.8243
2		9.302	13.25	7.8723	1.417
	40.6	7.833	7.15	1.6116	0.9129
3		9.508	12.25	6.8018	1.344
	60.9	7.954	7.35	1.7027	0.9241
4		9.479	12.95	6.5860	1.295
	81.3	7.990	6.95	2.2663	0.8698
5		9.565	12.45	6.7005	1.336
	101.6	7.916	7.35	1.7994	0.9285

Opposite side configuration 442 g/s output periodically, In each 30 minutes output interval 2 minutes, $T_{avg,o}$ = 19.67 °C, Tmakeup = 19.87 °C.

No.	Voutput %	Tavg - Tmakeup °C	Toutput - Tmakeup °C	ST	COEF
1	0	9.667	13.03	14.3620	1.3582
	20.2	7.920	7.43	1.8162	0.9381
2		9.543	12.23	6.3745	1.344
	40.4	7.591	7.63	1.2447	0.9596
3		9.549	12.23	6.3166	1.344
	60.7	7.823	7.63	0.8986	0.9753
4		9.366	11.73	5.6835	1.306
	80.9	7.993	8.73	1.8522	1.092
5		9.486	12.33	7.0772	1.363
	101.1	7.917	7.53	1.4451	0.9512

APPENDIX C

ADDITIONAL RESULTS FOR TEMPERATURE DISTRIBUTIONS IN THE TANK AT SPECIFIC TIMES

98.4 g/s continuous output 0 % of the tank volume

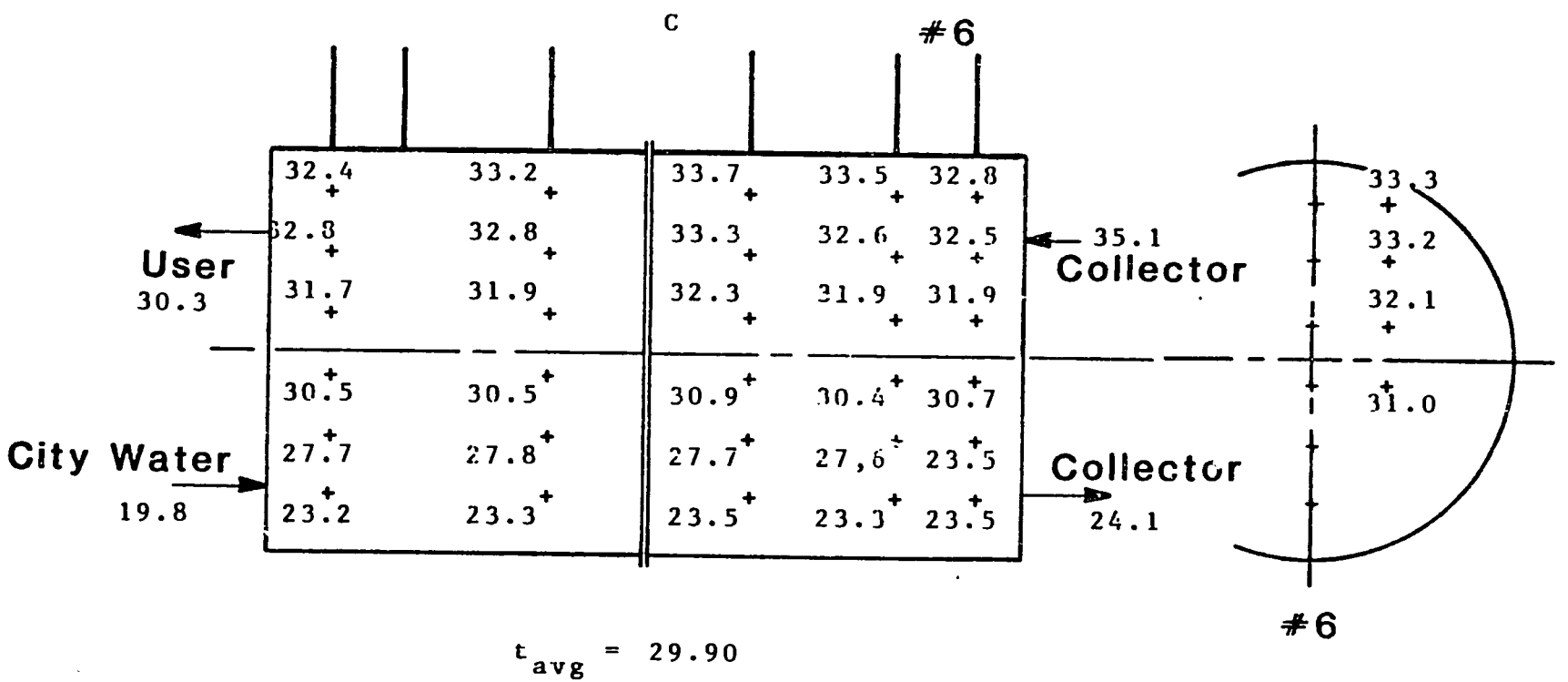

Fig. C.1: The Temperature Distribution in The Tank

98.4 g/s continuous output 17.9 % of the tank volume

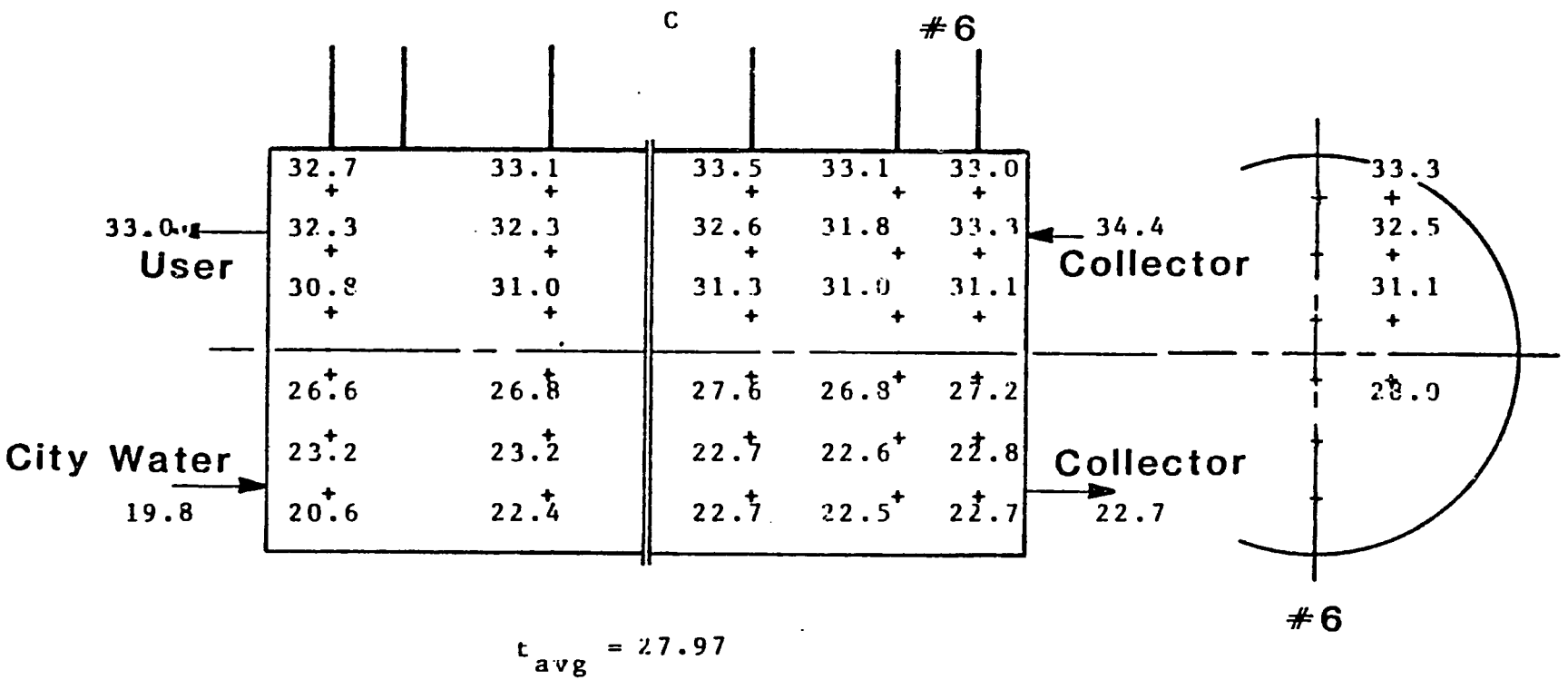

Fig. C.2: The Temperature Distribution in The Tank

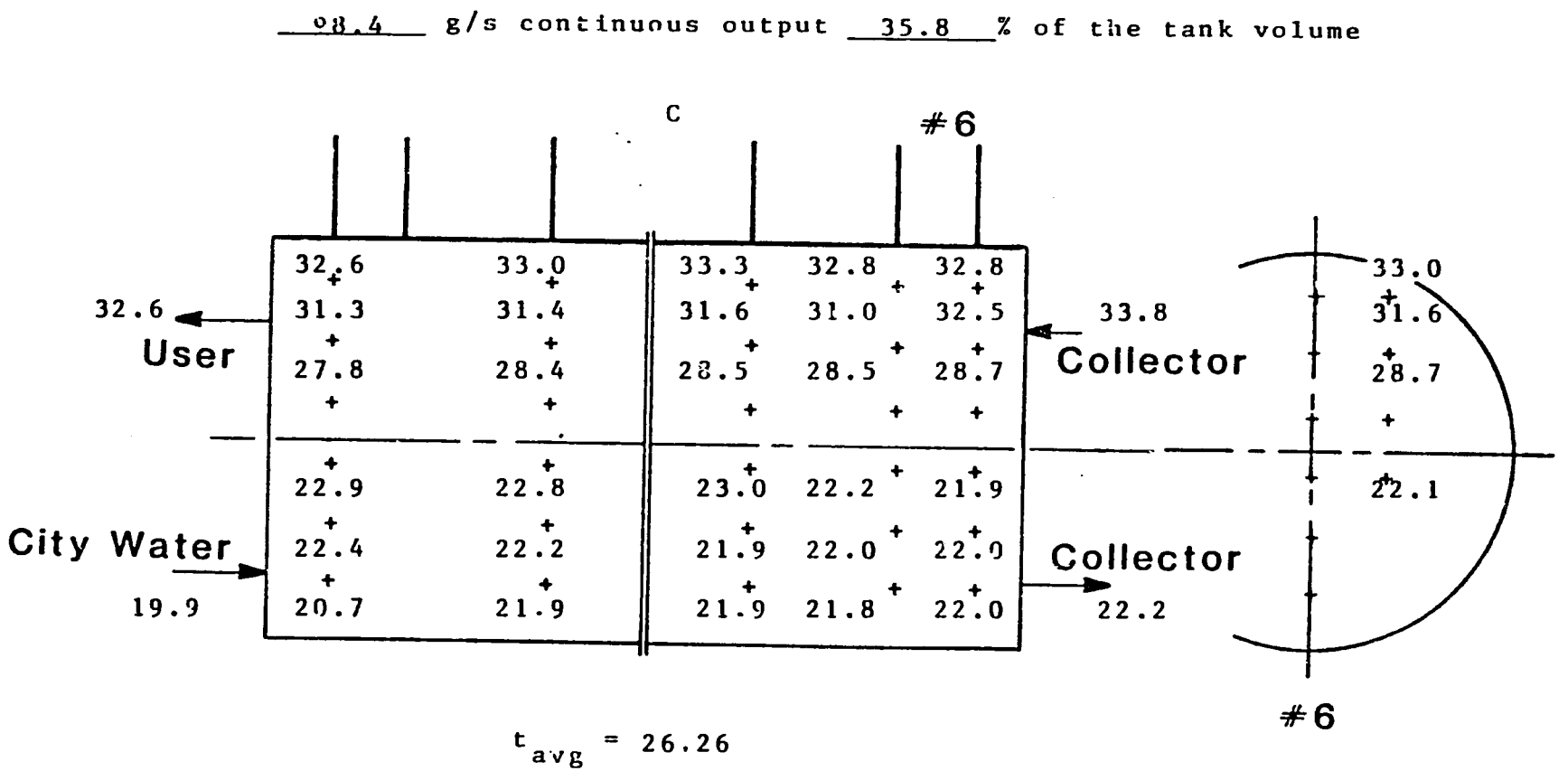

Fig. C.3: The Temperature Distribution in The Tank

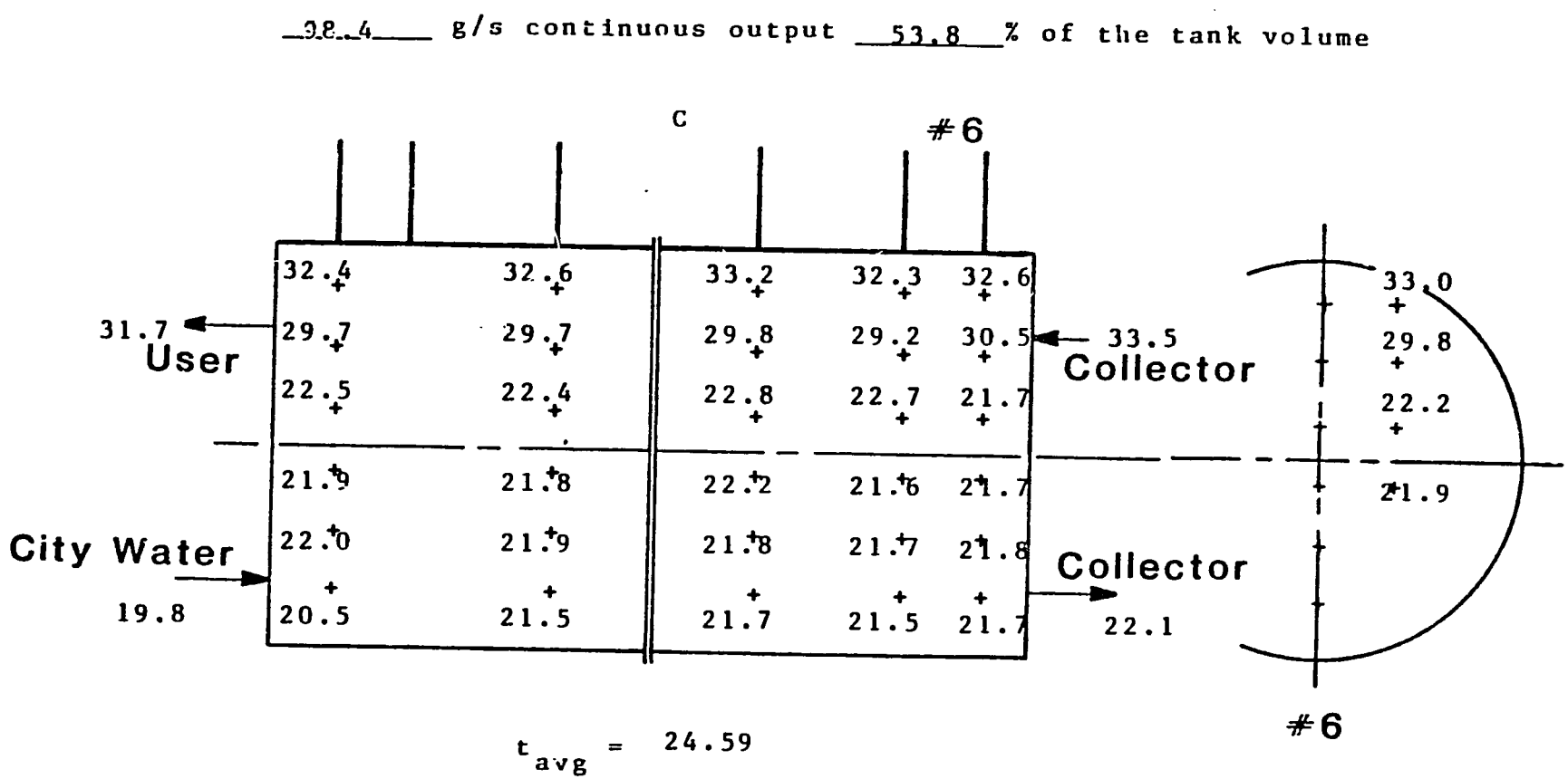

Fig. C.4: The Temperature Distribution in The Tank

98.4 g/s continuous output 71.7 % of the tank volume

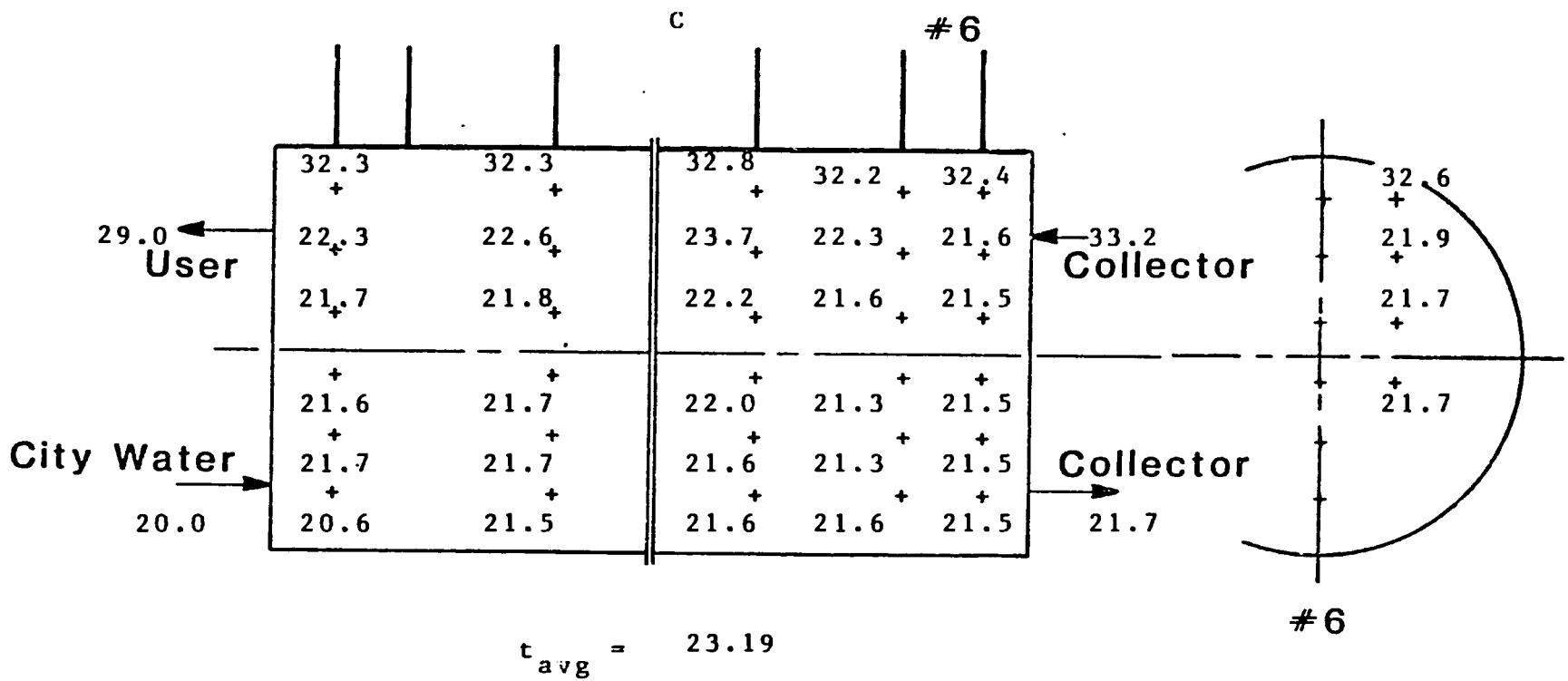

Fig. C.5: The Temperature Distribution in The Tank

98.4 g/s continuous output 89.6 % of the tank volume

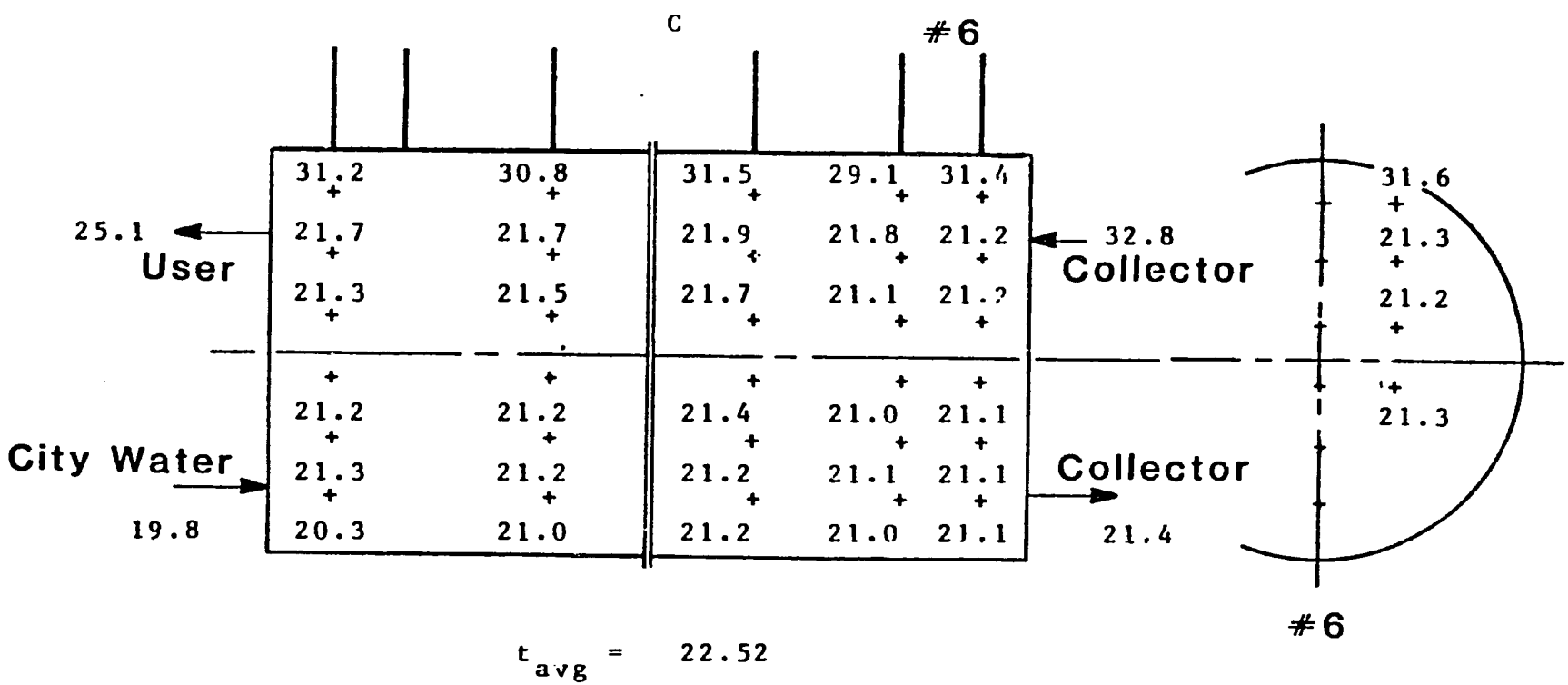

Fig. C.6: The Temperature Distribution in The Tank

151.4 g/s continuous output 17.2 % of the tank volume

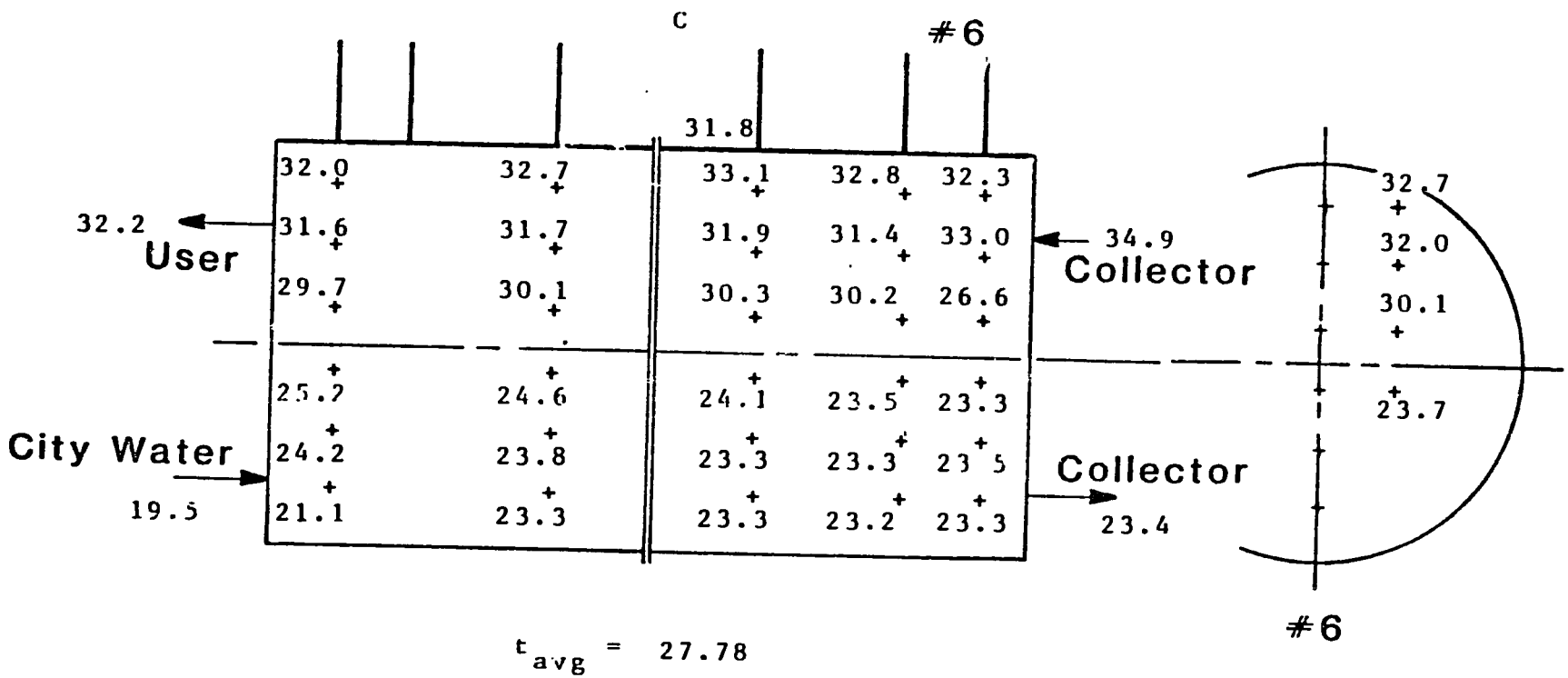

Fig. C.7: The Temperature Distribution in The Tank

151.4 g/s continuous output 34.5 % of the tank volume

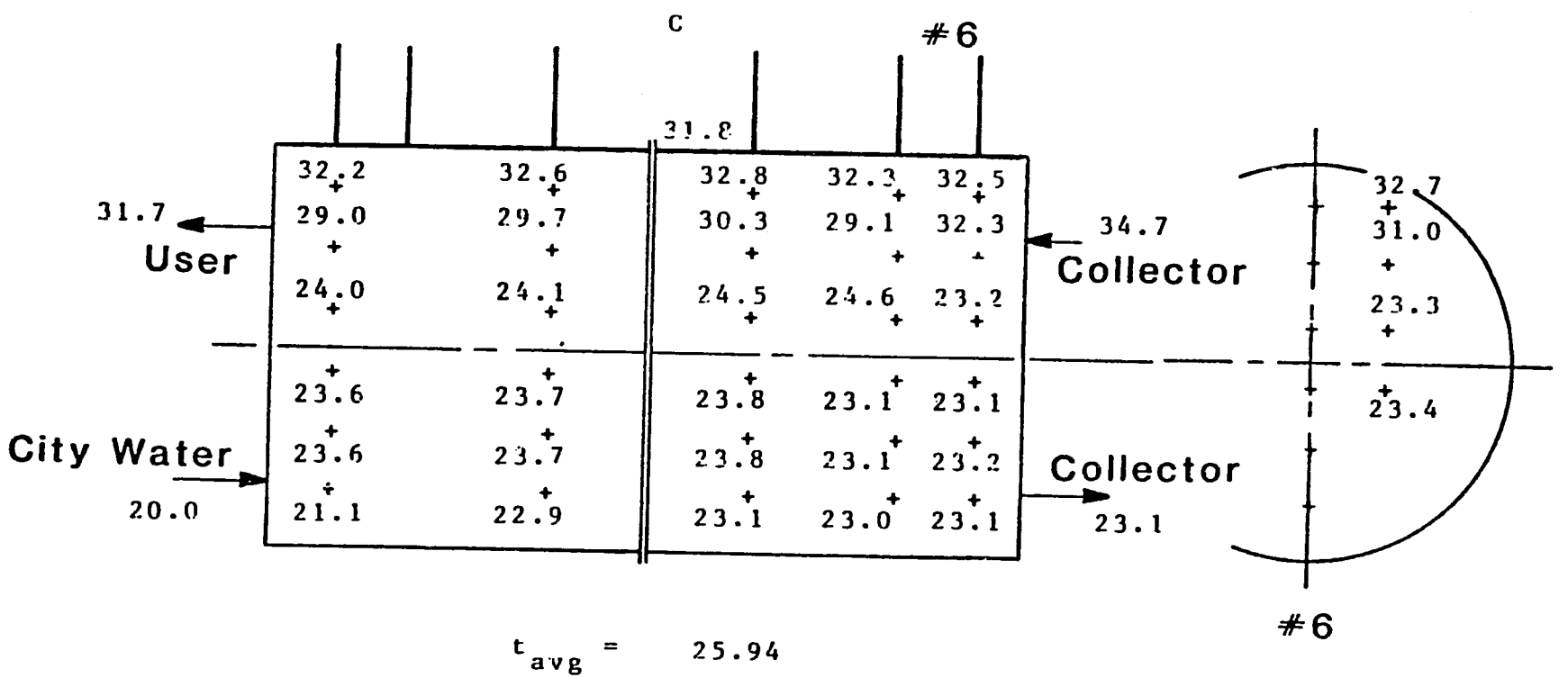

Fig. C.8: The Temperature Distribution in The Tank

151.4 g/s continuous output 51.69 % of the tank volume

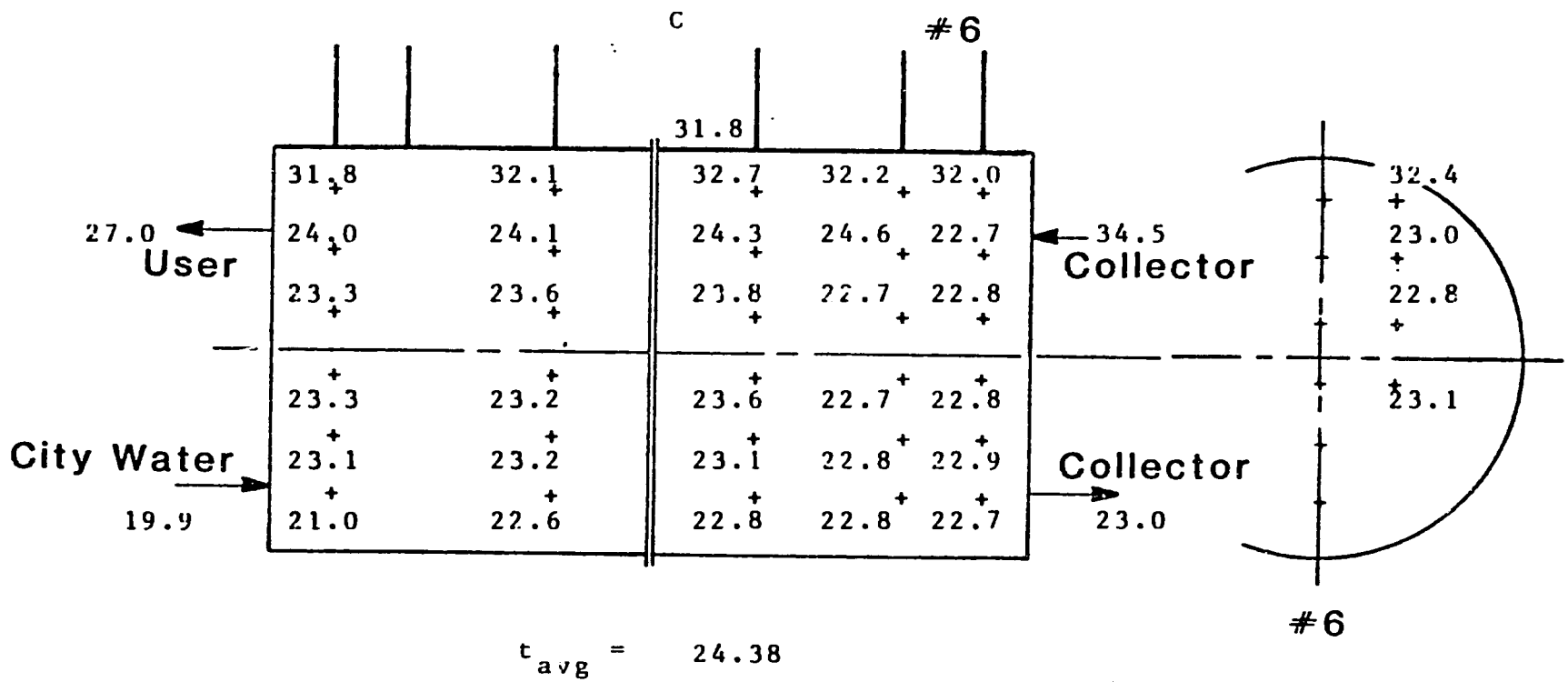

Fig. C.9: The Temperature Distribution in The Tank

151.4 g/s continuous output 68.9 % of the tank volume

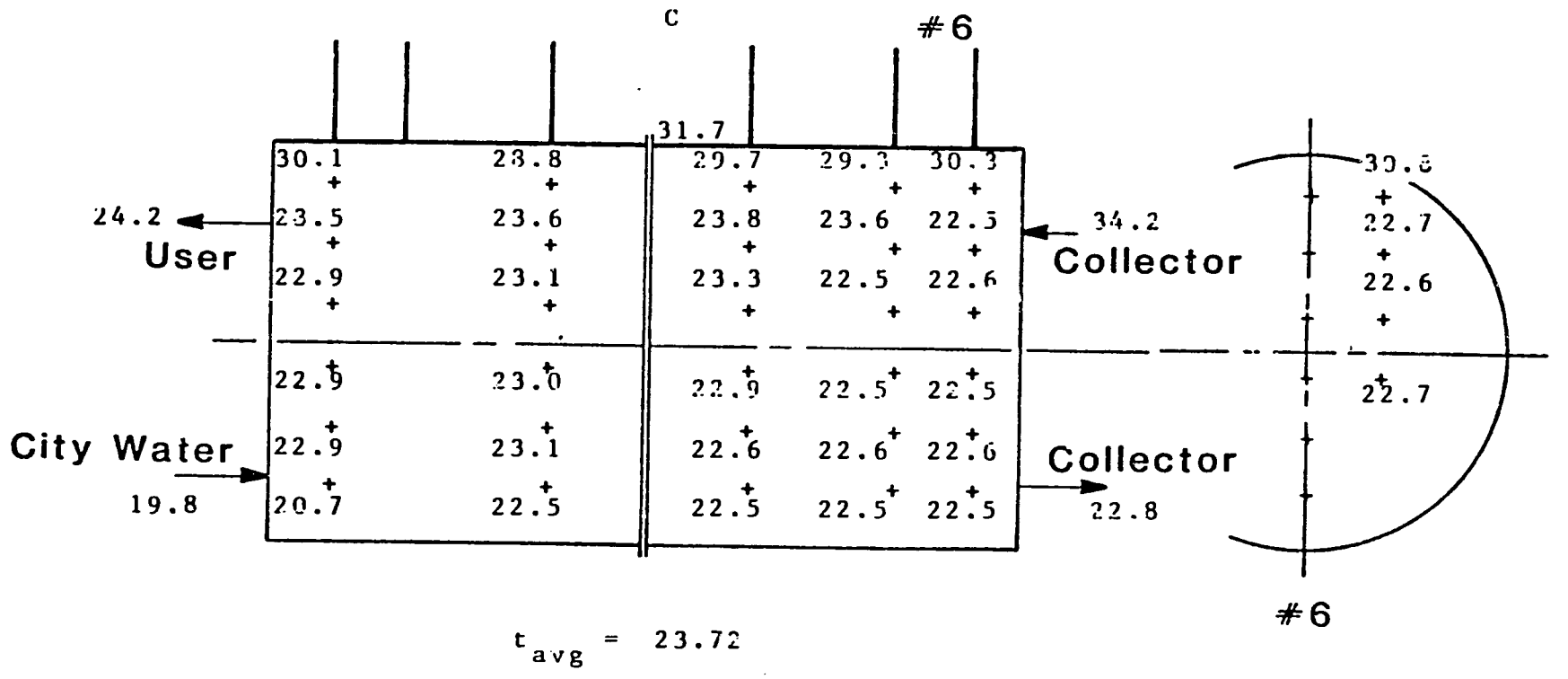

Fig. C.10: The Temperature Distribution in The Tank

151.4 g/s continuous output 86.2 % of the tank volume

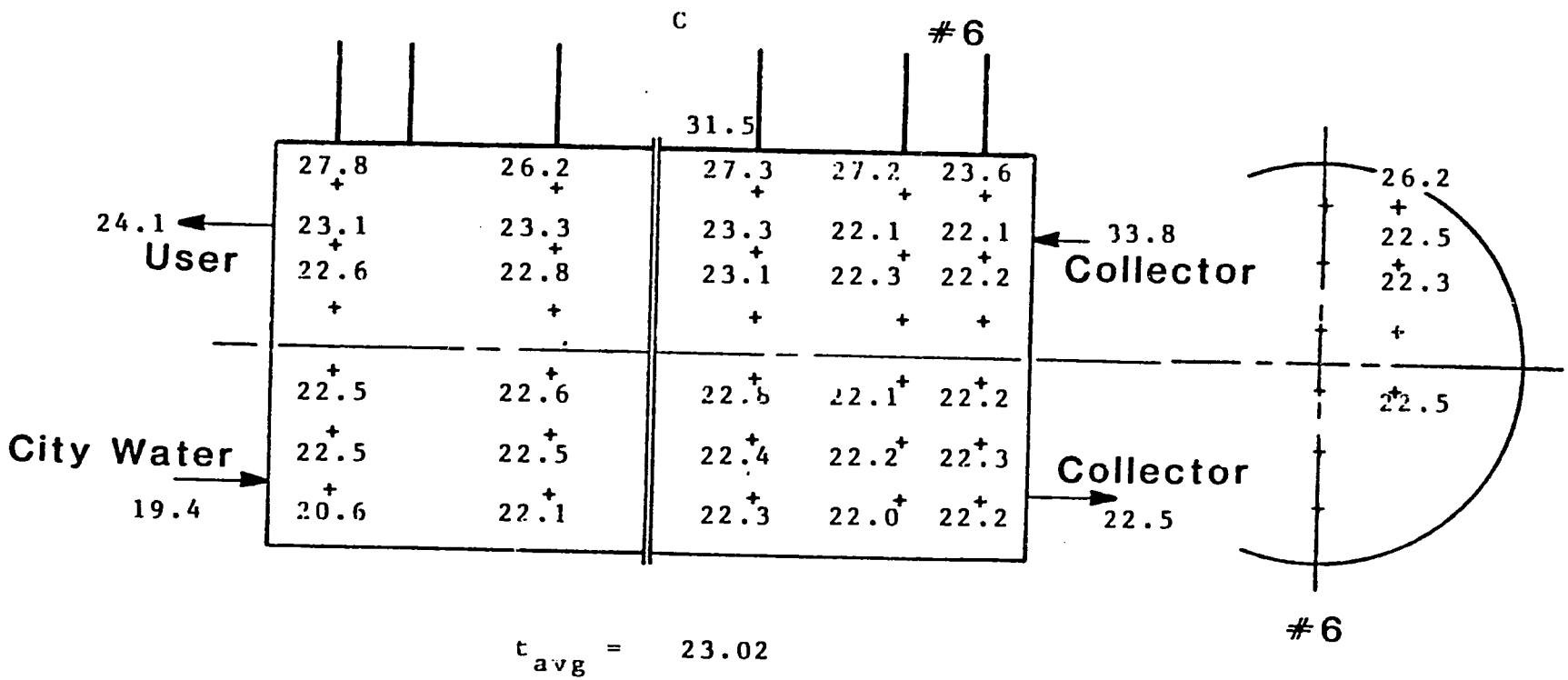

Fig. C.11: The Temperature Distribution in The Tank

442 g/s continuous output 0 % of the tank volume

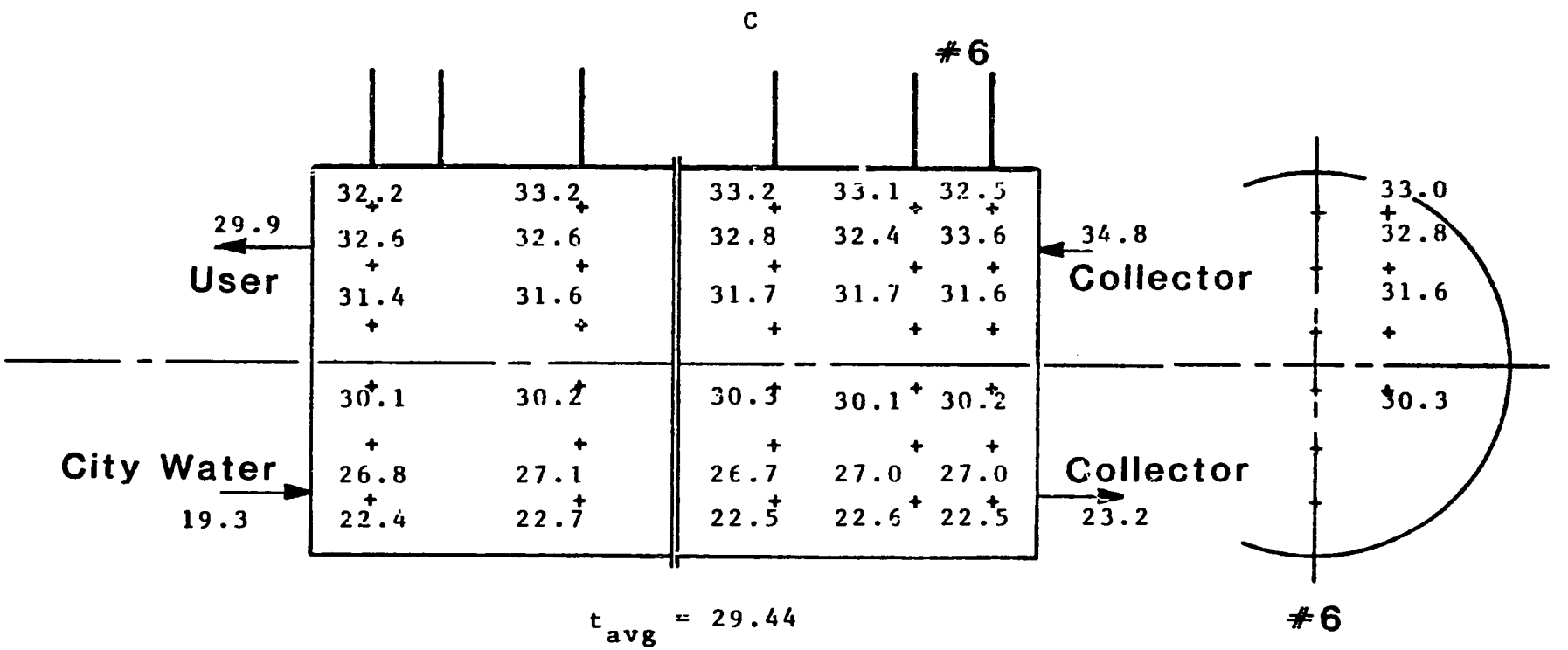

Fig. C.12: The Temperature Distribution in Tank

442 g/s continuous output 20 % of the tank volume

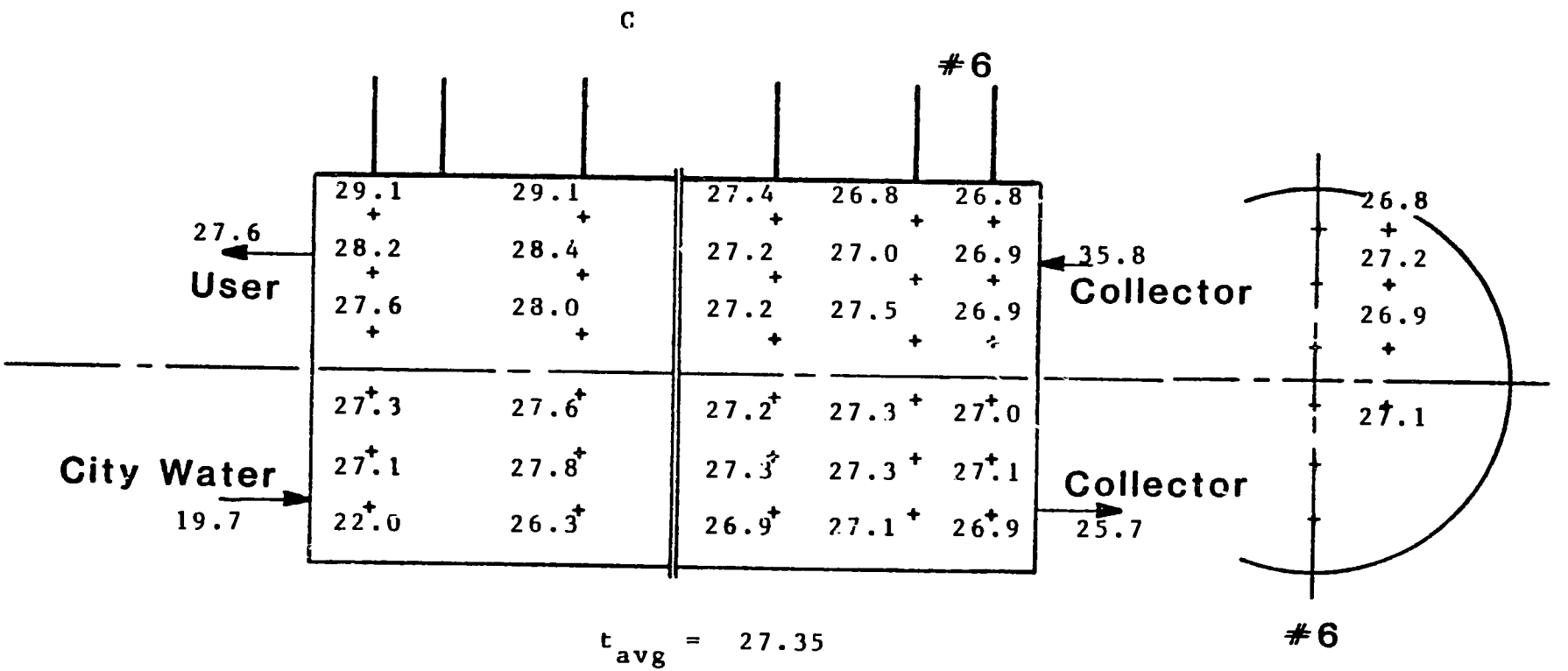

t_{avg} = 27.35

Fig. C.13: The Temperature Distribution in Tank

442 g/s continuous output 40 % of the tank volume

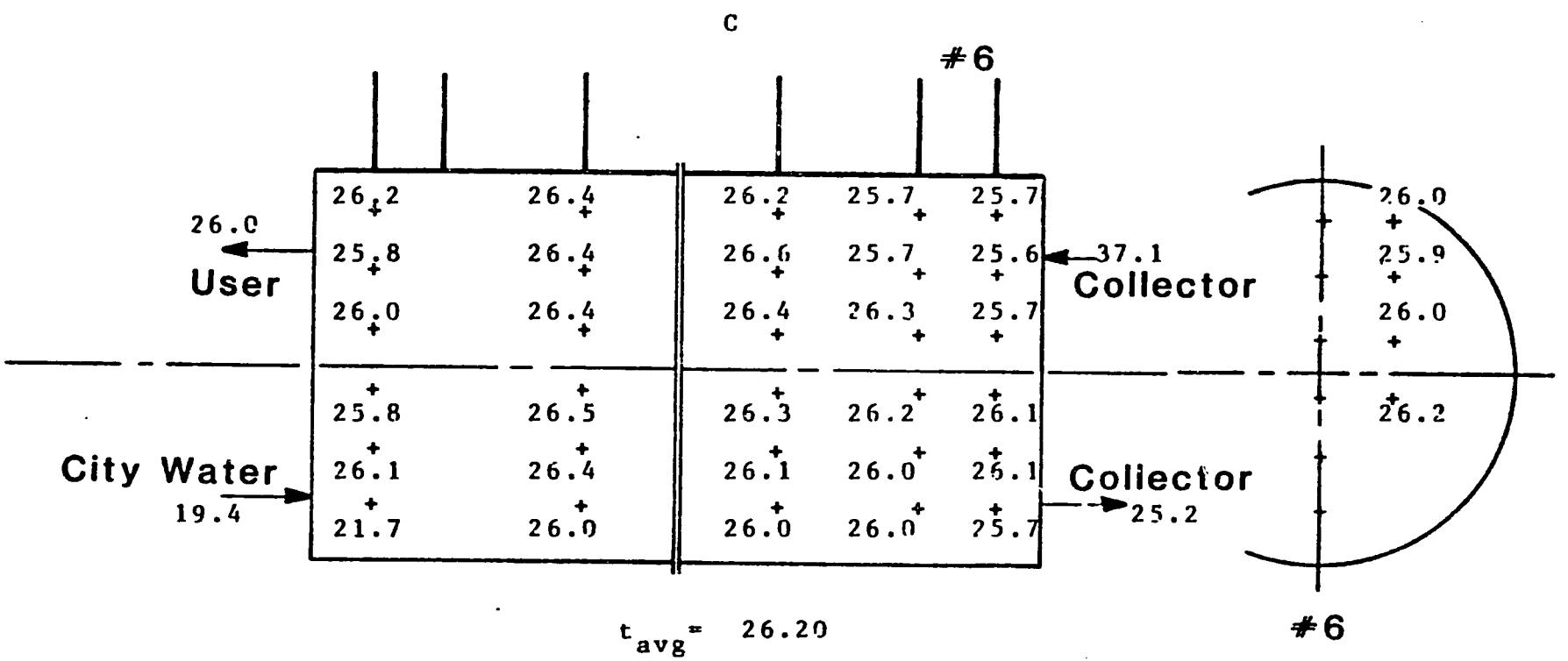

Fig. C.14: The Temperature Distribution in Tank

98.4 g/s continuous output 17.9 % of the tank volume

C

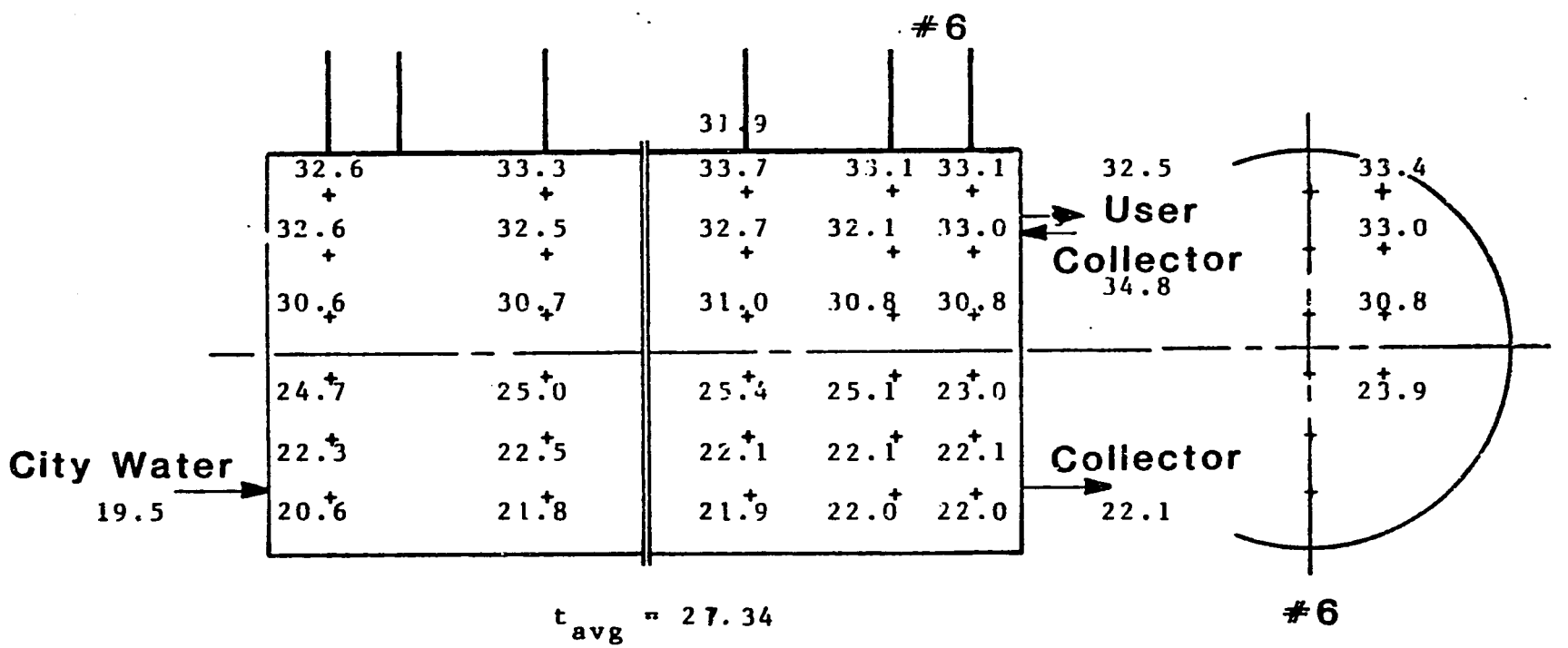

Fig. C.15: The Temperature Distribution in Tank

98.4 g/s continuous output 35.8 % of the tank volume

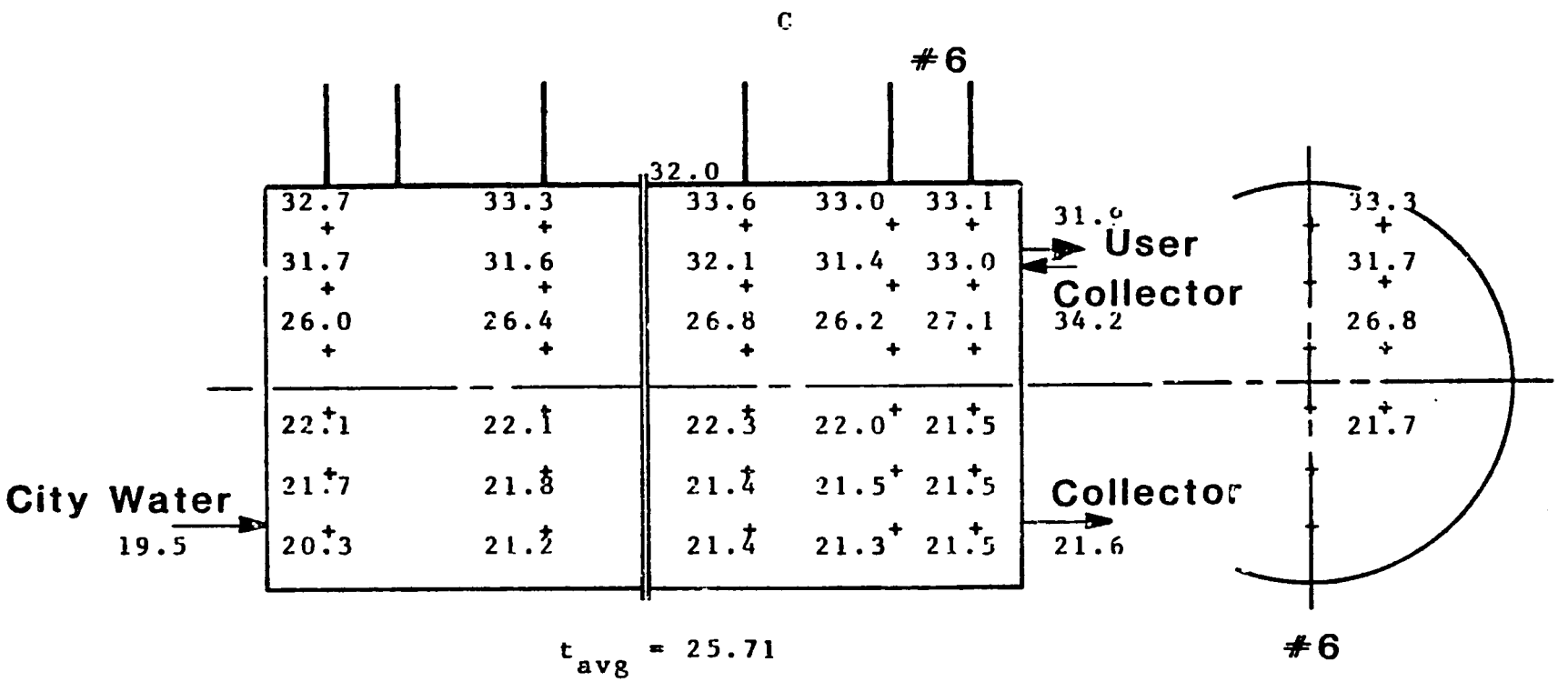

Fig. C.16: The Temperature Distribution in Tank

98.4 g/s continuous output 53.8 % of the tank volume

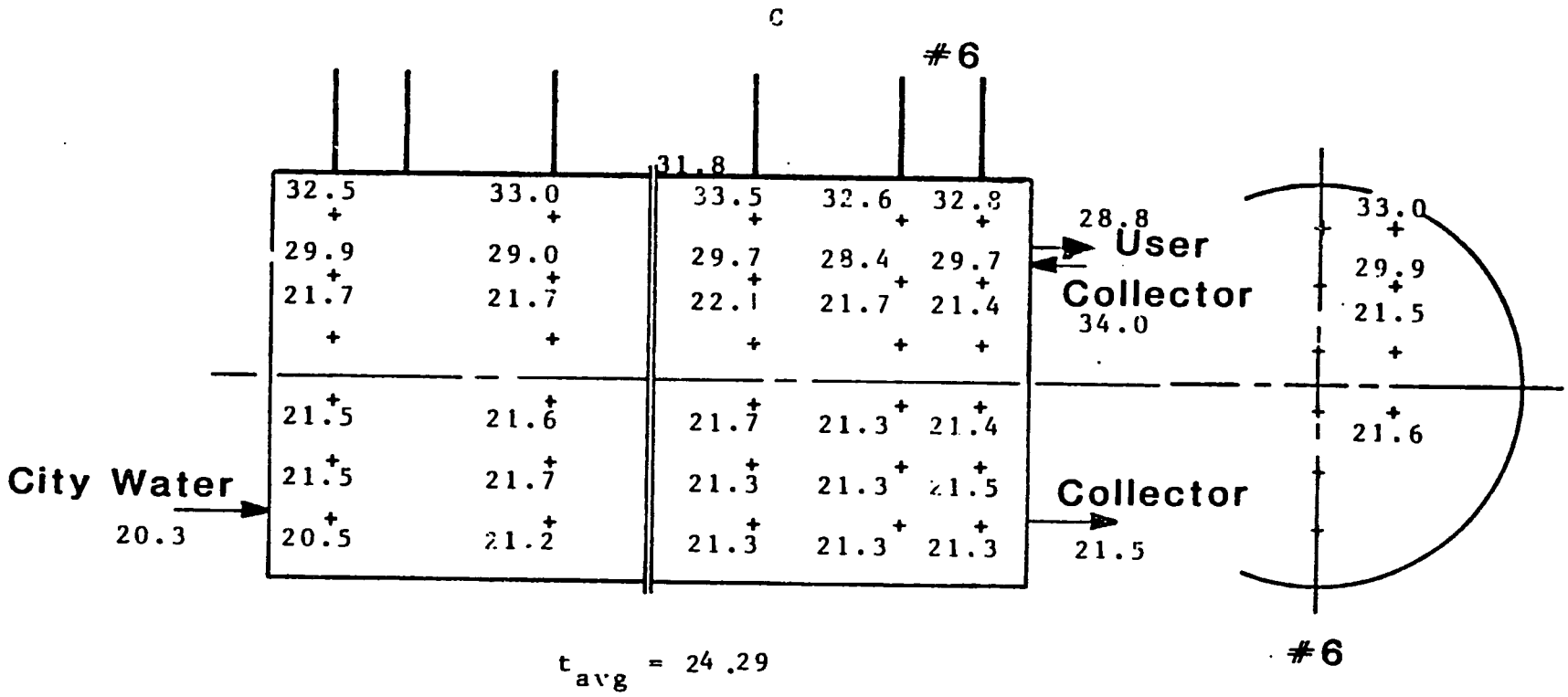

Fig. C.17: The Temperature Distribution in Tank

98.4 g/s continuous output 71.7 % of the tank volume

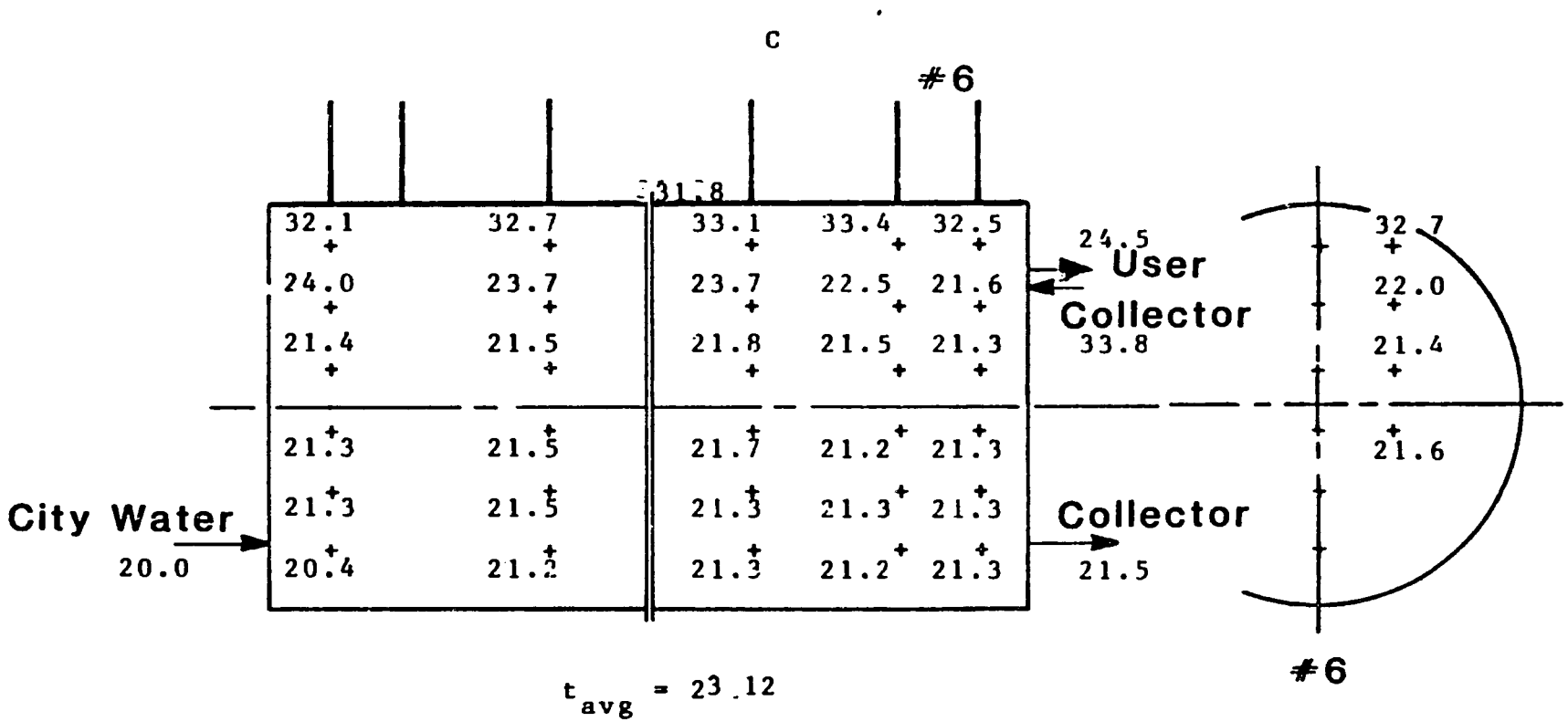

Fig. C.18: The Temperature Distribution in Tank

98.4 g/s continuous output 89.6 % of the tank volume

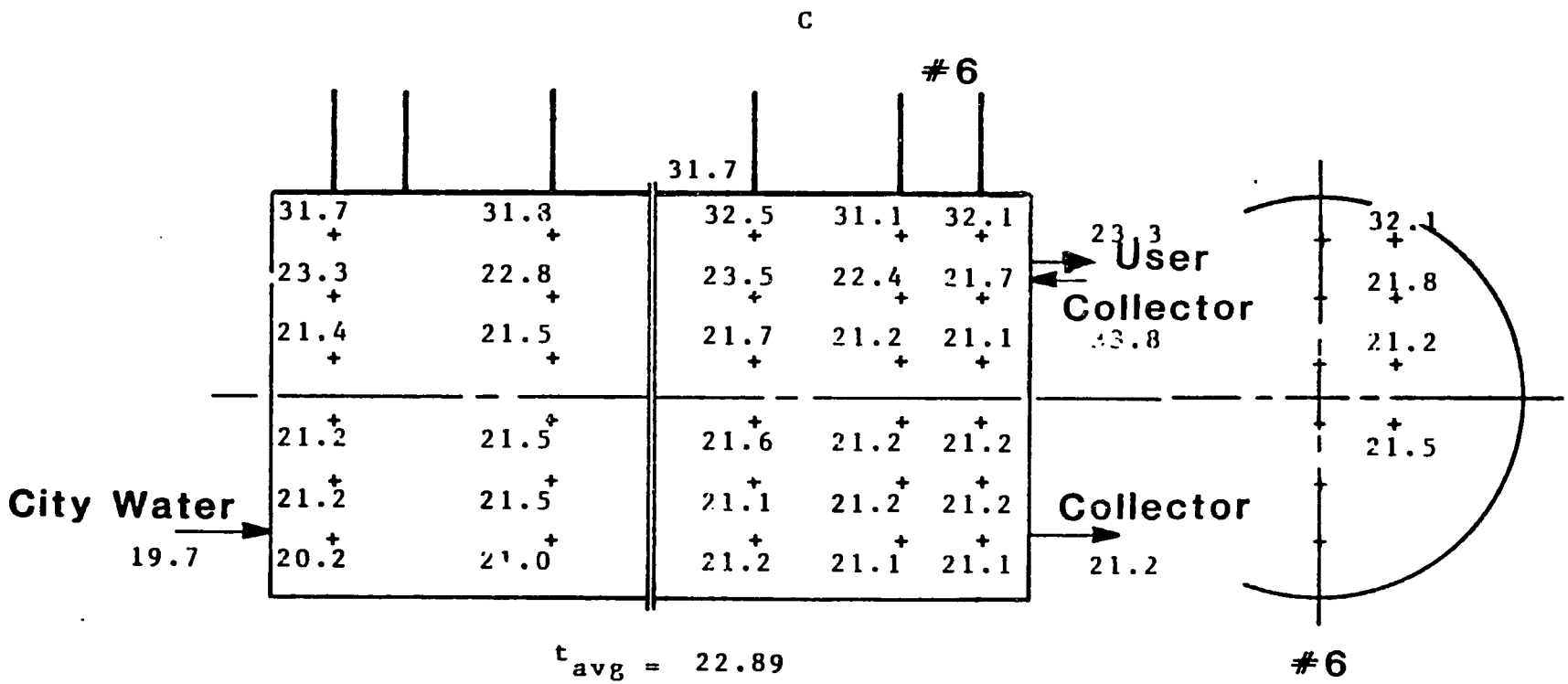

Fig. C.19: The Temperature Distribution in Tank

151.4 g/s continuous output 17.2 % of the tank volume

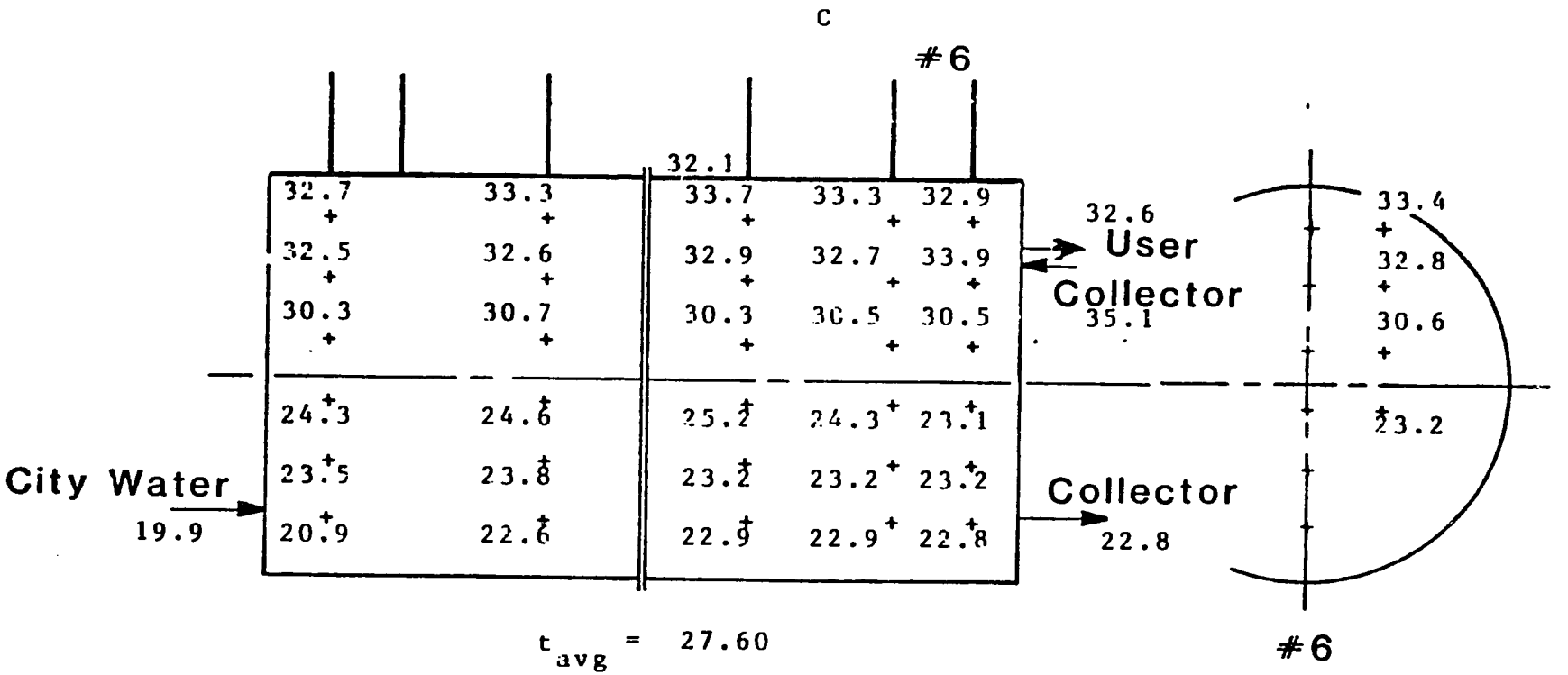

t_{avg} = 27.60

Fig. C.20: The Temperature Distribution in Tank

151.4 g/s continuous output 34.5 % of the tank volume

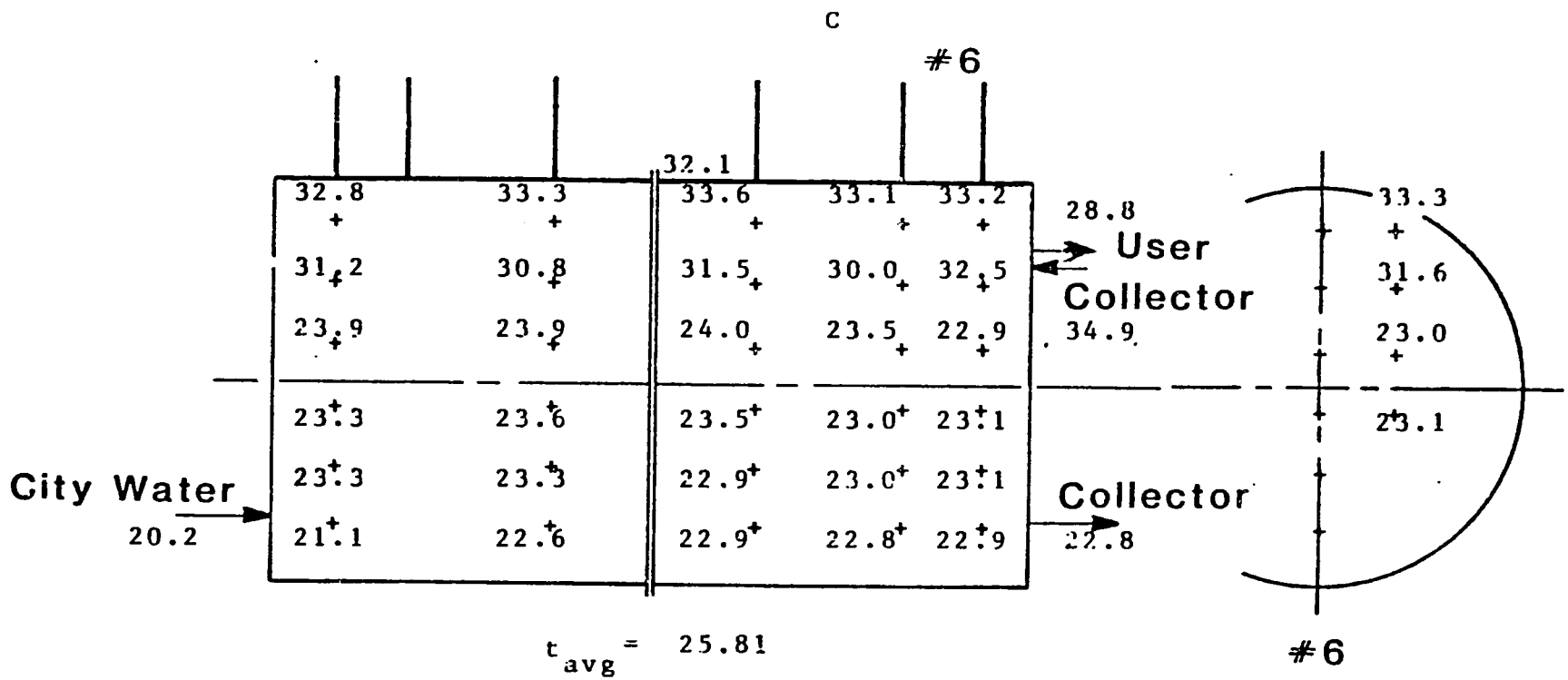

Fig. C.21: The Temperature Distribution in Tank

151.4 g/s continuous output 51.7 % of the tank volume

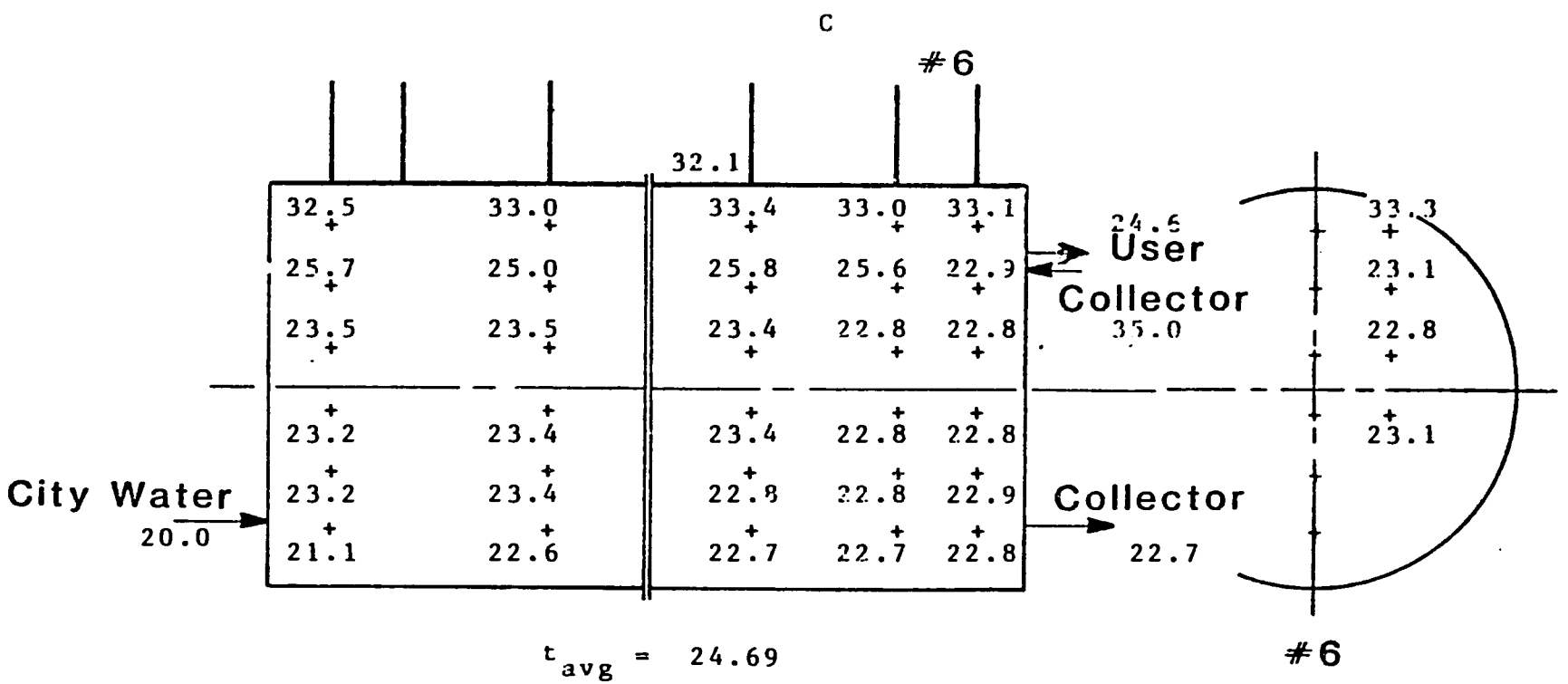

Fig. C.22: The Temperature Distribution in Tank

151.4 g/s continuous output 68.9 % of the tank volume

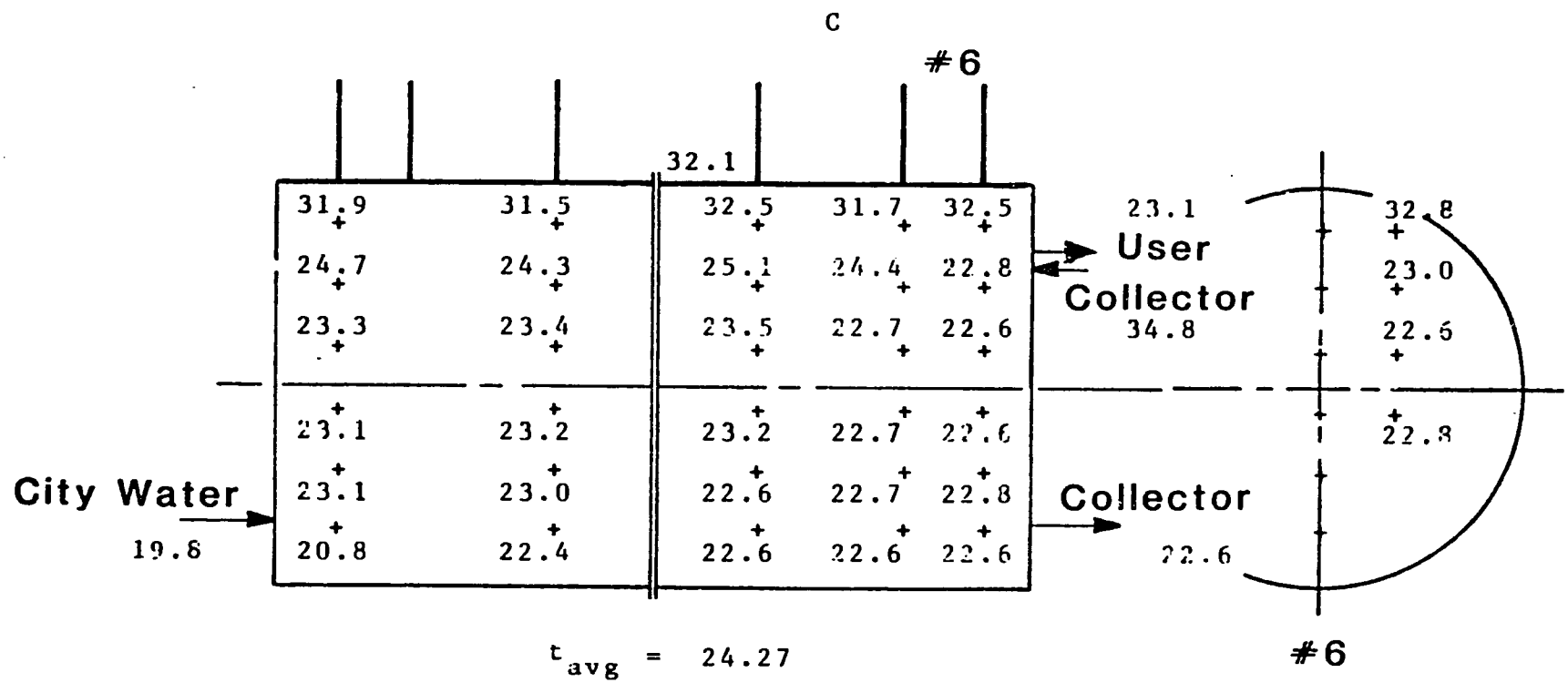

Fig. C.23: The Temperature Distribution in Tank

151.4 g/s continuous output 86.2 % of the tank volume

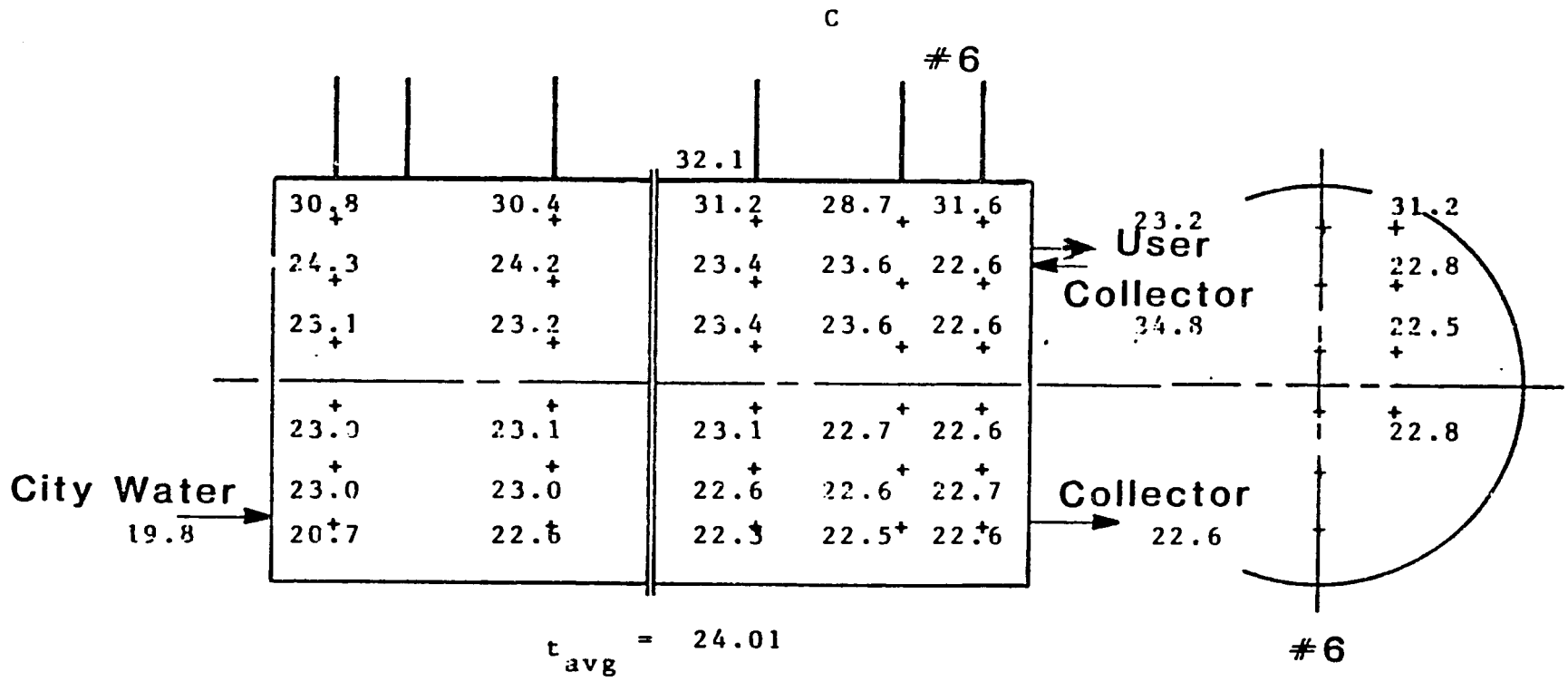

Fig. C.24: The Temperature Distribution in Tank

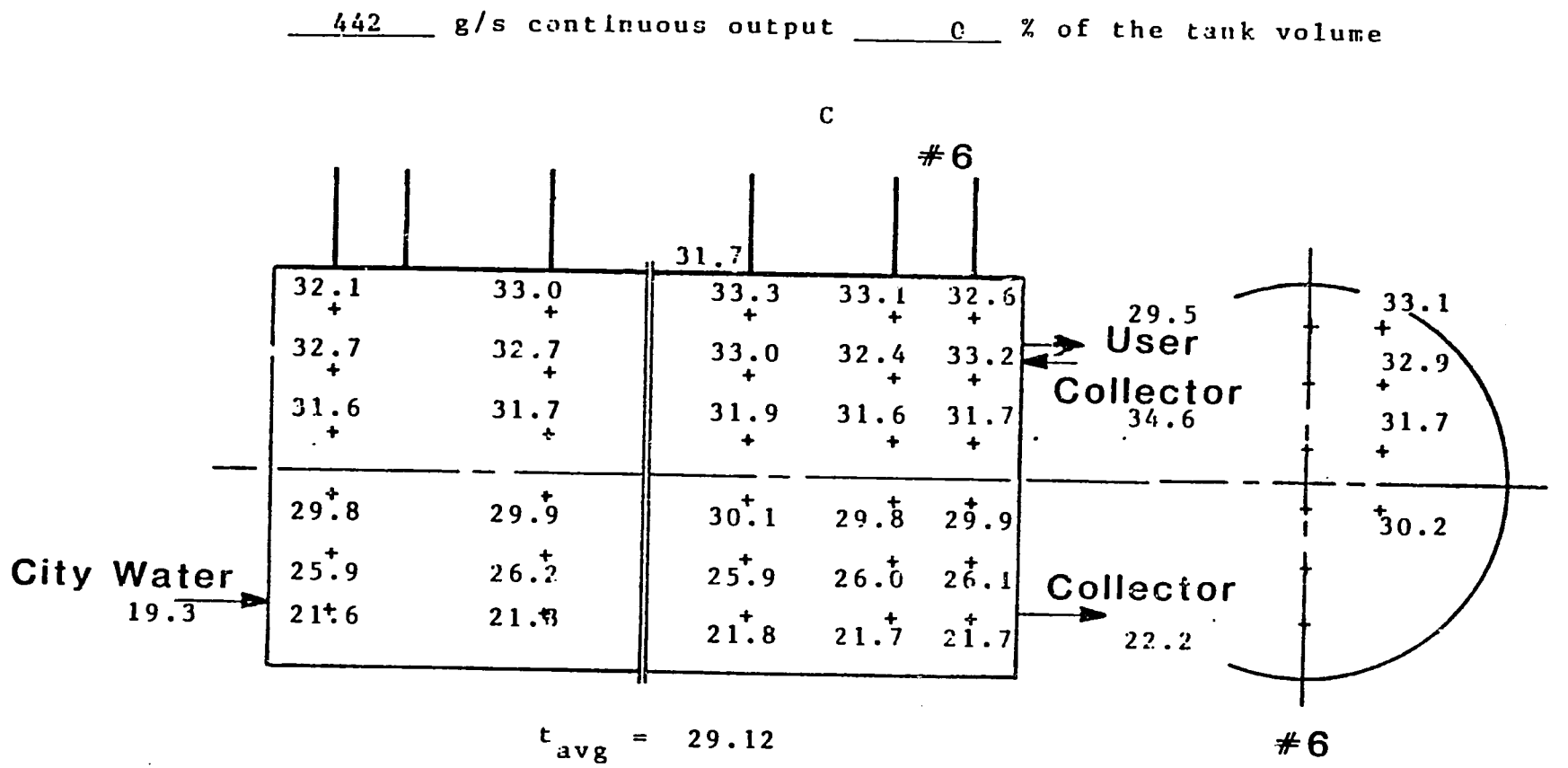

Fig. C.25: The Temperature Distribution in Tank

442 g/s continuous output 20.1 % of the tank volume

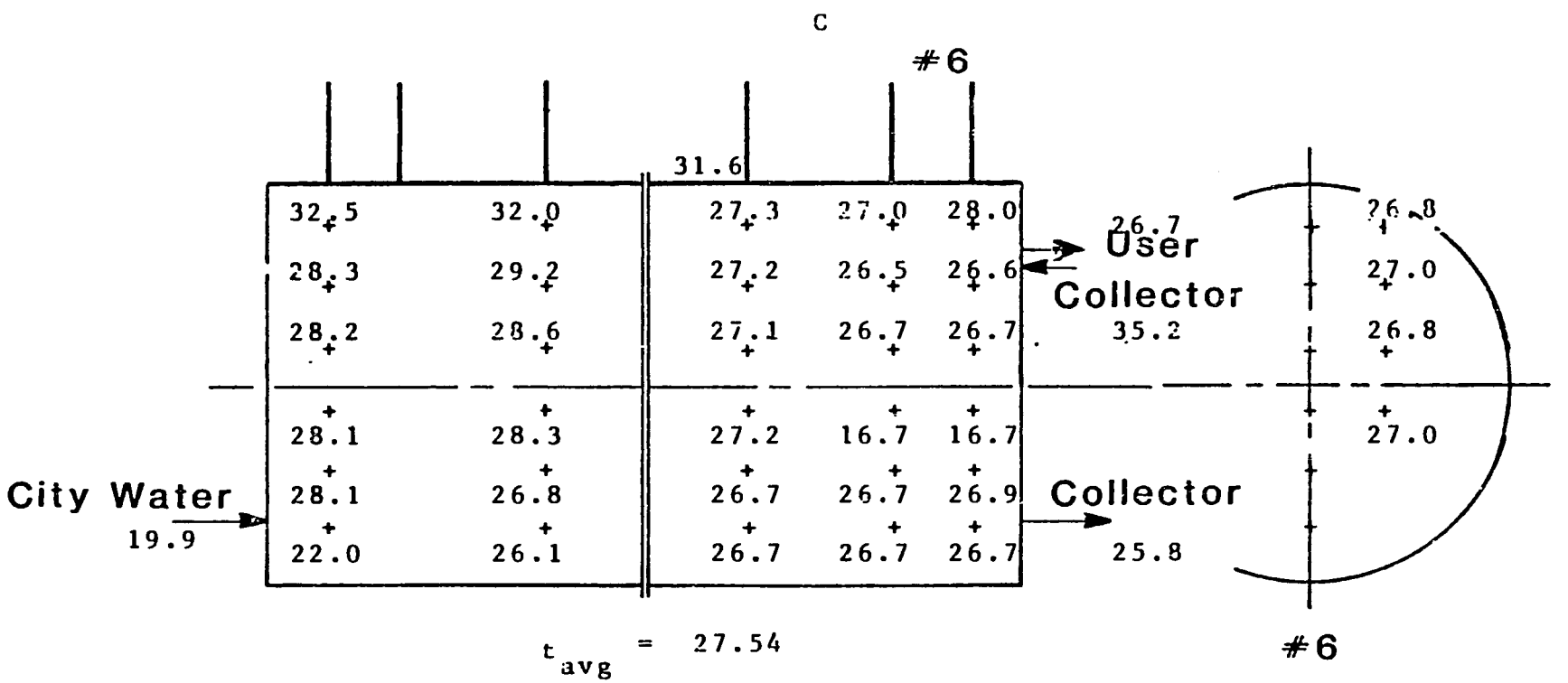

Fig. C.26: The Temperature Distribution in Tank

442 g/s continuous output 40.2 % of the tank volume

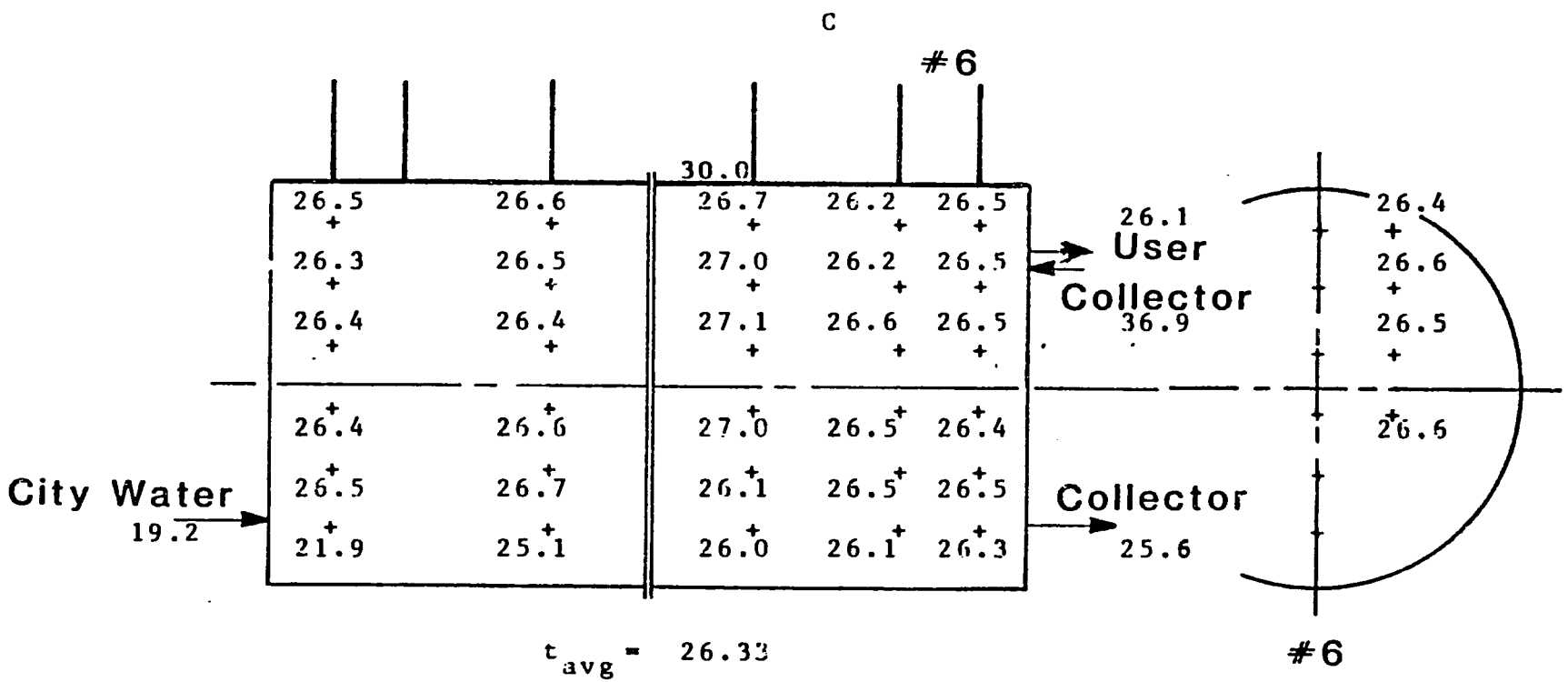

Fig. C.27: The Temperature Distribution in Tank